technische universität dortmund

ISF

Surface integrity depending on the machining process

Dipl.-Ing. Christian Rautert

October 2012

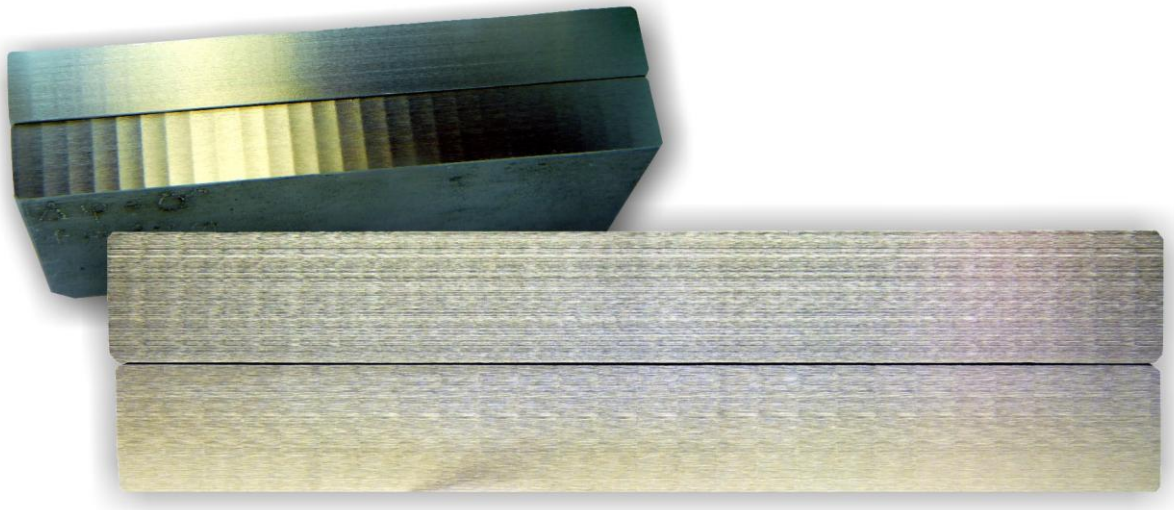

Overview

- Introduction
- Burr Minimization strategies in Machining Operations
- Micro-finishing of hard coated parts
- Detection of grinding burn and cracks by acoustic emission
- FEM in Internal Traverse Grinding
- Machining of low-sulfur steels
- Influence of coated surfaces on friction coefficients
- Machining of β-titanium alloys
- Waviness reduction
- Simulation strategies

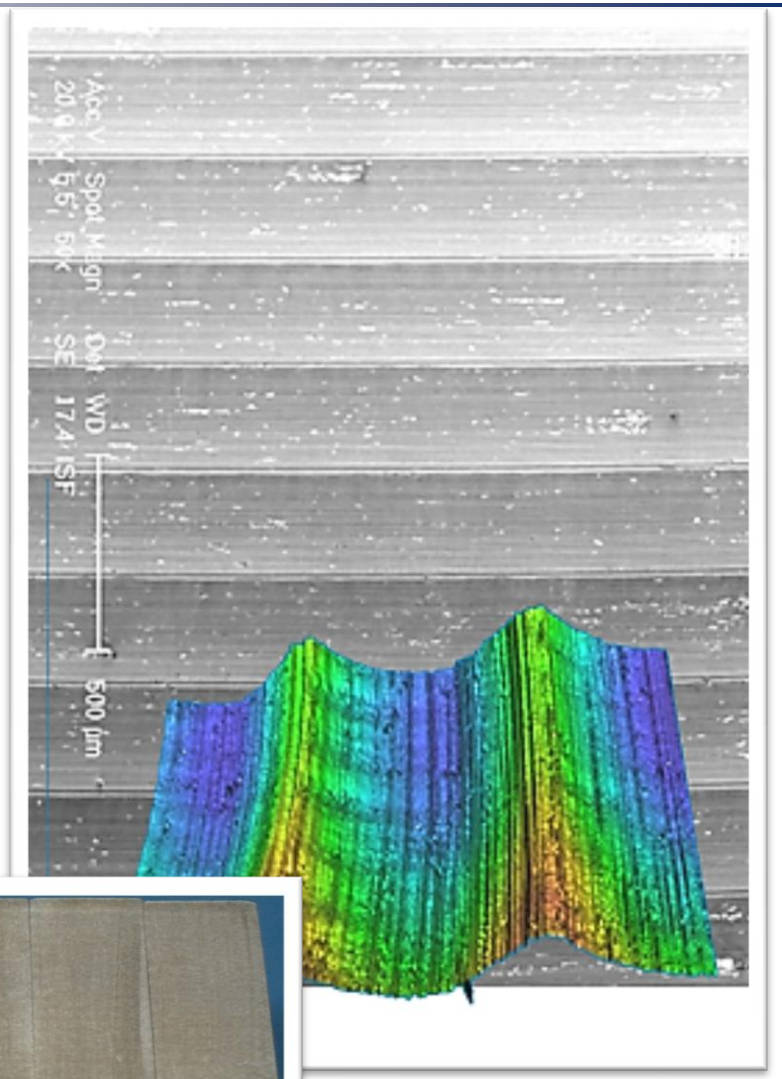

Applications of precise machining

Wear • Friction

Tools

Seals

Cylinders

Bearings

Drive components

Thin sheets

3D-Characterization by the use of optical microscopy

source: Nanofokus

Comparison of surface topographys generated in turning, grinding and honing processes

Turning

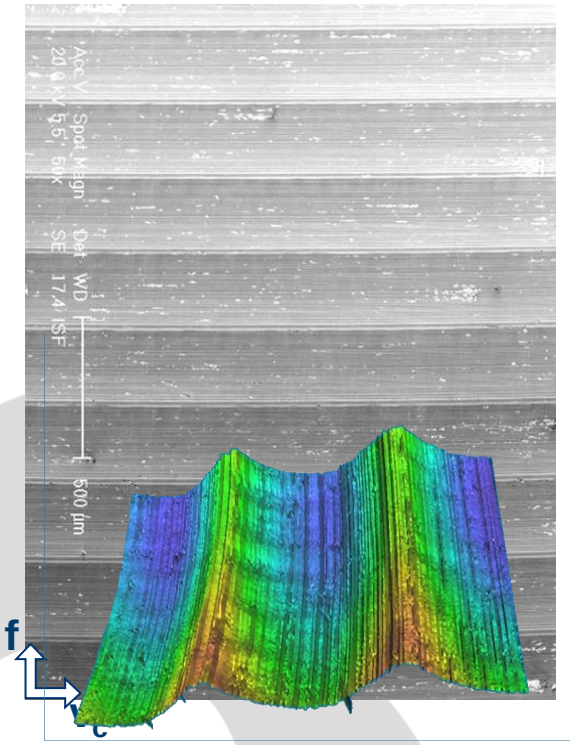

Grinding

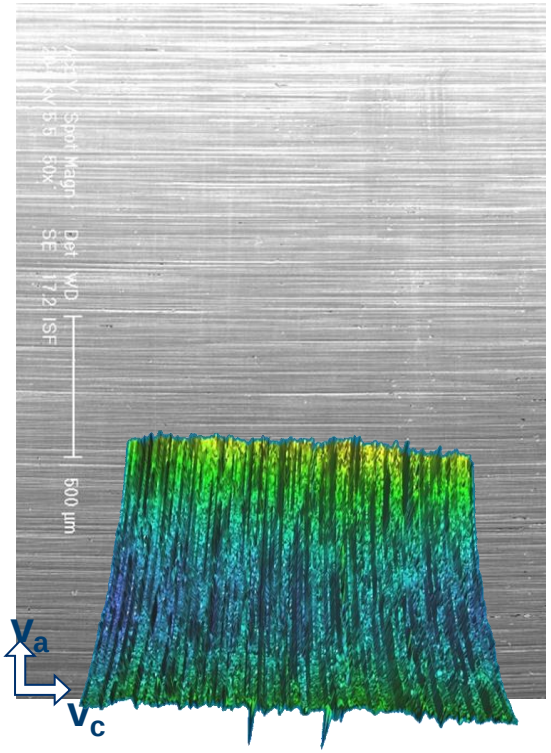

Honing

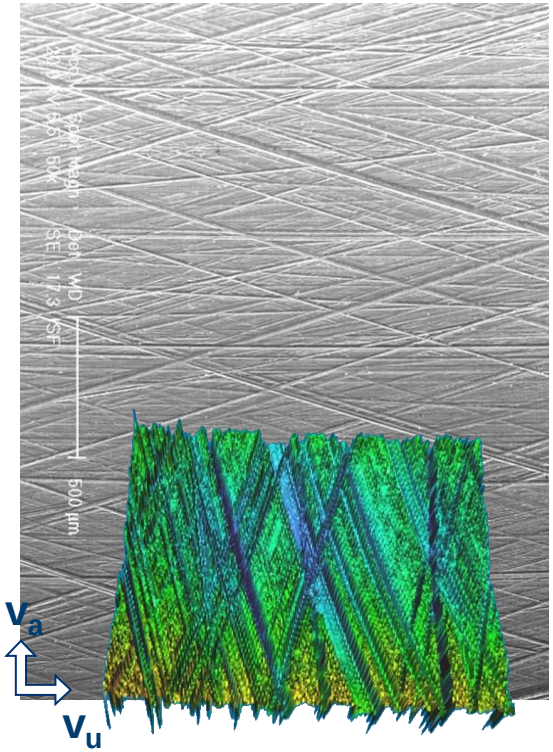

Three-point inside micrometer gauge

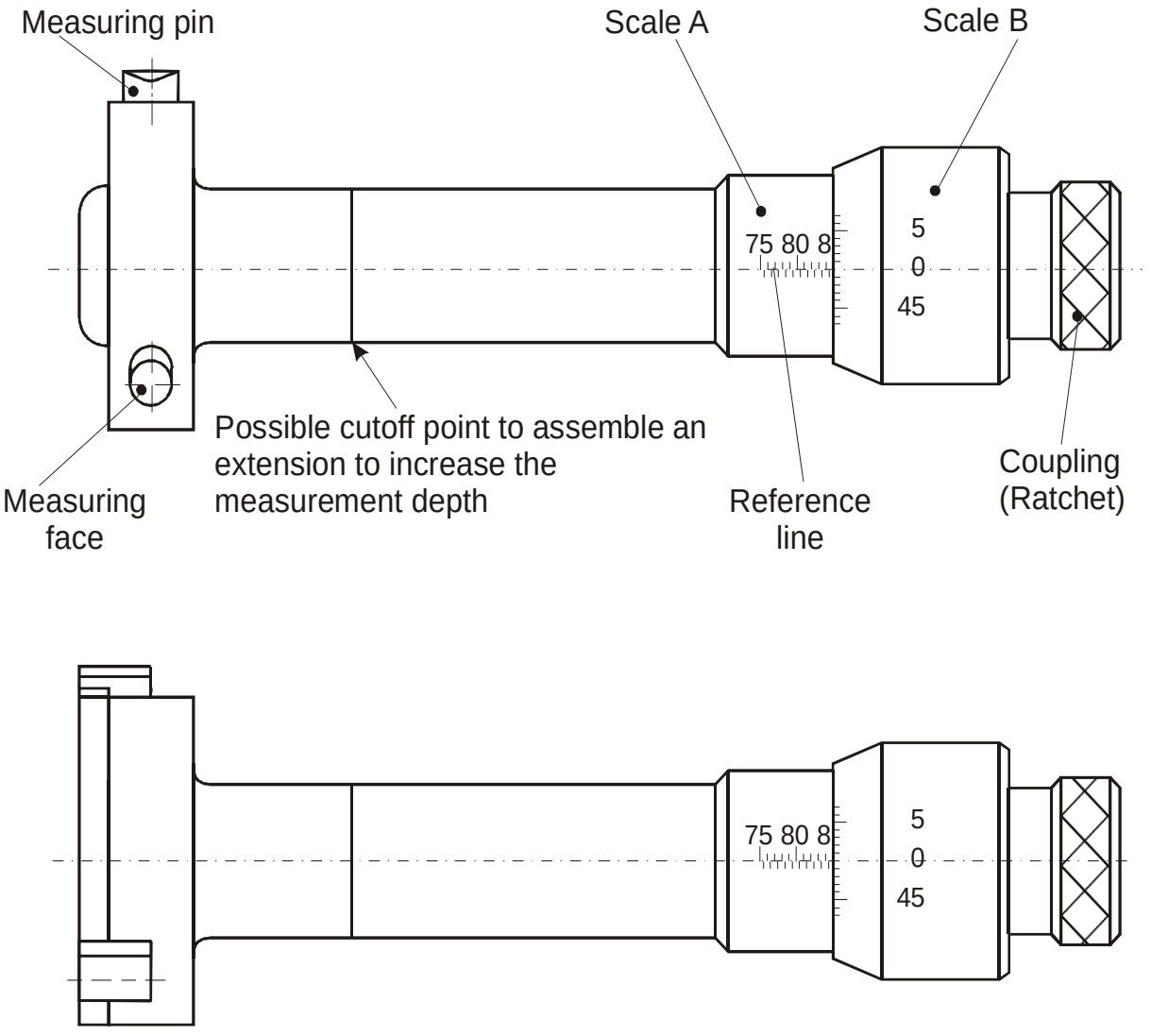

Applicable measurement principles of surface profilometers

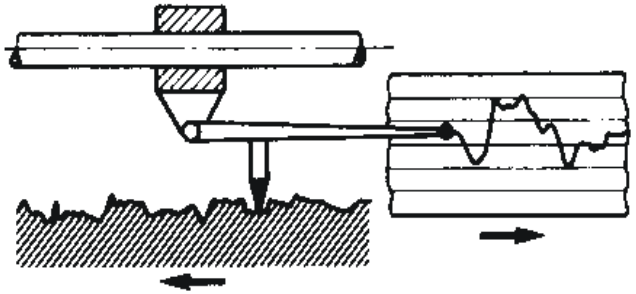

Mechanical

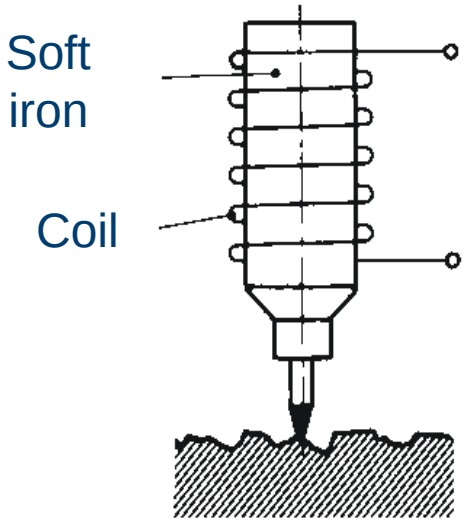

Inductive

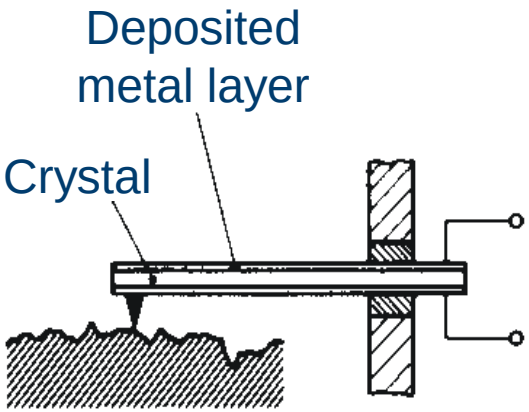

Piezoelectric

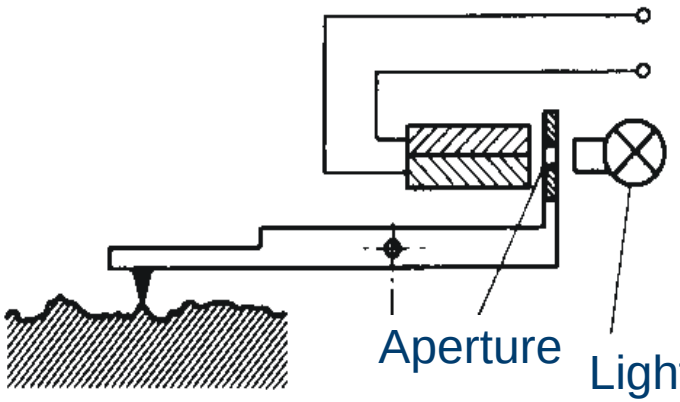

Opto-electrical

Measurement devices for the determination of circularity

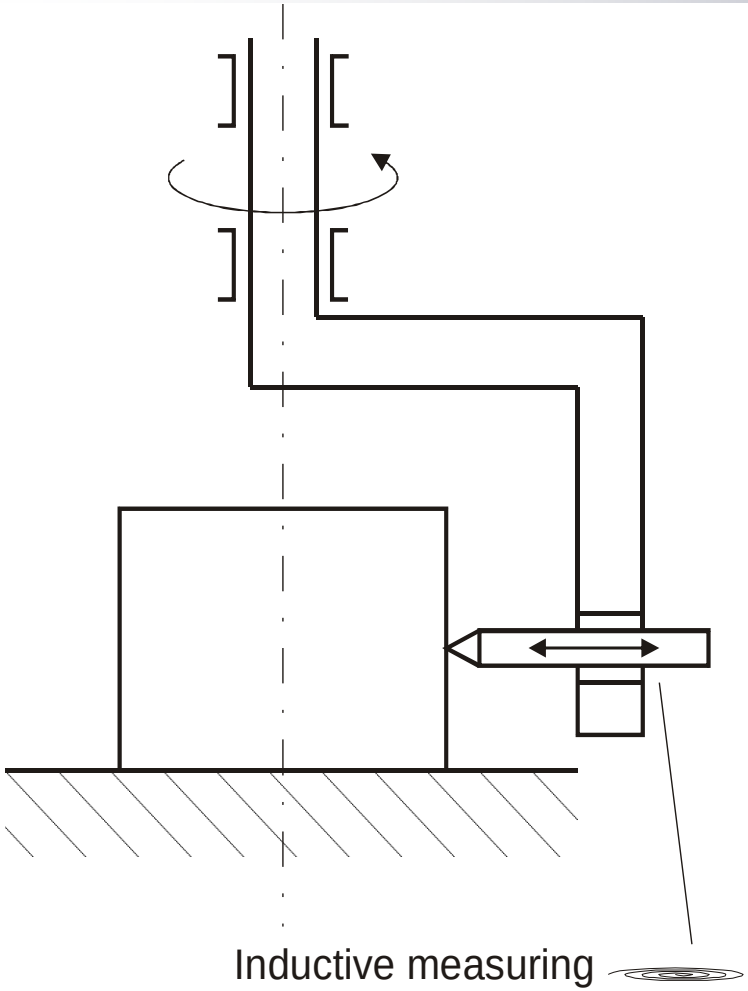

Talyrond - principle

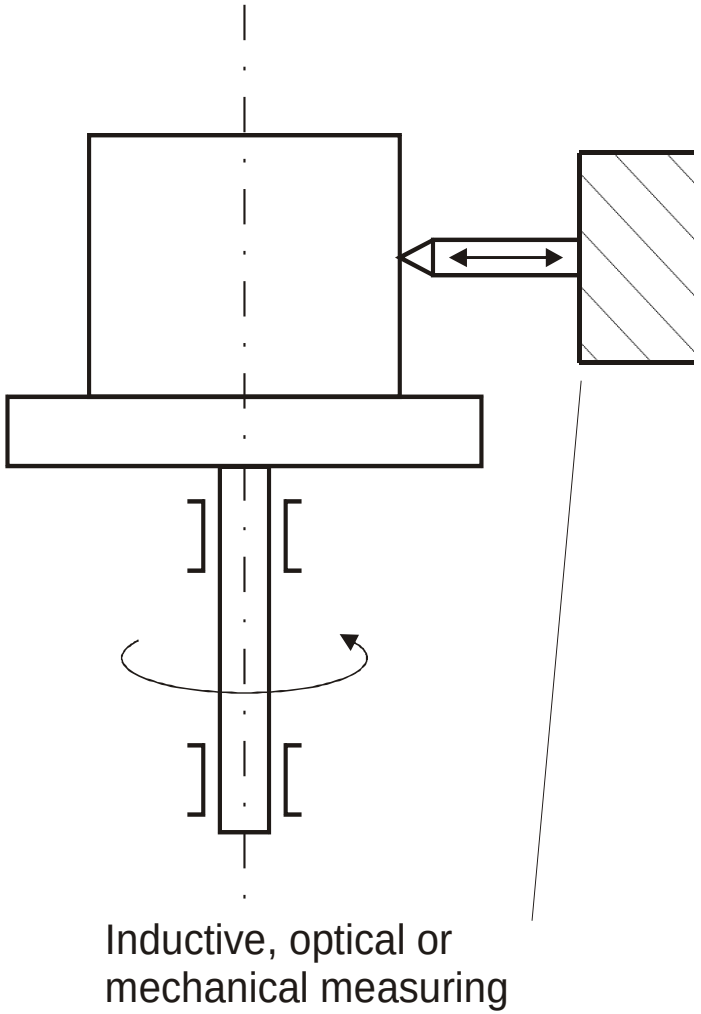

Form tester

Circularity measurement record

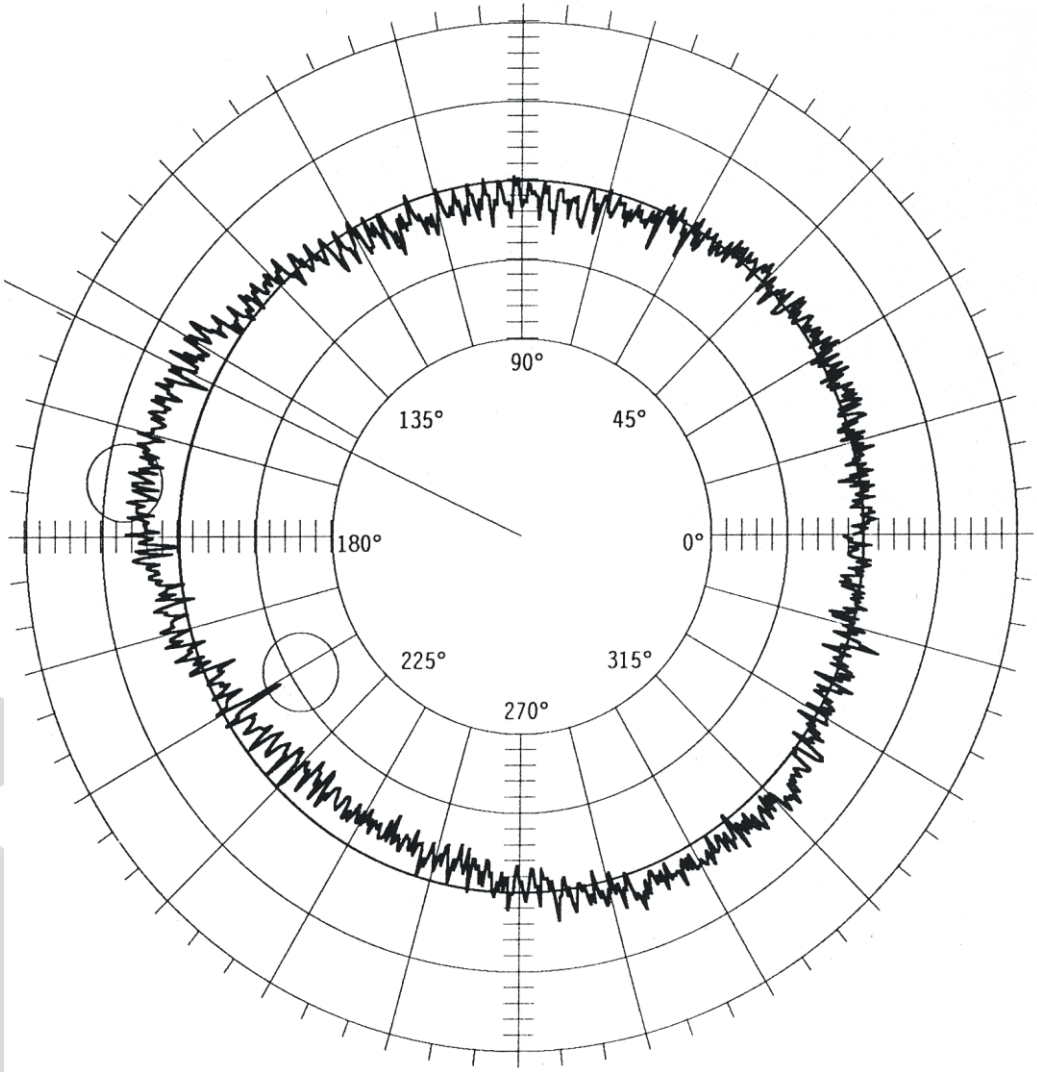

3D Coordinate measuring machine

Ruby probe and reference object

3D-Coordinate measuring machine Zeiss Prismo Vast

Drilling pattern

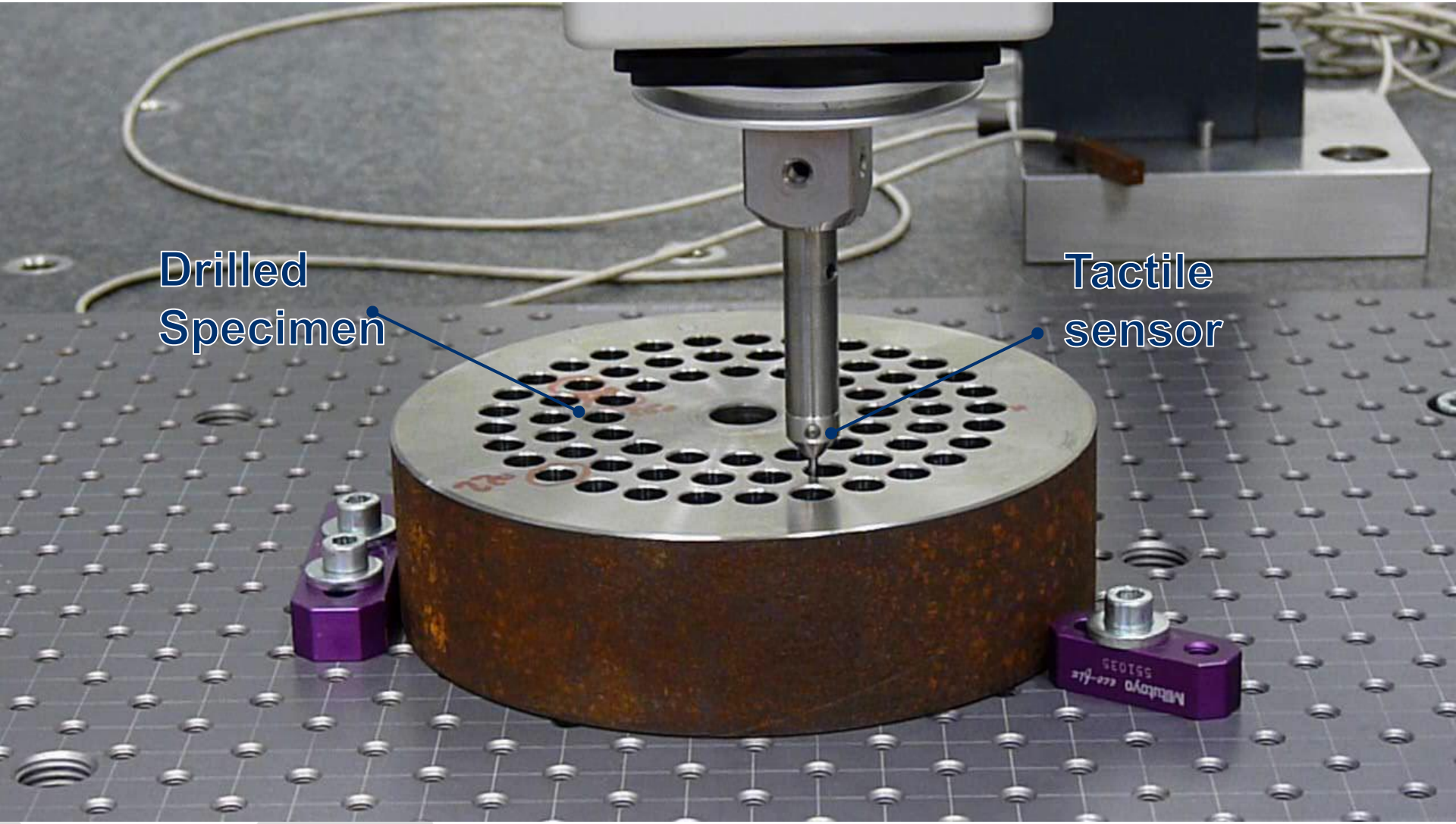

Overview

Introduction

Burr Minimization strategies in Machining Operations

Micro-finishing of hard coated parts

Detection of grinding burn and cracks by acoustic emission

FEM in Internal Traverse Grinding

Machining of low-sulfur steels

Influence of coated surfaces on friction coefficients

Machining of β-titanium alloys

Waviness reduction

Simulation strategies

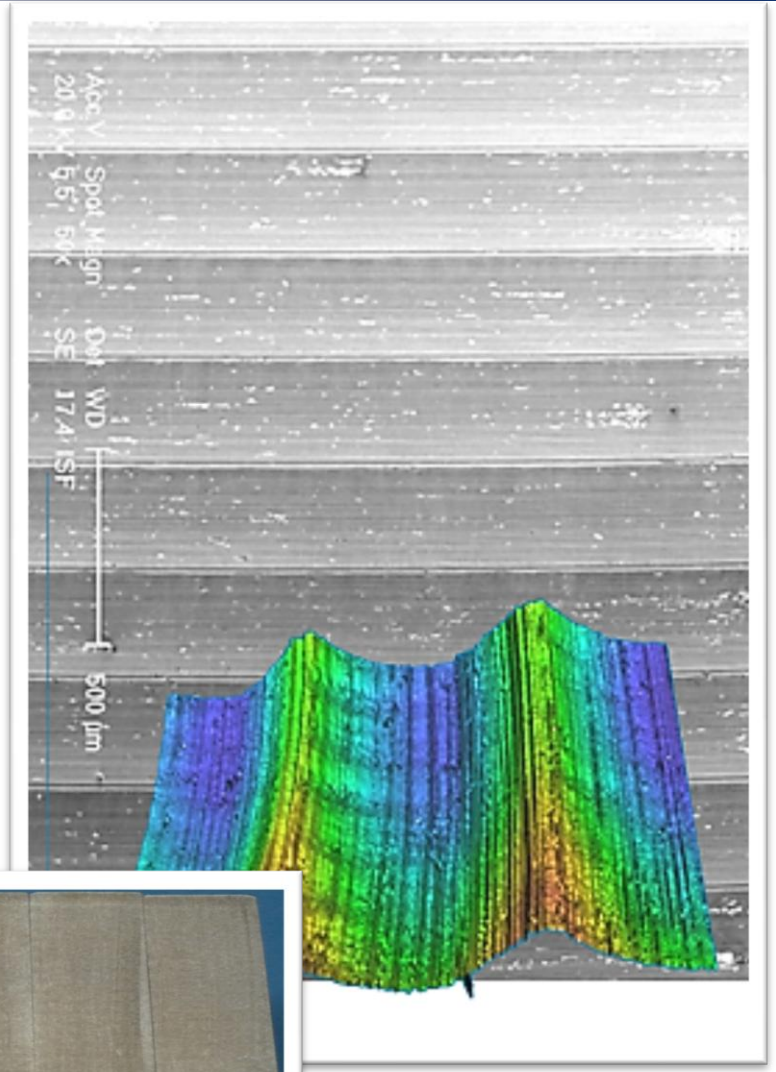

Burr Formation and Reduction Strategy in Turning Austenitic-Ferritic Stainless Steel

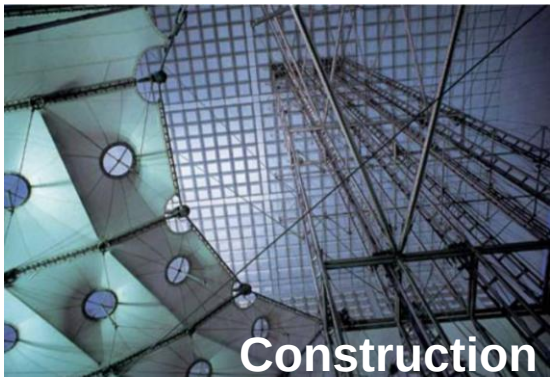

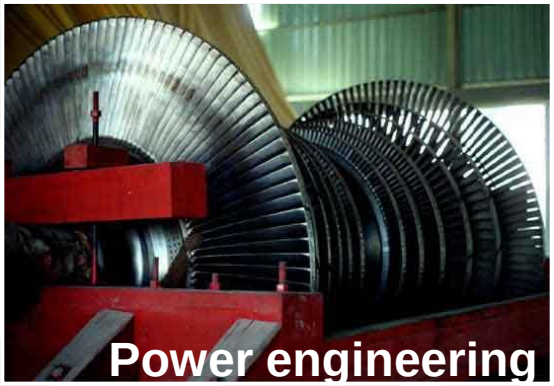

Material design:

- High percentage of alloying elements (Cr > 10.5 %)
- Microstructure:
  - ferritic
  - martensitic
  - austenitic
  - austenitic-ferritic

Main properties:

- Chemical resistance against corrosive media
- Favorable values for strength and toughness
- Low heat conductivity and high specific heat capacity

Burr Formation and Reduction Strategy in Turning Austenitic-Ferritic Stainless Steel

Experimental set-up – Workpiece material

X2CrNiMoN22-5-3

Mechanical Properties	
Hardness HRC	28.2
Tensile yield strength $R_{p0,2}$	531 N/mm^2
Tensile strength R_m	737 N/mm^2
Elongation at fracture A_{min}	36.7 %
Reduction at fracture Z_{min}	75 %
Notched bar impact work A_v at RT	100 J

Machining behavior

- The favorable values for strength and toughness lead to high thermomechanical loads in machining operations.
- Low heat conductivity increases the thermal tool loads.
- The adhesion tendency leads to material deposits on the tool.
- High ductility exacerbates chip breakage.

High loads on the tool and the workpiece

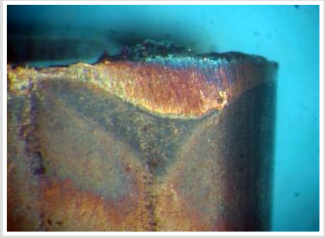

Unfavorable chip breakage and affection to burr formation

Low tool life and process reliability

Burr Formation and Reduction Strategy in Turning Austenitic-Ferritic Stainless Steel

Material:	X2CrNiMoN22-5-3	Cutting Speed:	v_c = 150 m/min
Cutting material:	HC-M25	Feed:	f = 0.15 mm
Tool:	CNMG120408	Depth of cut:	a_p = 2.5 mm
Cooling concept:	Emulsion	Volume removed:	Varies

α_0	γ_0	κ_r	r_ε
6°	9°	95°	0.8 mm

Process begin
Furrowing load at the end of contact zone

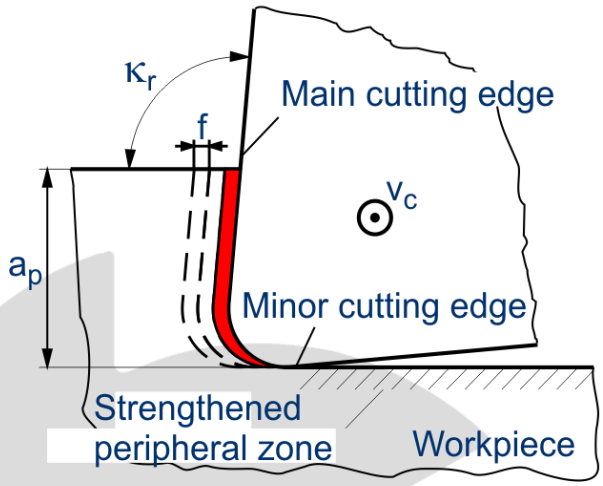

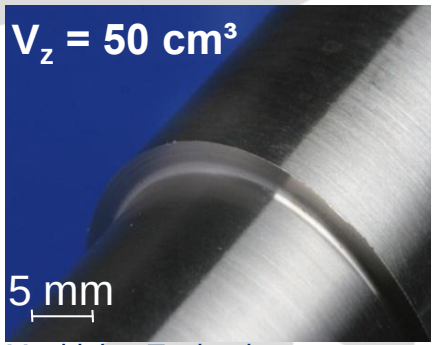

Phase 1
Beginning notch wear and burr formation

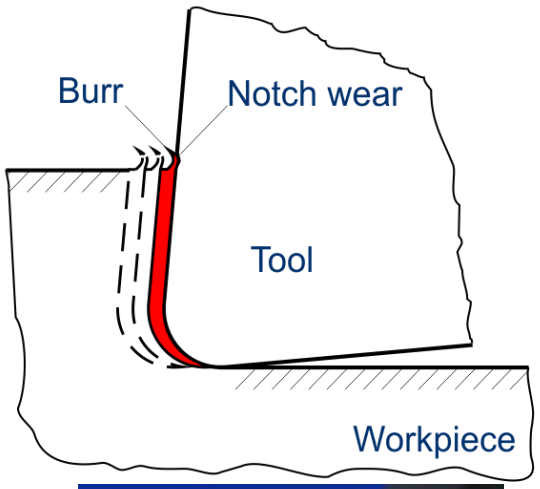

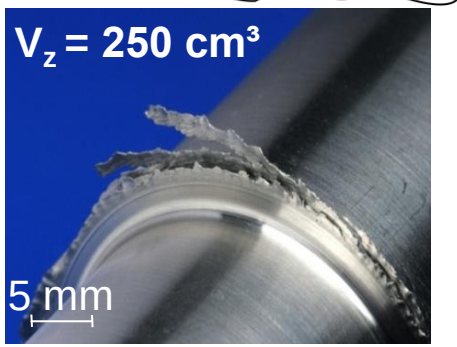

Phase 2
Interaction between notch wear and burr formation and their progression

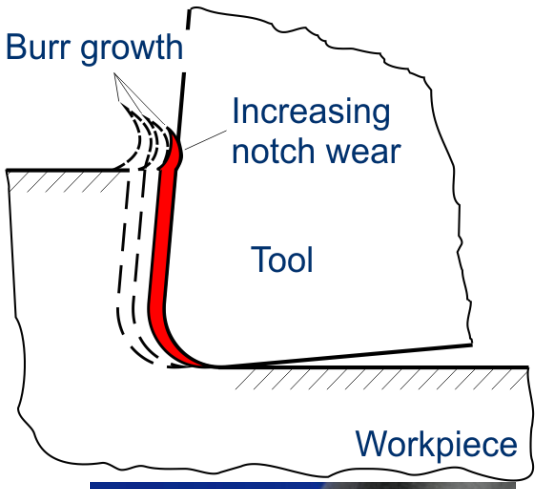

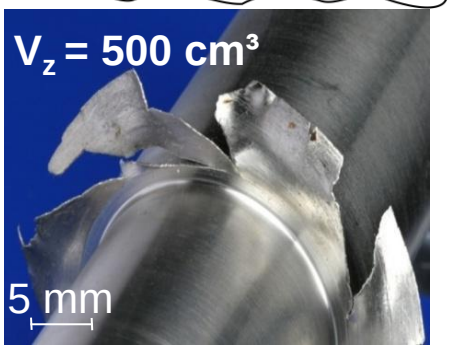

Burr Formation and Reduction Strategy in Turning Austenitic-Ferritic Stainless Steel

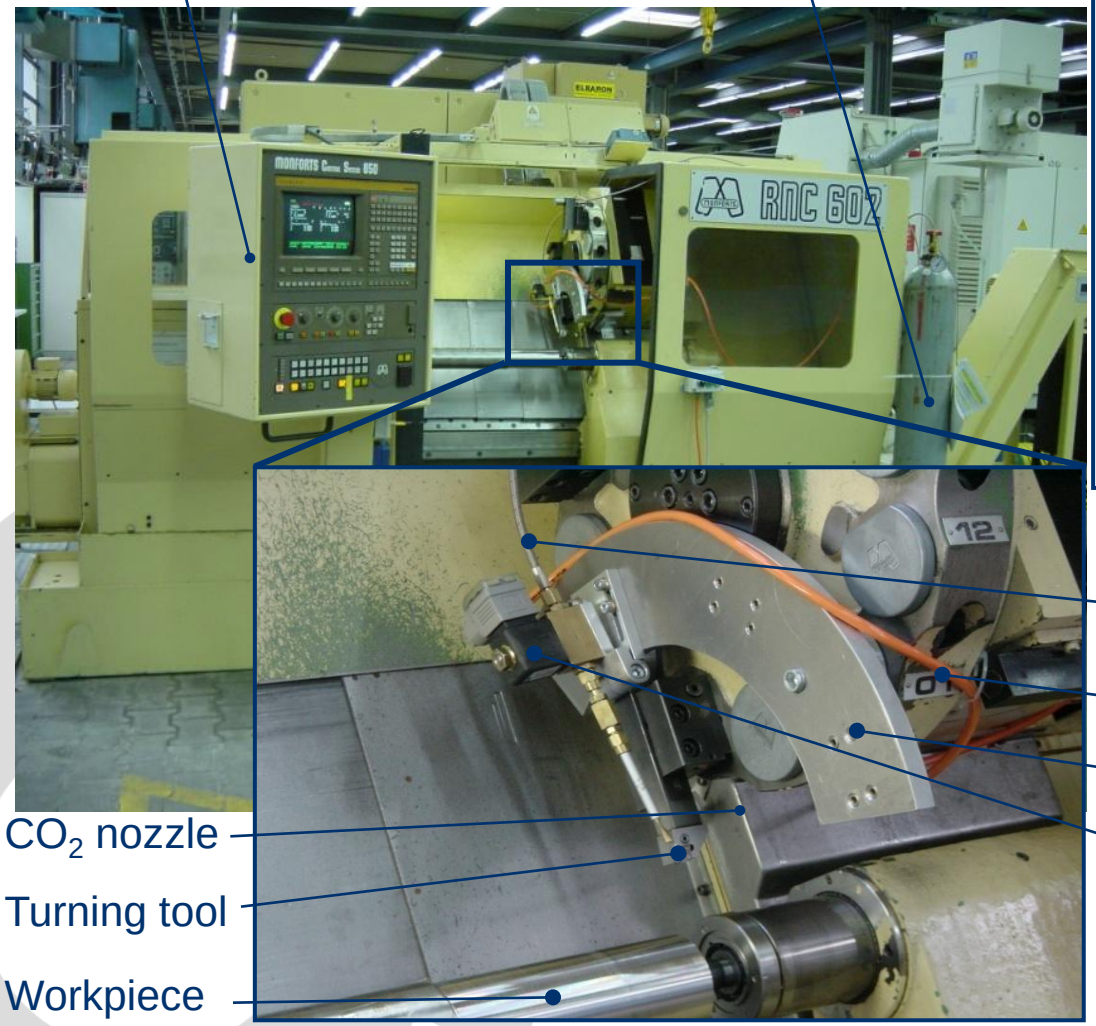

Lathe Monforts RNC 602

Driving power:	30 KW at 100 % ED
Drive torque:	755 Nm at 30 kW
Speed range:	28 up to 4000 min^{-1}
Tool magazine:	12
Max. Diameter:	210 mm
Max. length:	600 mm

Burr Formation and Reduction Strategy in Turning Austenitic-Ferritic Stainless Steel

Experimental set-up – Cooling medium

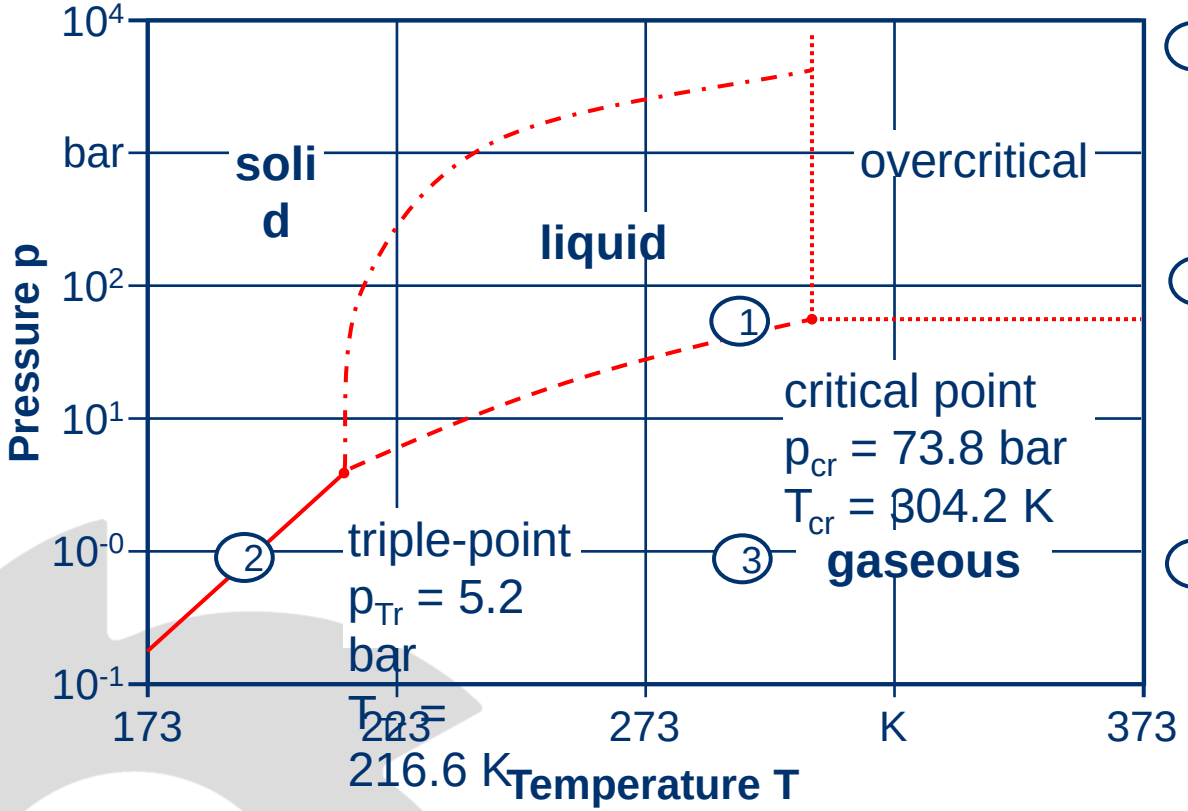

1. The liquid carbon dioxide is stored at a pressure of p = 60 bar in pressure gas cylinders at room temperature.
2. At relaxation, the liquid CO_2 cools down rapidly (Joule-Thomson-Effect). Because of that, a mixture of solid particles and cold gas is produced.
3. The dry ice particles, in particular, are an efficient cooling medium because of the high cooling capacity based on their high enthalpy of sublimation. In addition, the cooling of the chilled goods is achieved by the convection of the cold gas.

Properties of CO_2:

Non-toxic, incombustible, non-corrosive, odorless, higher density than air

Burr Formation and Reduction Strategy in Turning Austenitic-Ferritic Stainless Steel

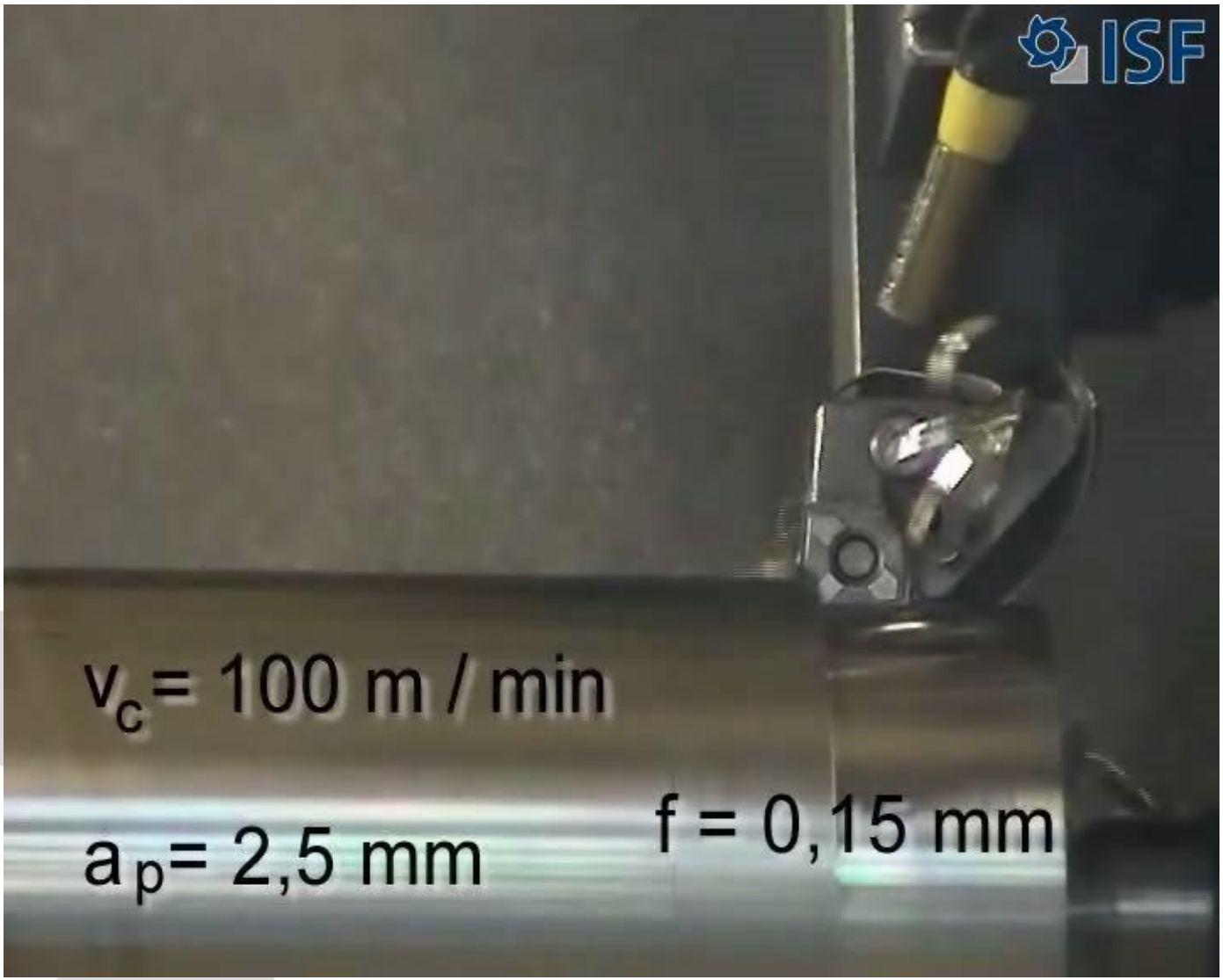

Burr Formation and Reduction Strategy in Turning Austenitic-Ferritic Stainless Steel

Material:	X2CrNiMoN22-5-3	Cutting Speed:	v_c = 150 m/min
Cutting material:	HC-M25	Feed:	f = 0.15 mm
Tool:	CNMG120408	Depth of cut:	a_p = 2.5 mm
Cooling concept:	Varies	Volume removed:	Varies

α_0	γ_0	κ_r	r_ε
6°	9°	95°	0.8 mm

Dry machining	MQL	Emulsion	CO_2
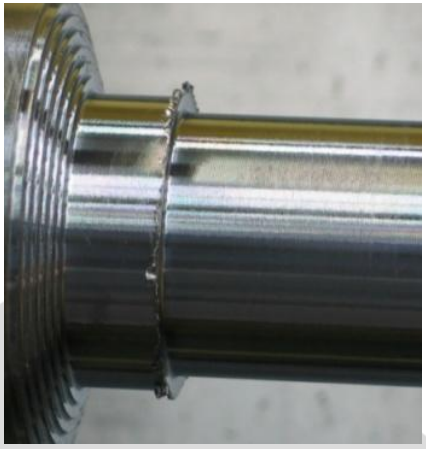	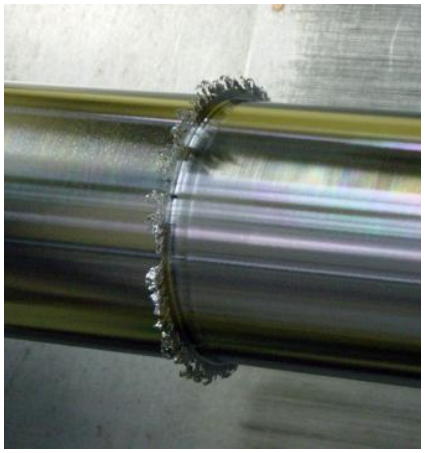		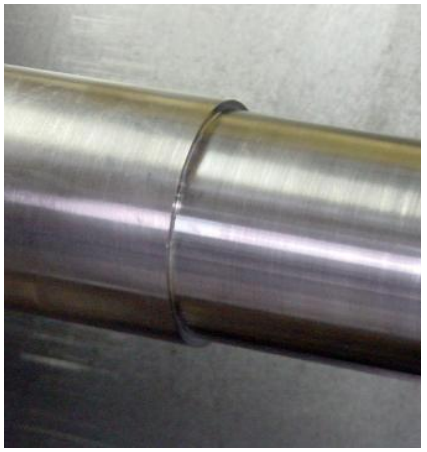
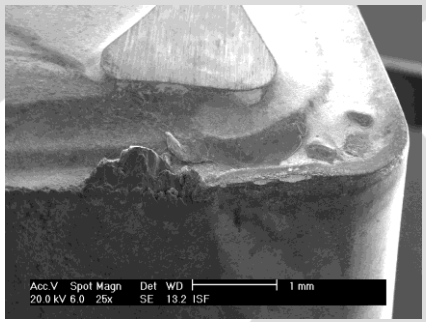	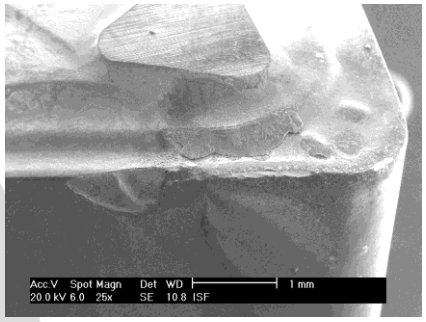	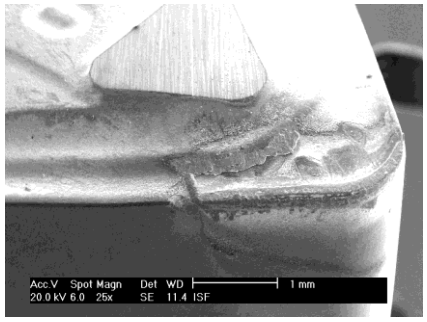	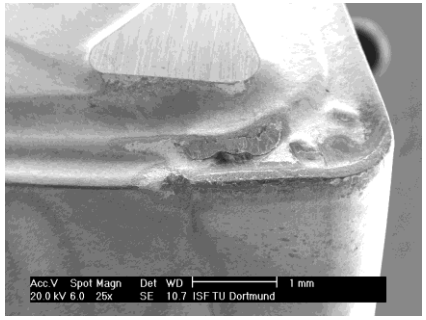

CO_2 Process Cooling for Burr Reduction in Face Milling of Aluminum Alloys

Experimental set-up – Workpiece material

EN AW-6060 (AlMgSi0.5)

Mechanical properties	
Hardness HBW	50
Yield point $R_{p0.2}$	60 N/mm²
Min. tensile strength R_m	120 N/mm²
Elongation at fracture A	16 %

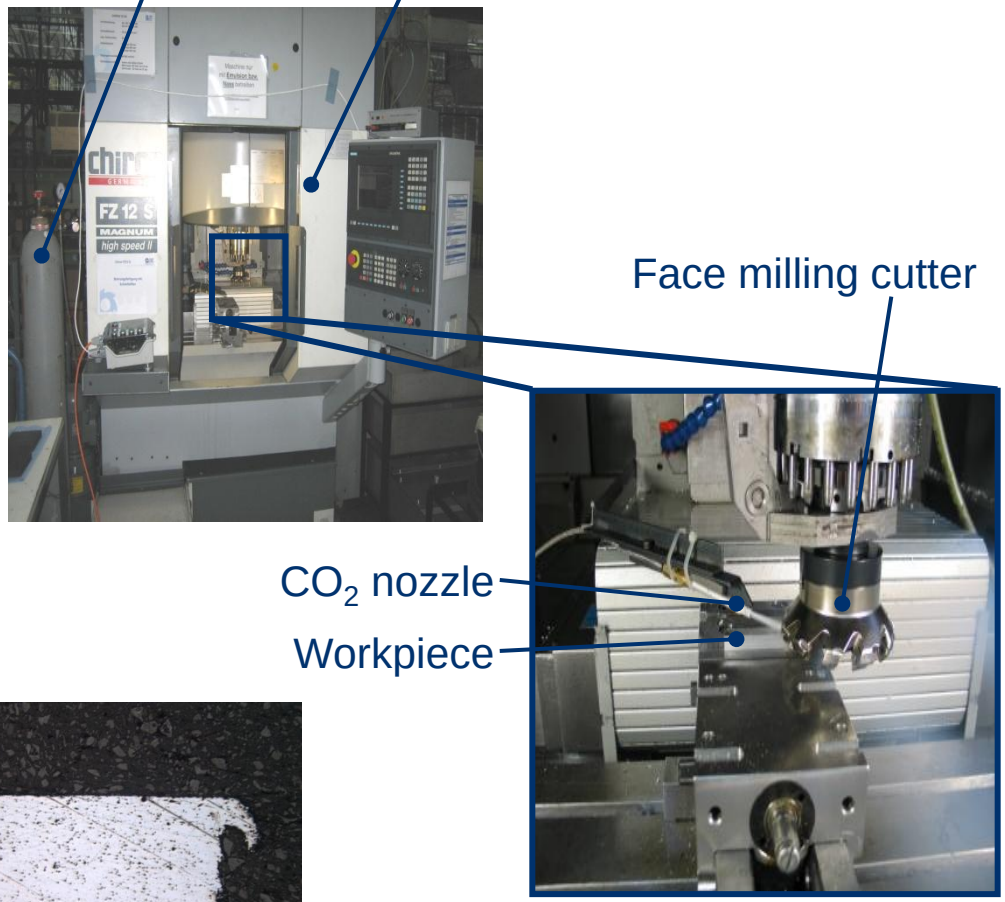

Machining Properties

- High tendency to adhesion leads to material deposits on the tool.
- High formability makes chip breakage more difficult and leads to burr formation.

CO_2 Process Cooling for Burr Reduction in Face Milling of Aluminum Alloys

CO_2 Process Cooling for Burr Reduction in Face Milling of Aluminum Alloys

Material:	EN AW-6060	Cutting Speed:	v_c = 3000 m/min
Tool:	Face milling cutter	Feed per tooth:	f_z = 0.1 mm
Cutting material:	HW-N25	Depth of cut:	a_p = 1.0 mm
Cooling concept:	Varies		

Dry machining

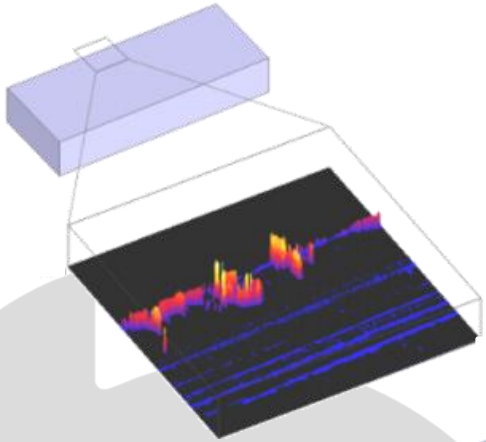

Pre-cooling

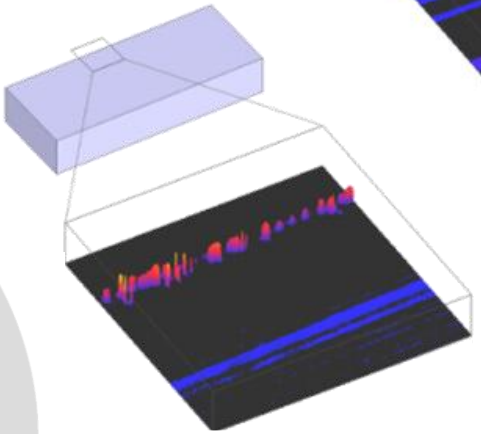

In-process cooling (P = 7.6 kW)

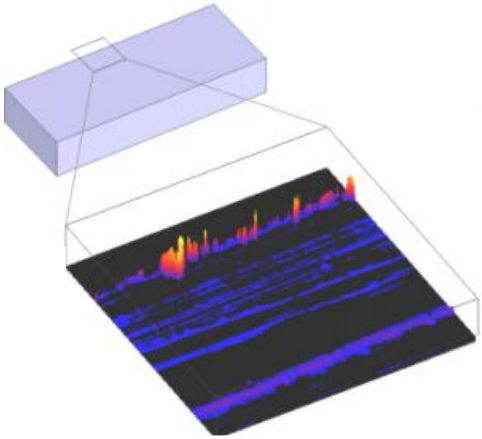

In-process cooling (P = 4.5 kW)

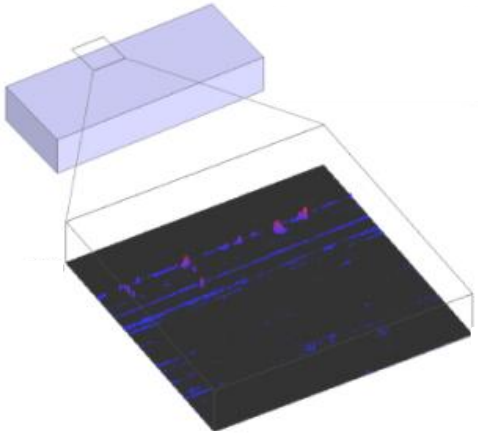

Burr height

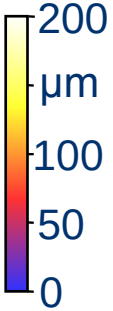

CO_2 Process Cooling for Burr Reduction in Face Milling of Aluminum Alloys

Material:	EN AW-6060	Cutting Speed:	v_c = 1000 … 3000 m/min
Tool:	Face milling cutter	Feed per tooth:	f_z = 0.4 … 1.0 mm
Cutting material:	HW-N25	Depth of cut:	a_p = 1.0 mm
Cooling concept:	Varies		

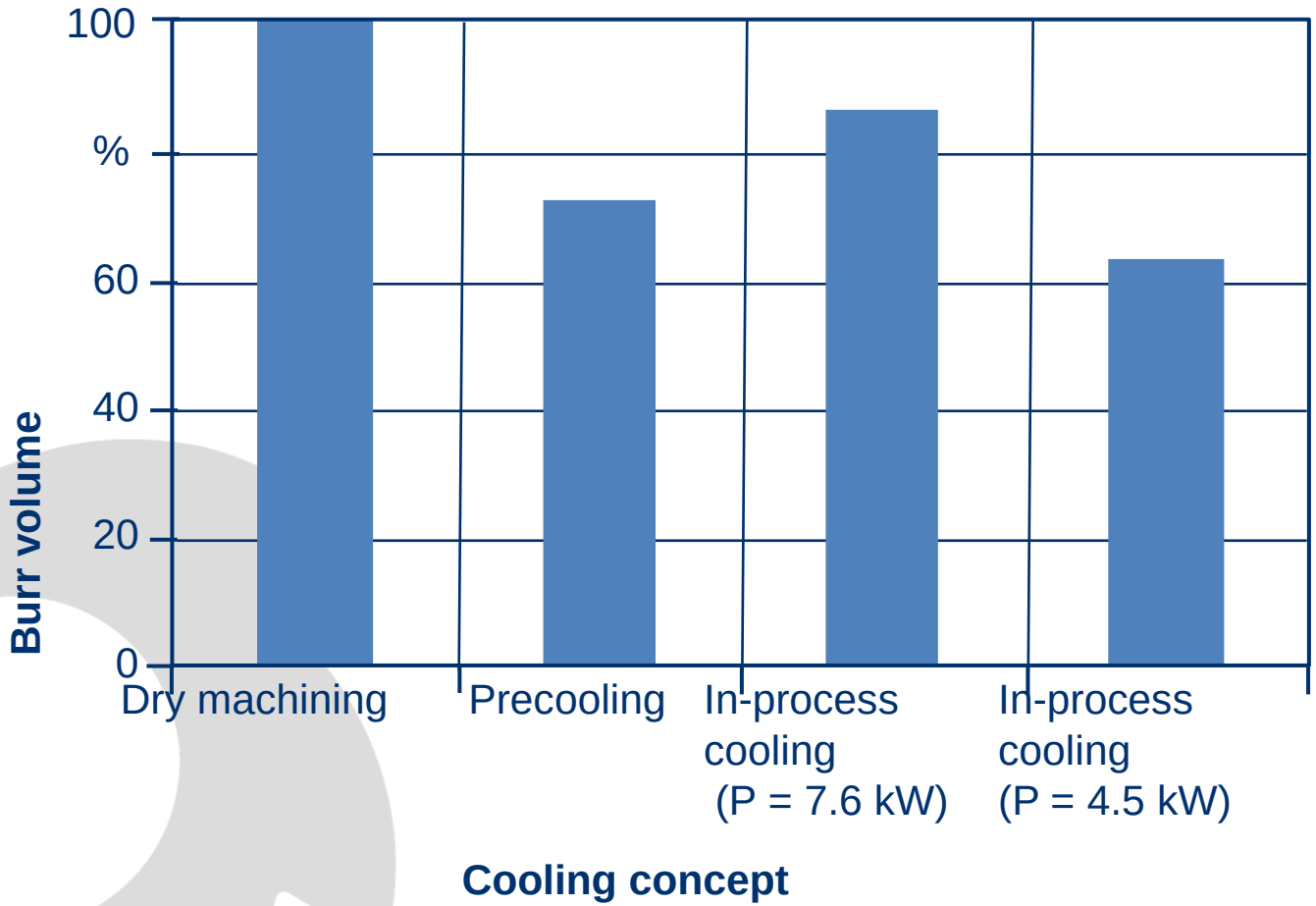

Burr Formation and Reduction in Machining Thin-Walled Light-Metal Frame Structures

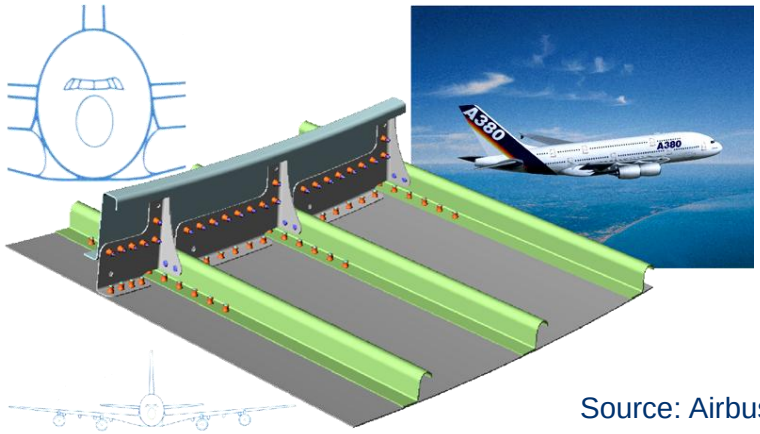

Source: Airbus

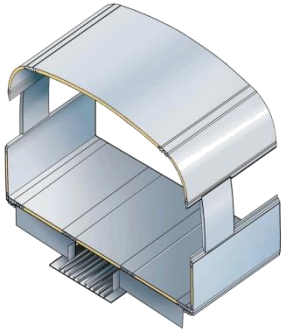

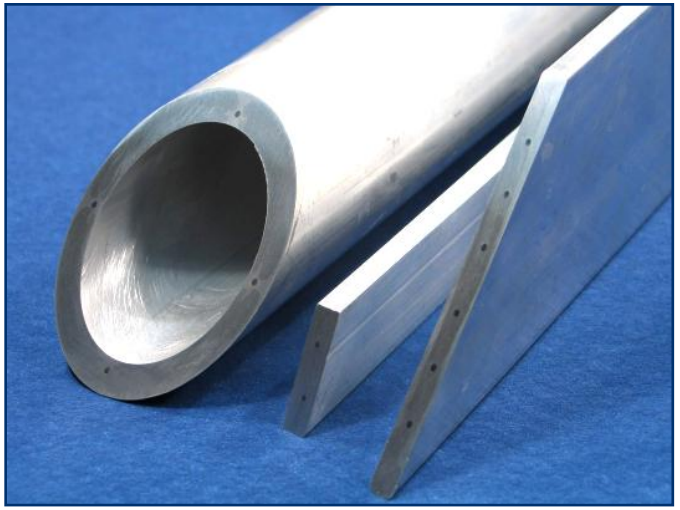

Source: Bombardier

Concept:

Source: IUL, Technische Universität Dortumund

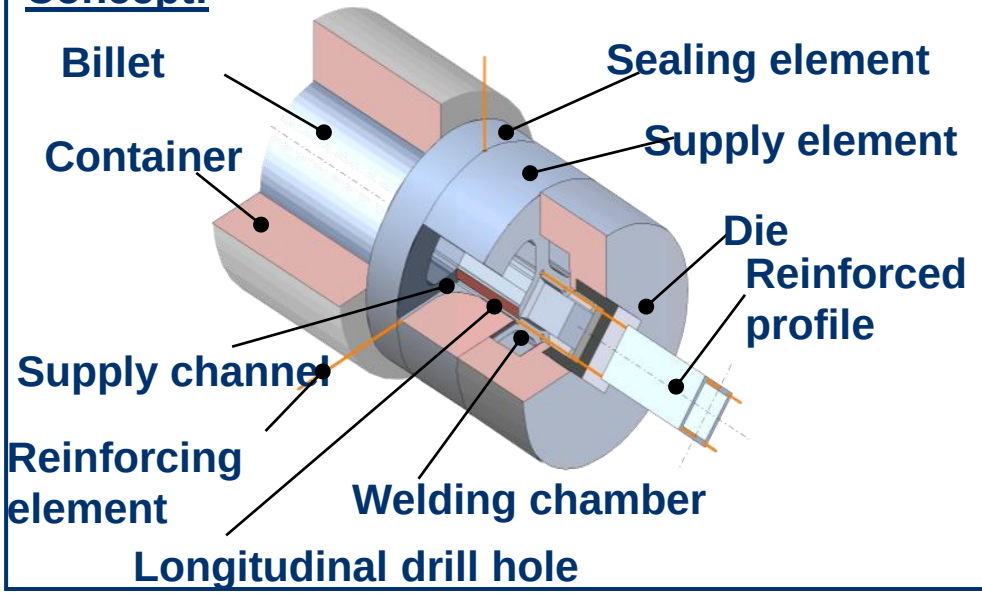

Burr Formation and Reduction in Machining Thin-Walled Light-Metal Frame Structures

Drilling:

Tool:	Twist drill
Cutting material:	HW-K30
Diameter:	d = 8.5 mm
Cutting speed:	v_c = 220 m/min
Feed:	f = 0.2 mm
Bore hole diameter:	d = 8.5 mm

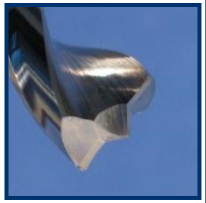

Orbital milling:

Tool:	End milling cutter
Cutting material:	HW
Diameter:	d = 5 mm
Cutting speed:	v_c = 375 m/min
Feed:	f = 0.024 mm
Depth of cut:	a_p = 4 mm
Bore hole diameter:	d = 8.5 mm

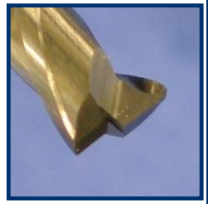

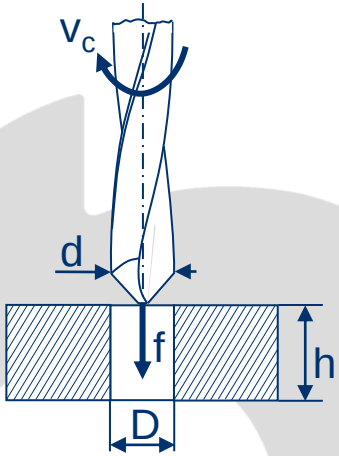

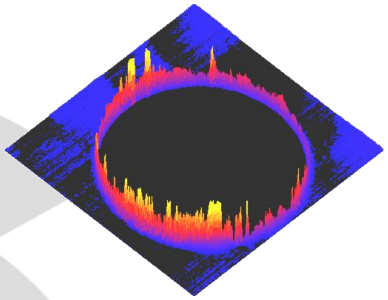

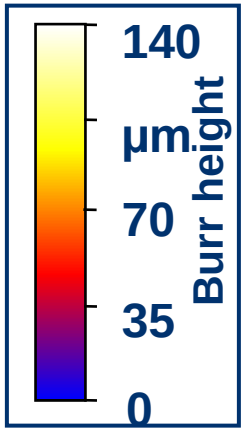

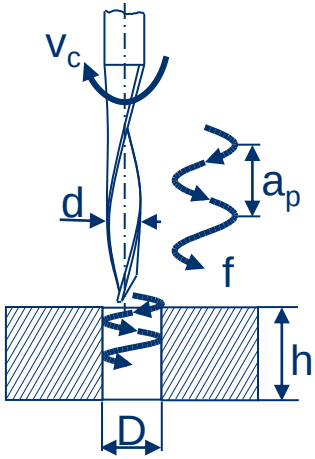

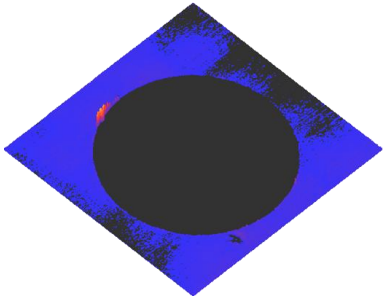

+ Short cutting time
+ Minimal machine tool requirements
+ Slight thermal influences on the workpiece

+ High flexibility
+ Favorable chip breakage and removal
+ Low axial and radial forces

Burr Formation and Reduction in Machining Thin-Walled Light-Metal Frame Structures

Workpiece material:	EN AW-6060	Cutting speed:	v_c	= 375 m/min
Reinforcement material:	1.4310 (X10CrNi18-8)	Feed:	f	= 0.05 mm
Reinforcment position:	Centrical	Depth of cut:	a_p	= 3 mm
Cooling concept:	MQL	Bore hole diameter:	D	= 8.5 mm
Cutting material:	HW-K20	Tool diameter:	d	= 5 mm

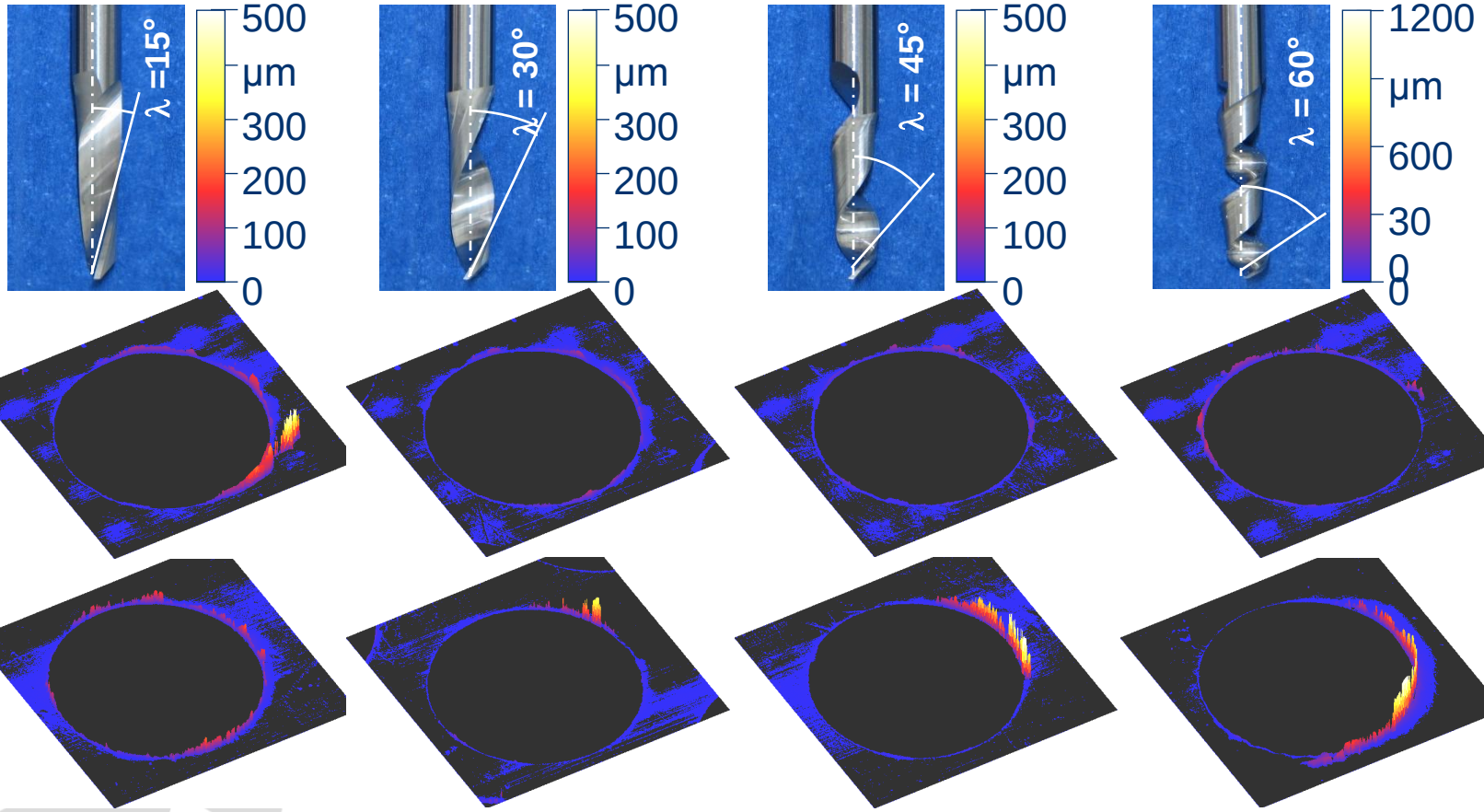

Delamination Reduction strategys in Machining Fiber-Reinforced Plastics

Advantages of reinforced polymer plastics

- Low density (1.6 g/cm^3)
- High stiffness
- Adequate fatigue strength
- Good damping
- High creep strength
- High corrosion resistance

Delamination Reduction strategys in Machining Fiber-Reinforced Plastics

Material:	Carbon fiber	Drilling tool:	Twist drill, d = 8 mm
Fabric type:	2.2 twist	Cutting material:	HW
Polymer matrix:	Epoxy resin	Cutting Speed:	v_c = 120 m/min
		Feed:	f = 0.15 mm

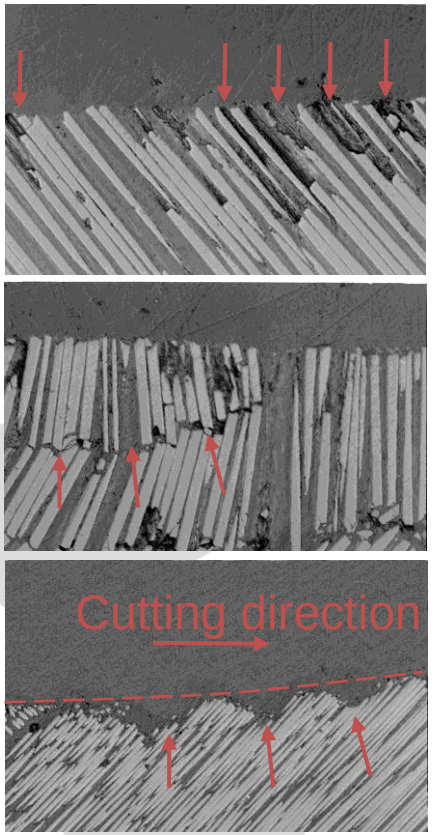

Fiber pull-outs

Delaminations

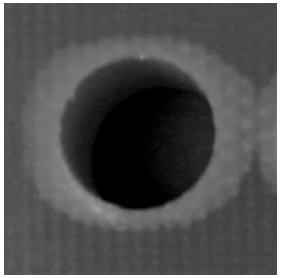

Fiber bundle cracks

Burr formation

Fiber bundle pull-outs

Break outs

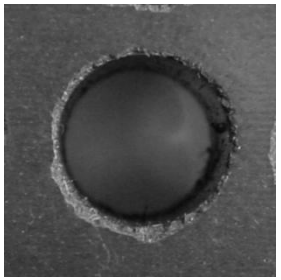

Negative effects on drill hole integrity

Delamination Reduction strategys in Machining Fiber-Reinforced Plastics

Material:	Carbon fiber	Tools:	Twist drill / end milling cutter
Fabric type:	2.2 twist	Diameter:	d = 8 mm / d = 5 mm
Cutting material:	HW –K10/ PCD	Cutting Speed:	v_c = 120 m/min / v_c = 60 m/min
Fiber volume:	70 %	Feed:	Varies
Polymer matrix:	Epoxy resin	Depth of cut:	Varies

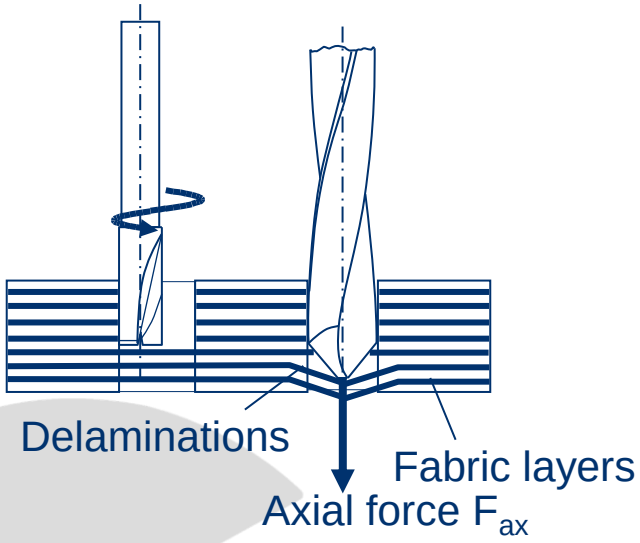

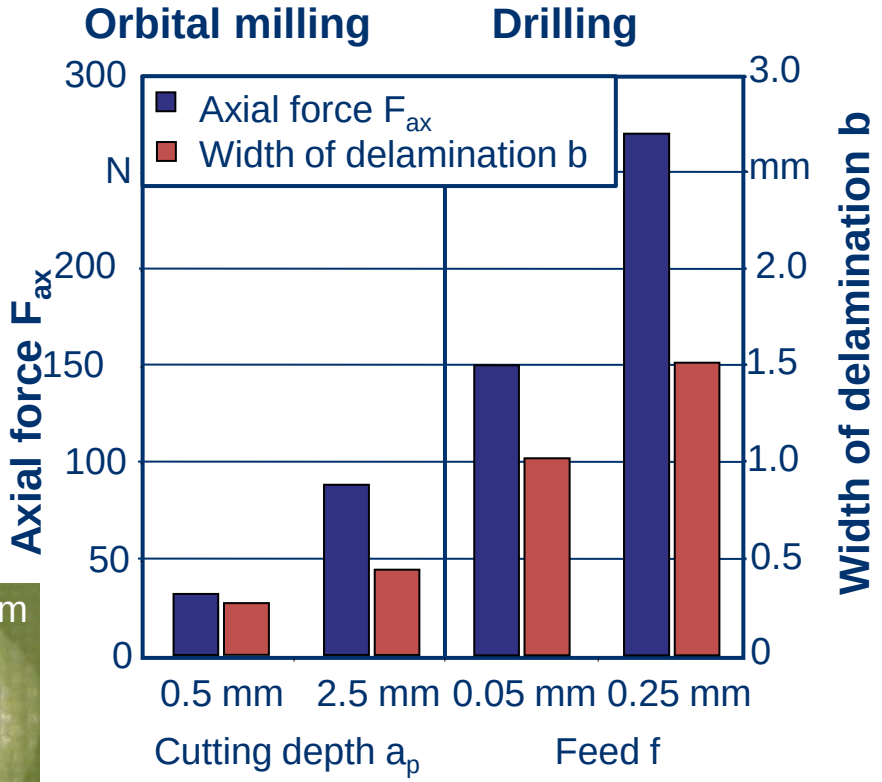

Orbital milling **Drilling**

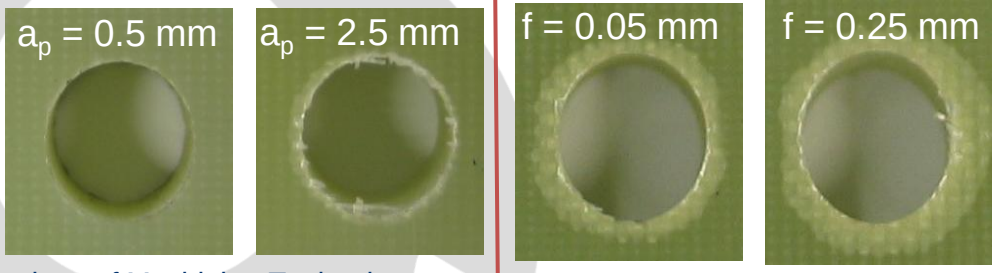

Burr Formation in Micro-milling of NiTi Alloys

Experimental set-up – Workpiece material

Material properties of β-NiTi (austenitic, pseudo-elastic)

Chemical composition		
Ni	at.-%	49.4
Ti	at.-%	50.6

Properties

- Fatigue resistance
- Damping
- Wear resistance
- Biocompatibility

Flexible picker arm

Tissue spreader

Memory-Metalle GmbH

Mechanical Properties
Tensile strength R_m: 707 MPa
Elongation at fracture δ_B: 20.1 %

Stent

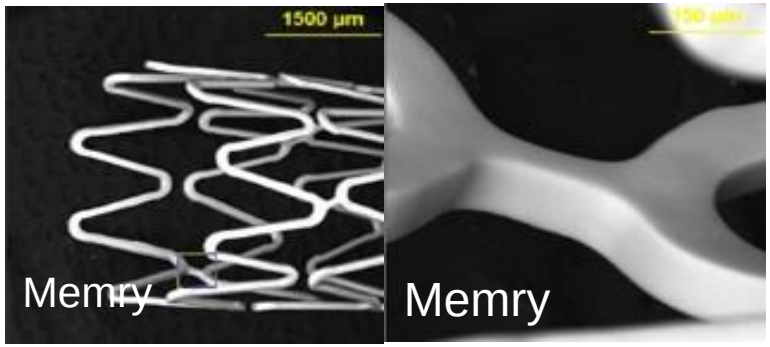

Burr Formation in Micro-milling of NiTi Alloys

Material:	β-NiTi	Cutting Speed:	v_c = 33 m/min
Tool:	End mill, d = 0.4 mm	Feed per tooth:	f_z = 12 µm
Cutting material:	HW (UF)	Depth of cut:	Varies
Coating:	TiAlN	Pocket width:	B = 0.8 mm
Cooling concept:	MQL	Pocket length:	l = 10 mm

a_p = 10 µm / a_e = 10 µm

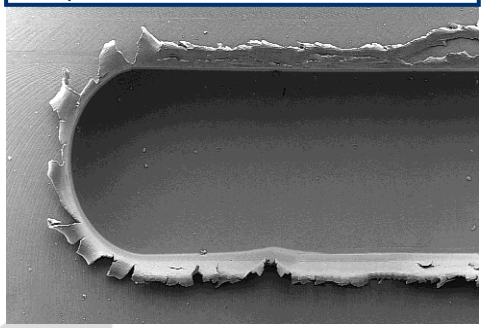

a_p = 20 µm / a_e = 20 µm

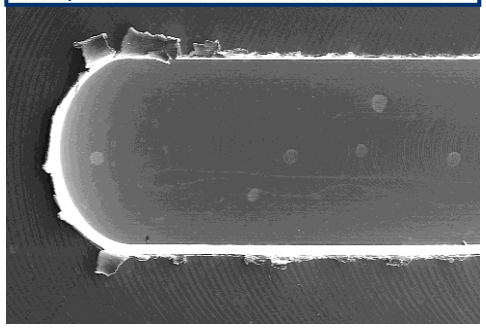

a_p = 40 µm / a_e = 40 µm

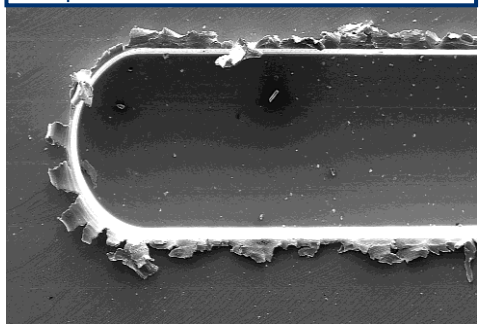

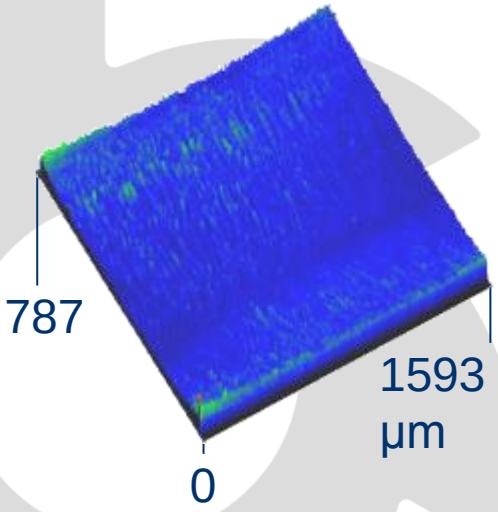

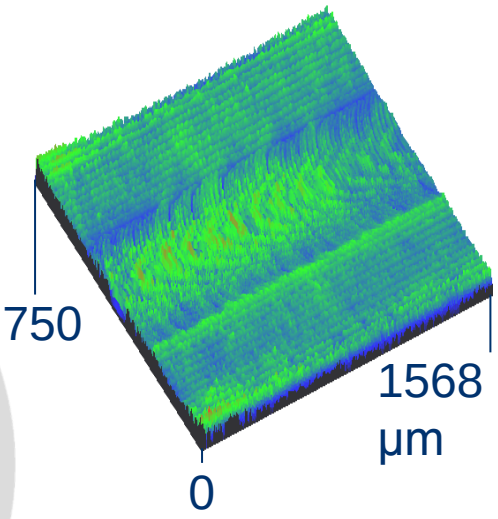

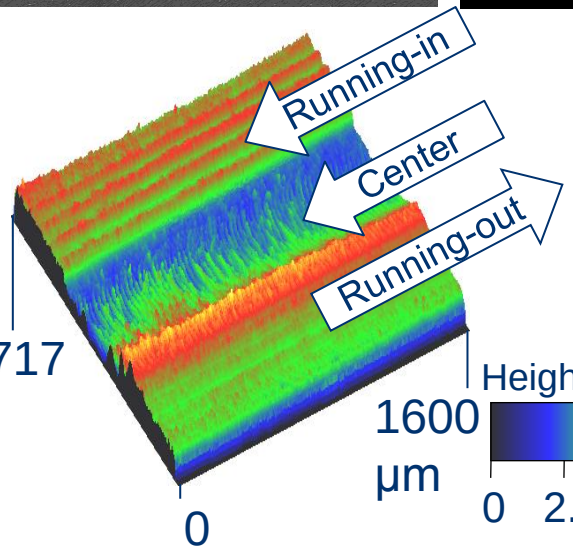

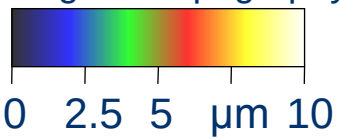

Burr Formation in Micro-milling of NiTi Alloys

	Workpiece surface	Tool side view	Surface topography
$\beta_f = 50°$	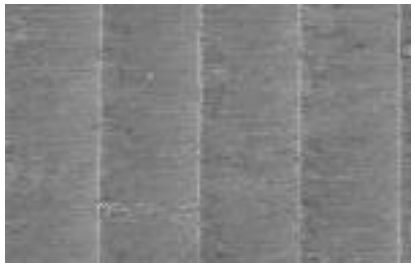	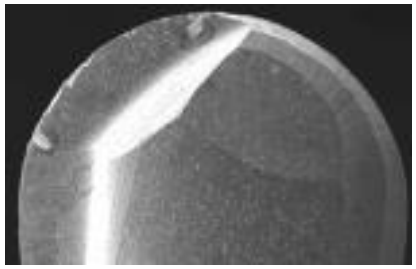	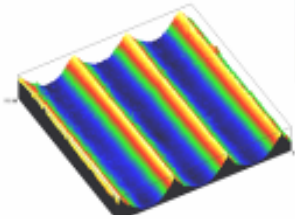
$\beta_f = -50°$	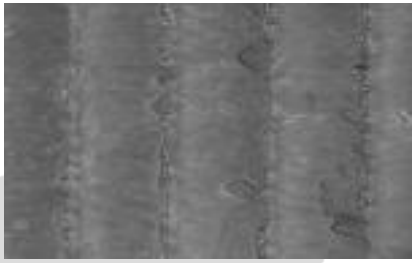	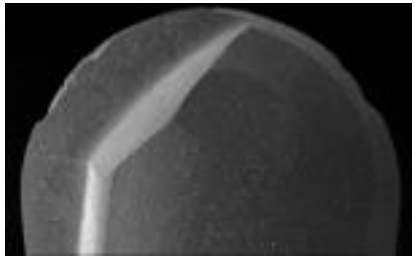	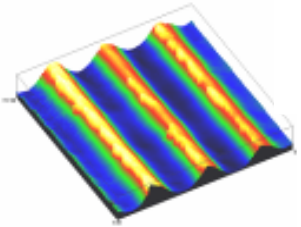
$\beta_{fN} = 50°$	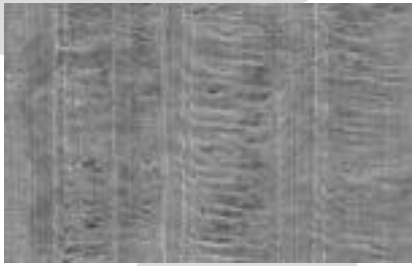	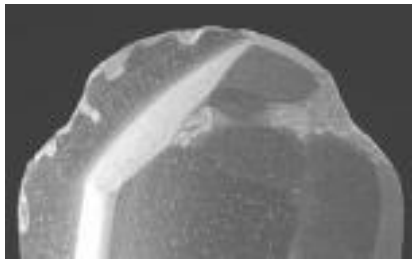	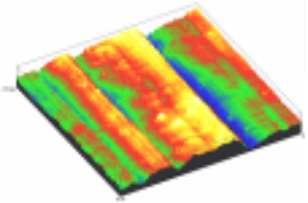

Tool: d = 1 mm

Milling strategy:
Down-milling

Material:
Austenitic NiTi

Cutting data:

v_c	= 47 m/min
a_e	= 0.25 mm
a_p	= 0,10 mm
f_z	= 0.006 mm
V_z	= 20 mm³

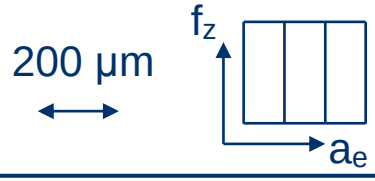

Burr Formation in Micro-milling of NiTi Alloys

$\beta_f = 50°$

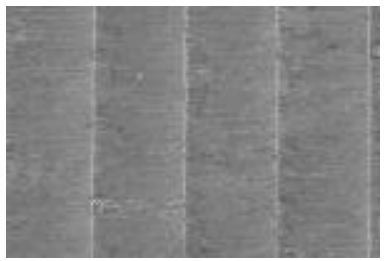

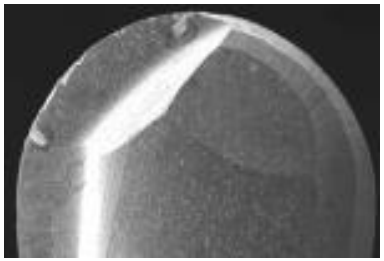

$\beta_{fN} = 50°$

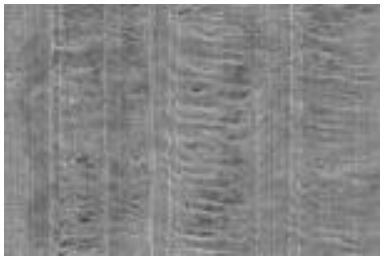

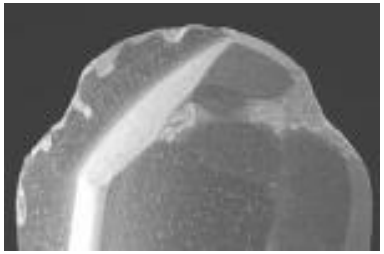

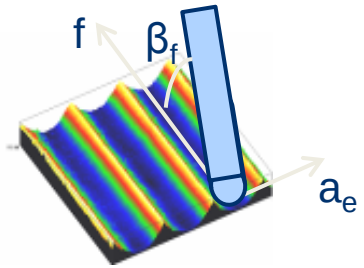

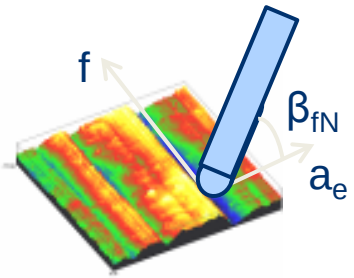

Cutting data:

v_c = 47 m/min
a_e = 0.25 mm
a_p = 0.10 mm
f_z = 0.006 mm
V_z = 20 mm³

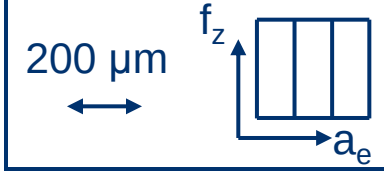

Transfer of experimental results into simulation:

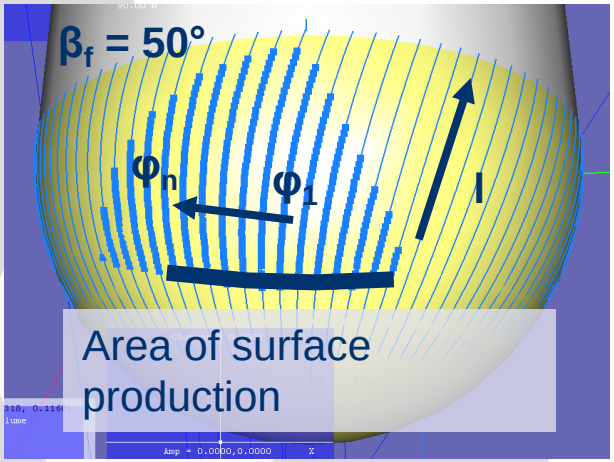

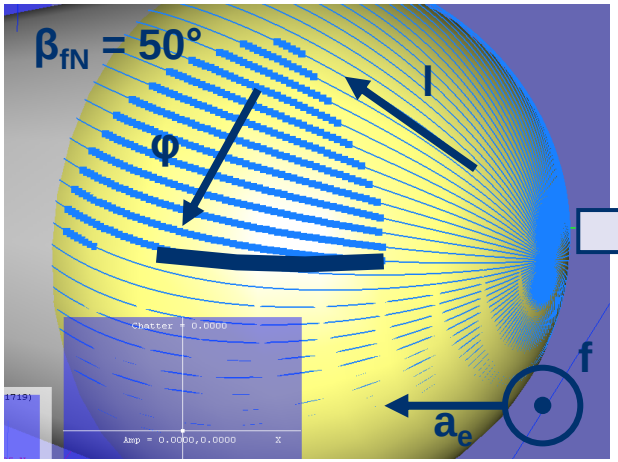

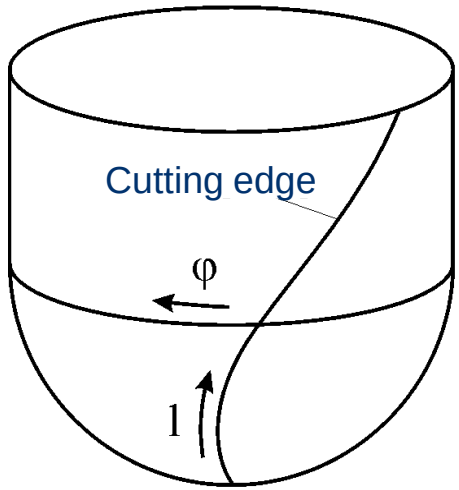

Burr Formation in Micro-milling of NiTi Alloys

$\beta_f = 50°$

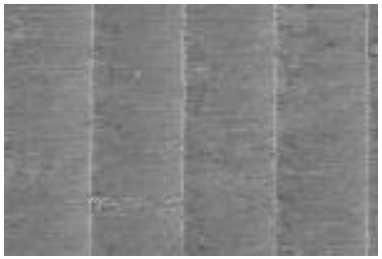

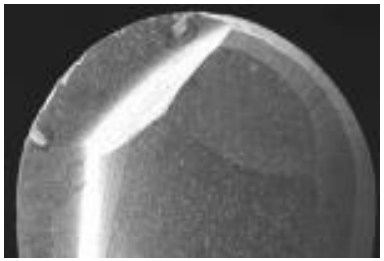

$\beta_{fN} = 50°$

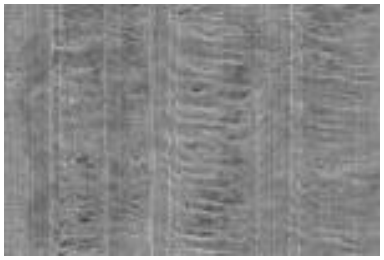

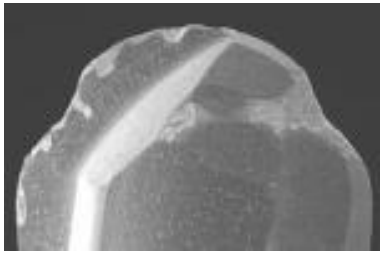

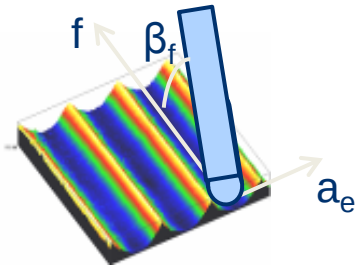

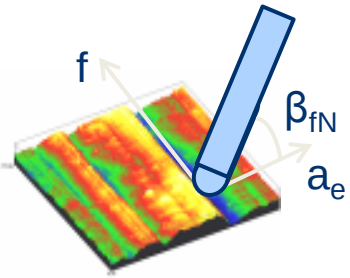

Cutting data:

v_c = 47 m/min
a_e = 0.25 mm
a_p = 0.10 mm
f_z = 0.006 mm
V_z = 20 mm³

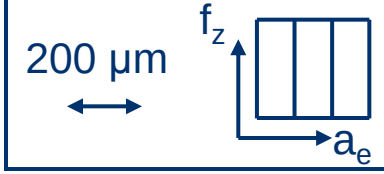

Transfer of experimental results into simulation:
with display of cutting edge kinematics:

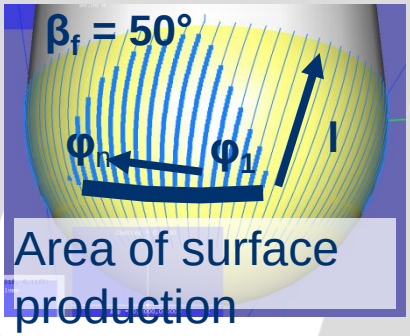

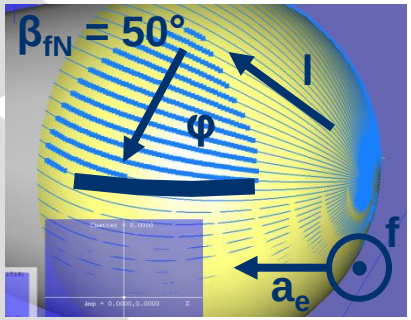

Optimization of β_f – adjustment (no contact of the tool center)

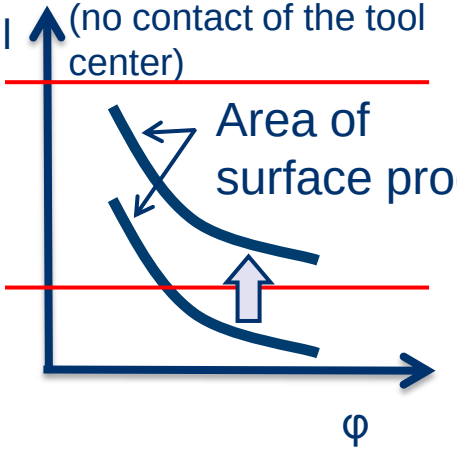

Optimization of the slope (adjustment of the NC-angle, avoidance of β_{fN})

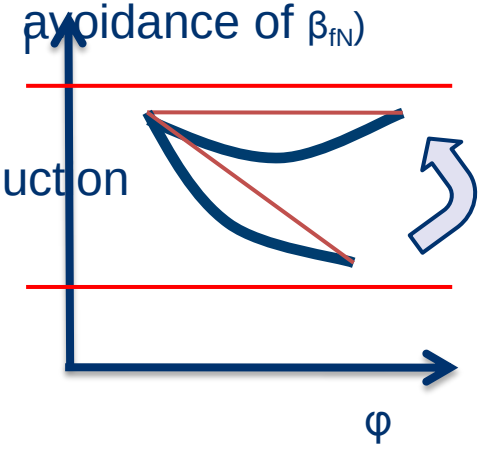

Summary

Burr Formation and Reduction Strategy in Turning Austenitic-Ferritic Stainless Steel

- The use of a carbon dioxide cooling leads to significant burr reduction and minimized adhesive tool wear as well as minimized notch wear.

CO_2 Process Cooling for Burr Reduction in Face Milling of Aluminum Alloys

- The cooling of the exit edge of the workpiece leads to a significant reduction in burr formation.

Burr Formation and Reduction in Machining Thin-Walled Light-Metal Frame Structures

- In comparison to drilling, orbital milling has advantages with respect to its flexibility, chip formation and bore hole quality.
- The helical angle has an influence both on the entry and on the exit burr.

Delamination Reduction strategys in Machining Fiber-Reinforced Plastics

- The reduction of axial forces causes a significant reduction in delamination.

Burr Formation in Micro-milling of NiTi Alloys

- In 5-axis-milling of NiTi shape memory alloys, the tool inclination angle has an influence on burr formation on the tips in direction of the previously machined paths.

Overview

Introduction

Burr Minimization strategies in Machining Operations

Micro-finishing of hard coated parts

Detection of grinding burn and cracks by acoustic emission

FEM in Internal Traverse Grinding

Machining of low-sulfur steels

Influence of coated surfaces on friction coefficients

Machining of β-titanium alloys

Waviness reduction

Simulation strategies

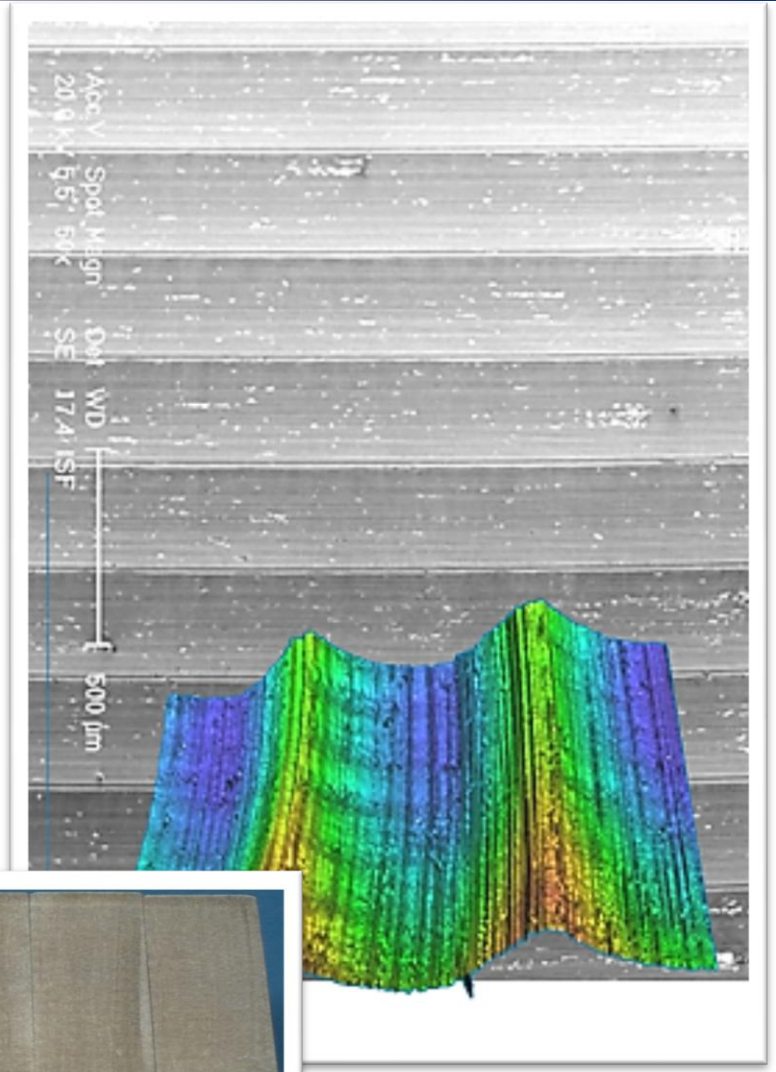

Microfinishing alias short-stroke honing

Process kinematics honing

Following german standard DIN 8589-14

- Abrasive process
- Multi-grain tool with two cutting motions
- Characteristics are the kind of cutting movement (long- and short stroke) and the processing point at the workpiece (internal, external)

External-cylindrical-shortstroke-honing

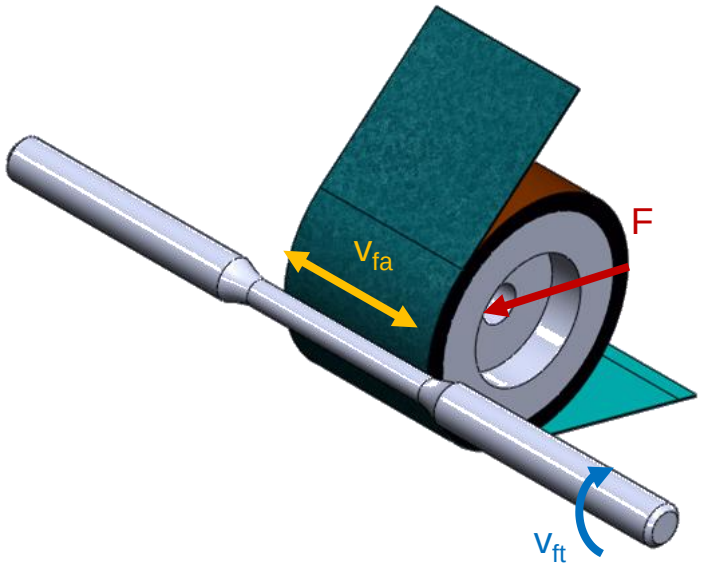

F = Force controlled infeed
v_{ft} = Tangential velocity
v_{fa} = Axial velocity

Tool machines

Lathe – MAG Boehringer M670

- Engine output P = 11…25kW
- Rotational speed range n = 7,1…1400 min^{-1}
- Feed range f = 0,04…2,8 mm/U

Finish equipment – Supfina 202

- Oscillation power P = 0,37 kW
- Oscillation frequency f_{os} = 2…21 Hz
- Amplitude range S = 0…5 mm
- Belt infeed velocity v_B = 0…64 mm/min
- Pressure p_n = variable

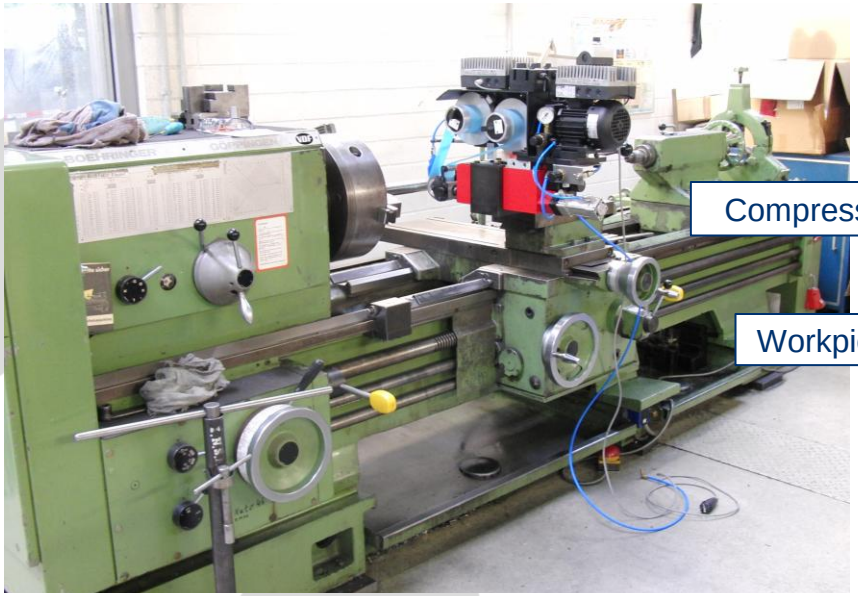

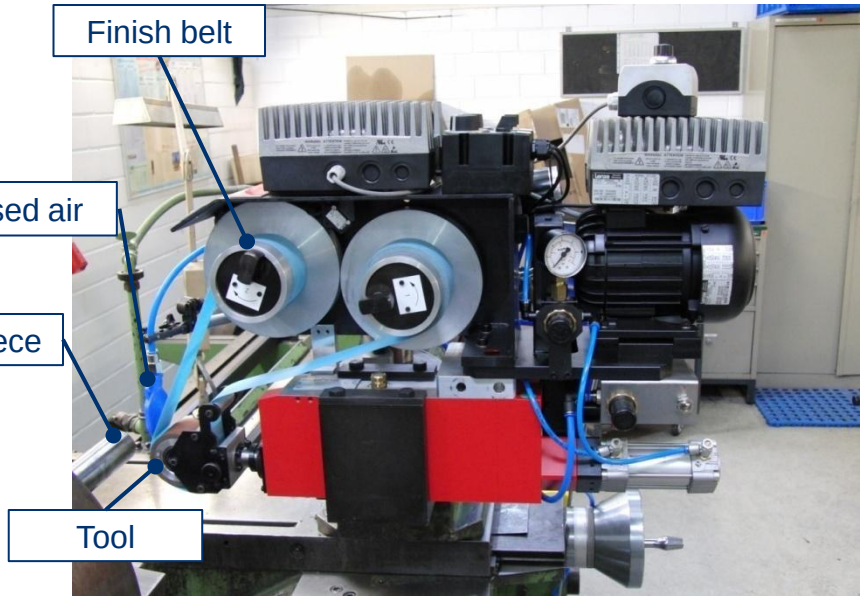

Tools

Press roll

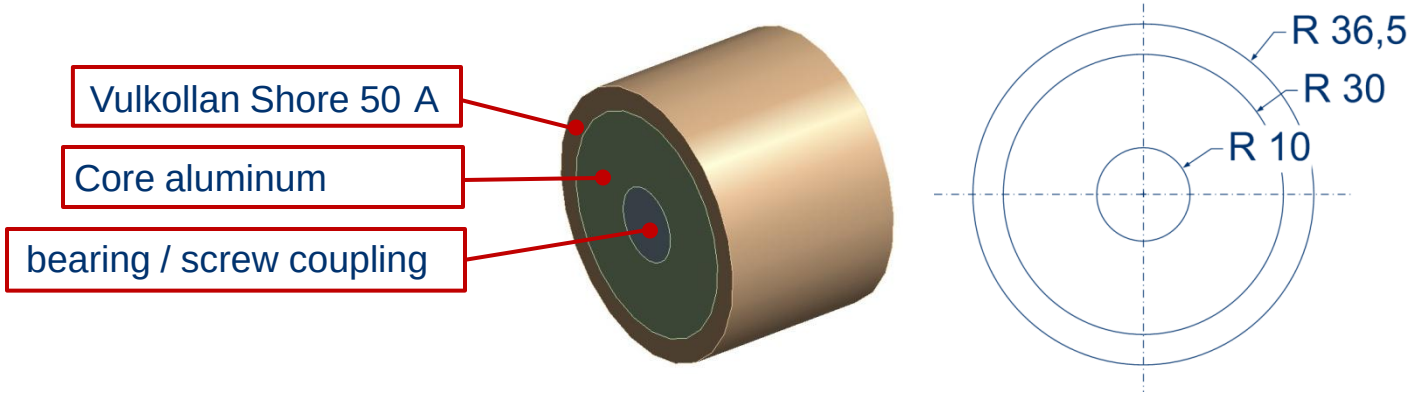

Finishbelt

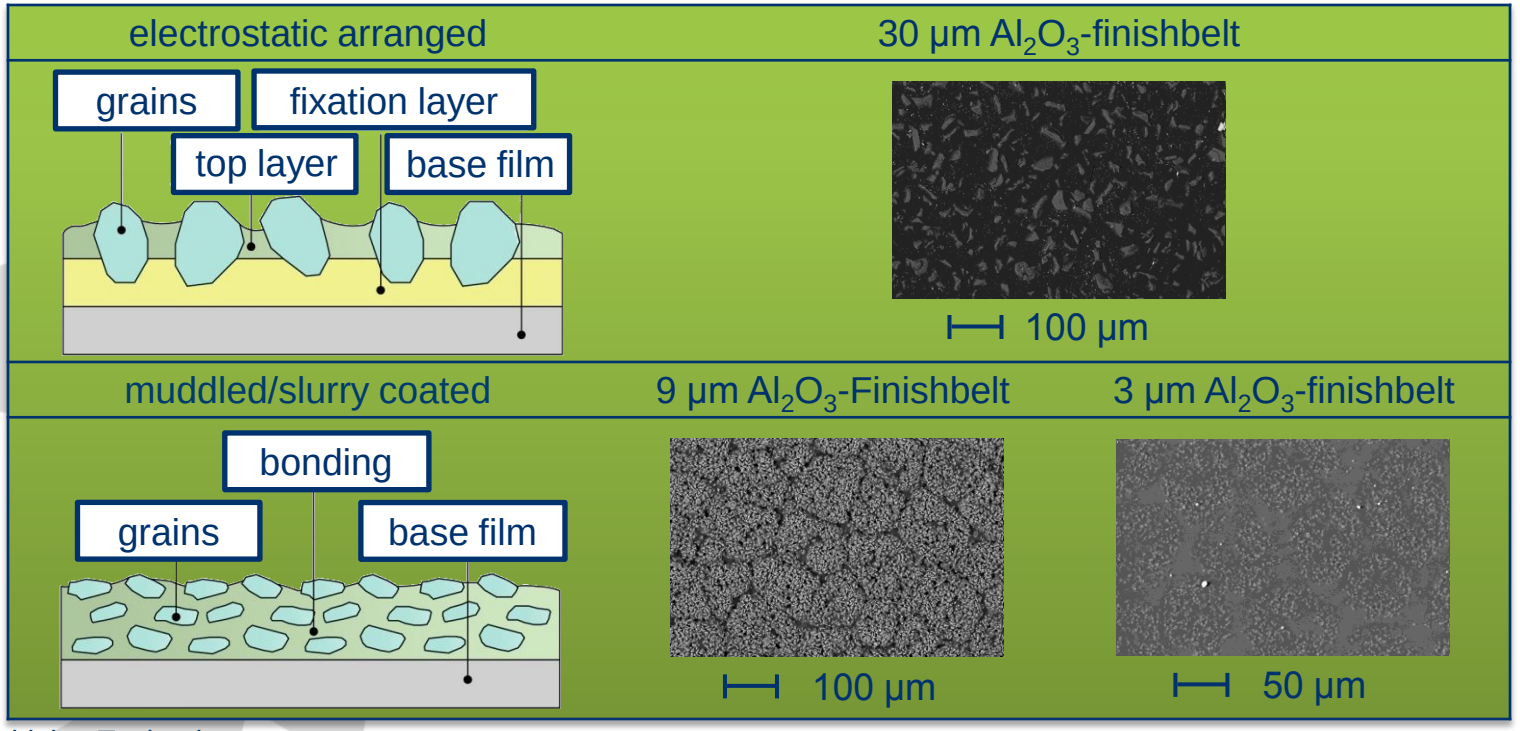

Project idea

- **Displace hard chromate plating** under
  - ⇒ Improvements of technological properties of the coating system and
  - ⇒ Reduction of the manufacturing costs

- **Solution approach:**
  - ⇒ Using multilayer-coating-systems made of thermal sprayed carbide-including layer and a DLC (Diamond-like-Carbon) top layer.
  - ⇒ Usage of new coating applications: Nano HVOF (high velocity oxygen fuel), FP PVD (focused plasma physical vapour deposition)
  - ⇒ Determination of process strategys to machine the carrier material and the HVOF-coating.

- **Project aim:**
  - ⇒ Development, qualification, machining and illustration of tribology-optimized high performance coatings

FE-Simulation loading cases

Meshing

- Fine meshing (l_e = 1 mm)
- Mid-level mashing (l_e = 2 mm)
- Rough meshing(l_e = 4 mm)

l_e – maximal elementsize
b_{wz} – width push roll
b_{ws} – width workpiece

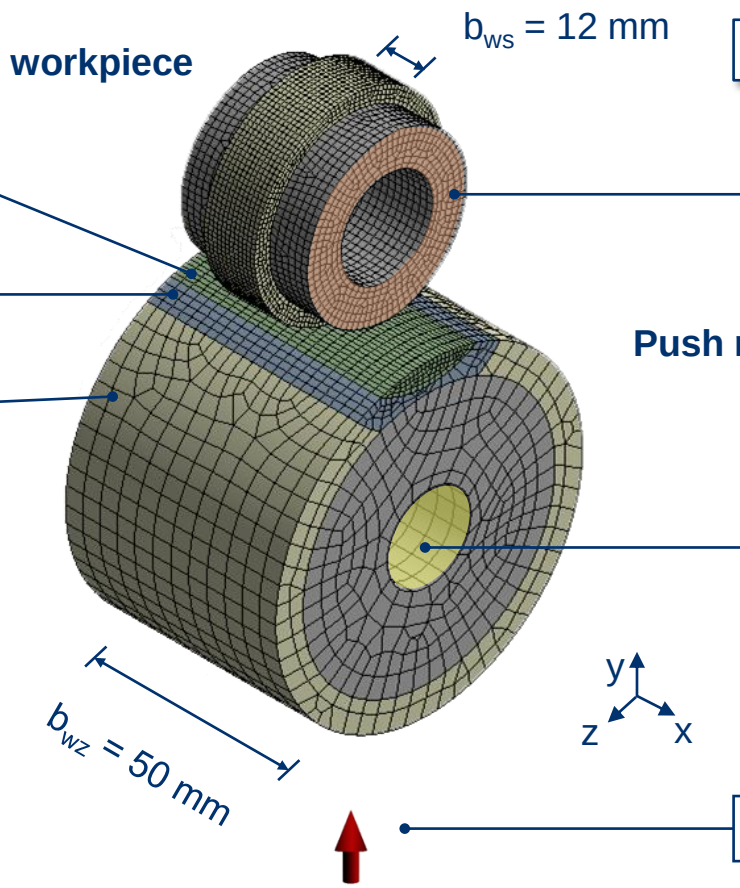

Boundary conditions

- Rotational bearing
- Fixed cylindrical bearing
- Push force F = 600 N

Analysis

- Deformation u_y of the tool
- Normal stress σ_n between tool und workpiece

Loading cases

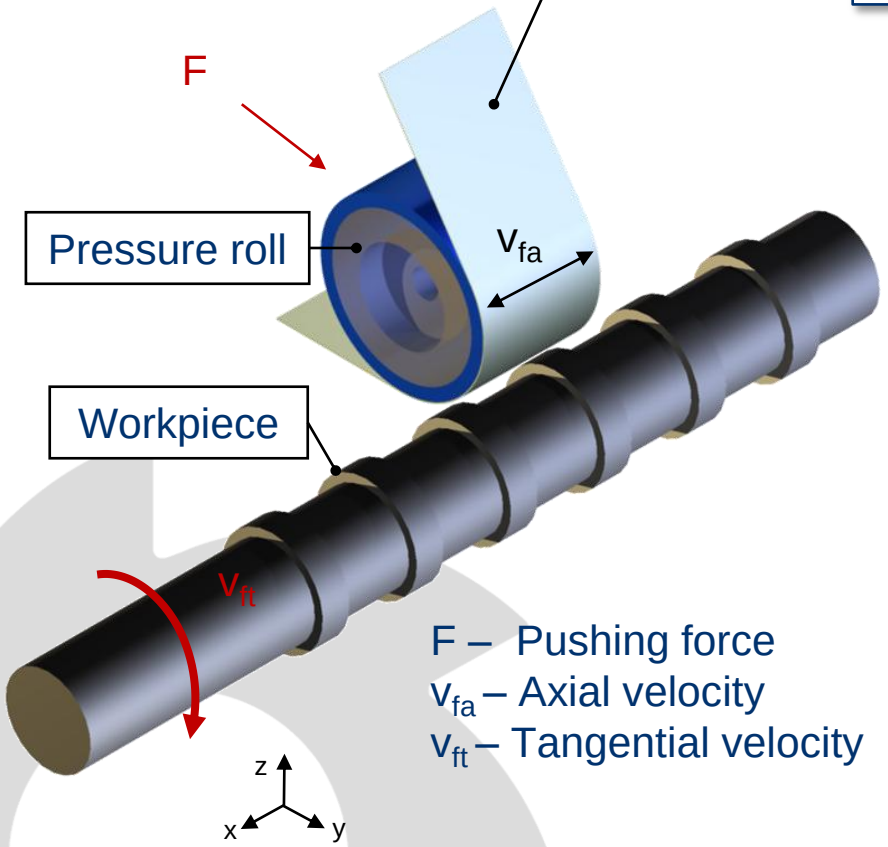

F – Pushing force
v_{fa} – Axial velocity
v_{ft} – Tangential velocity

Tool wider than workpiece

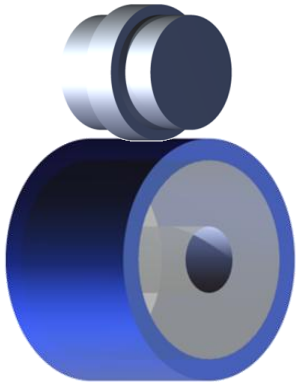

Tool and workpiece equal wide

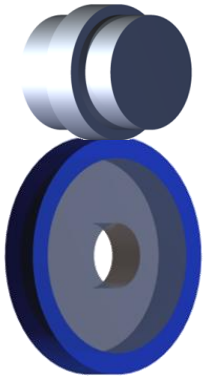

Tool slimmer than workpiece

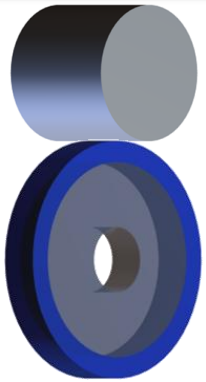

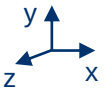

Load case
„tool width larger than workpiece width“

Displacement u_y on the tool

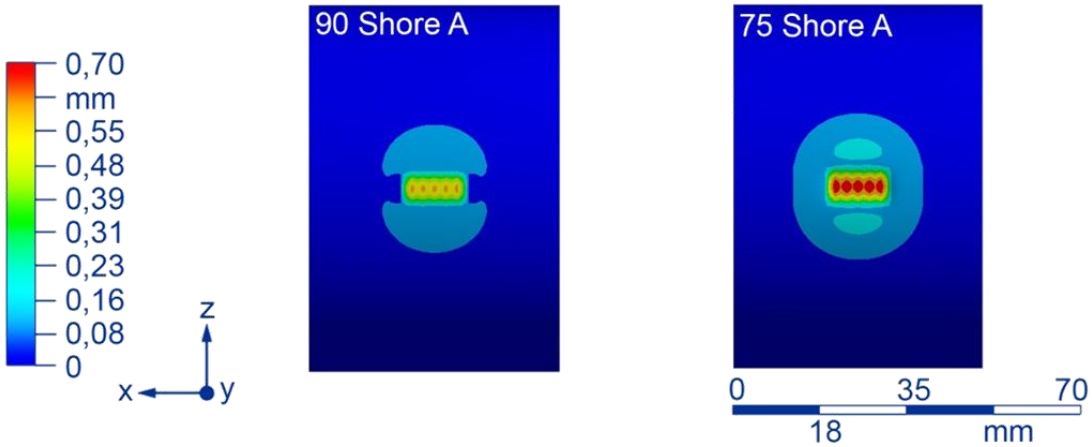

Principal stress σ_n on the workpiece

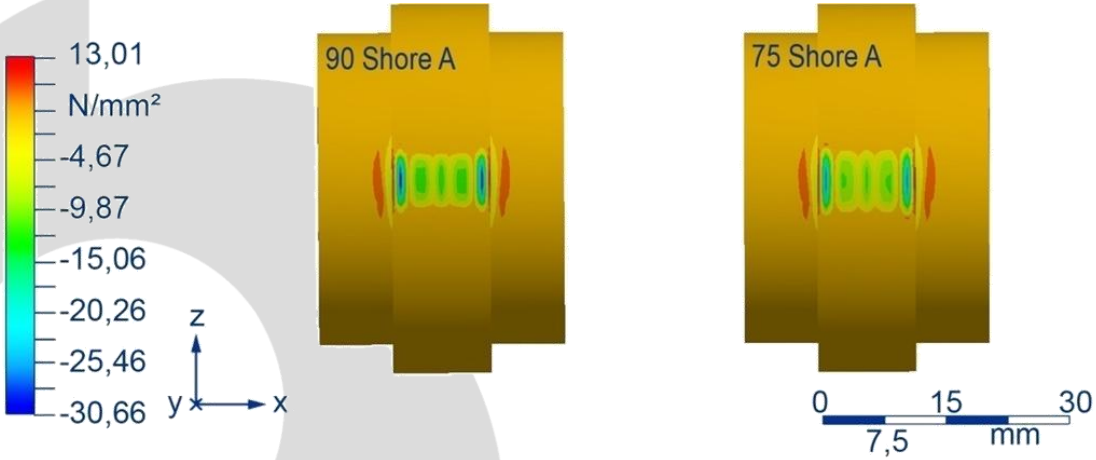

Push roll

Vulkollan 75/90 Shore A

Push force

F = 600 N

Simulation results

Max. displacement

u_y = 0,7 mm at 75 Shore A
$\Rightarrow$ wrap around angle α_u = 28,7°

u_y = 0,58 mm at 90 Shore A
$\Rightarrow$ wrap around angle α_u = 25,8°

Max. compressive stress

σ_n = 30,66 N/mm² bei 90 Shore A
σ_n = 27,31 N/mm² bei 75 Shore A

Validation by pressure films

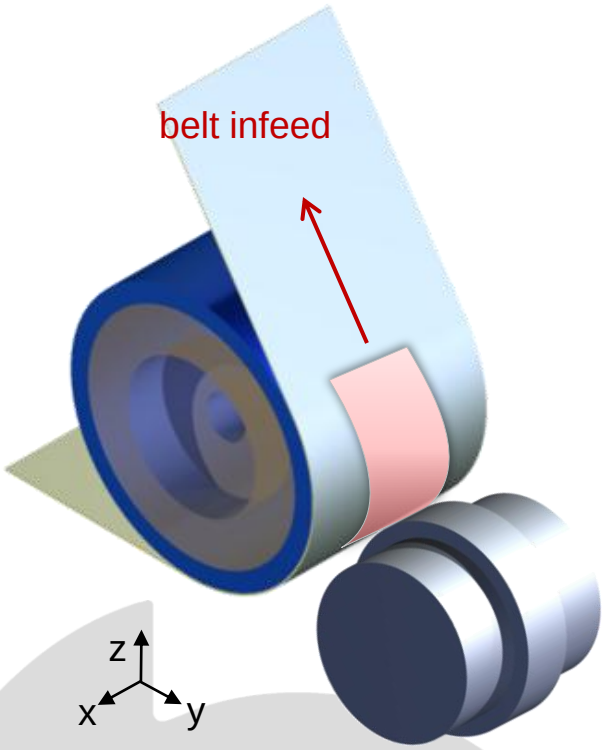

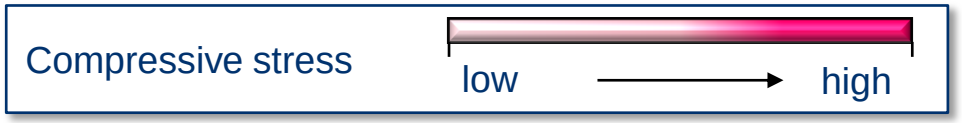

Pressure film: mid-level pressure

Pressure film: low pressure

Due to the low strength of the toolmaterial increases the contact pressure per unit area at the edge of the shaft shoulder

⇒ Confirmation of the simulation results
⇒ unsteady wear behaviour of the finishbelt possible

Formgenauigkeit

Material	Abrasive	Grain size	Force	Cutting speed v_c
42CrMo4 QT	Al_2O_3	d_K = 30; 9; 3 µm	F = 240…360 N	v_c = 21,2 m/min

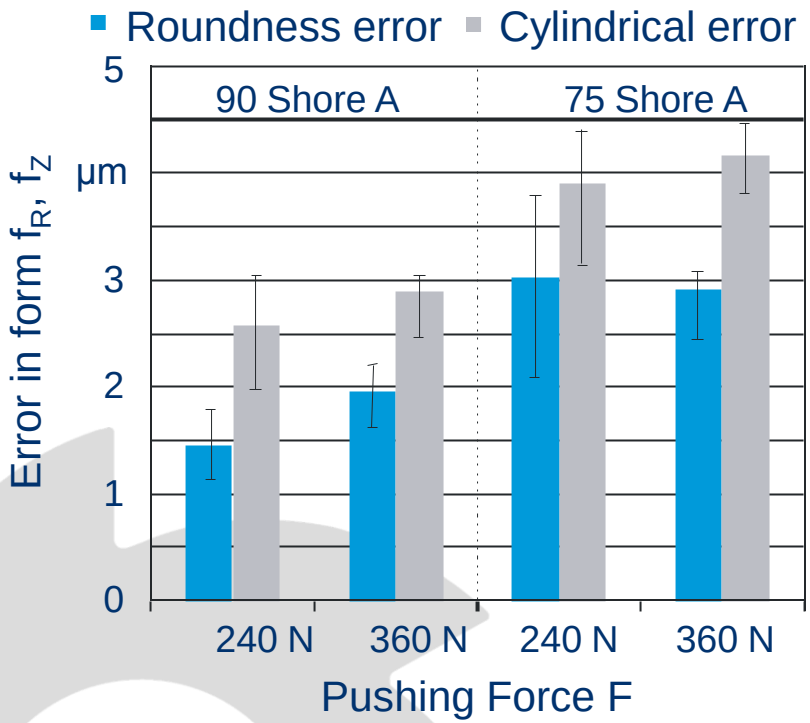

3D-model of the cylindrical form

90 Shore A

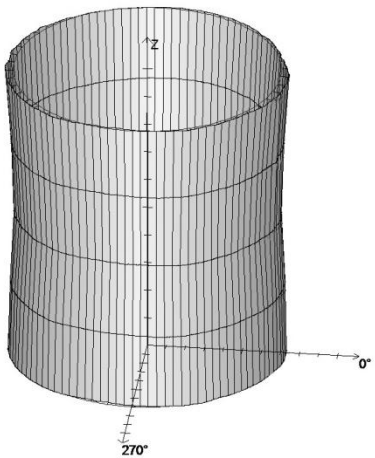

75 Shore A

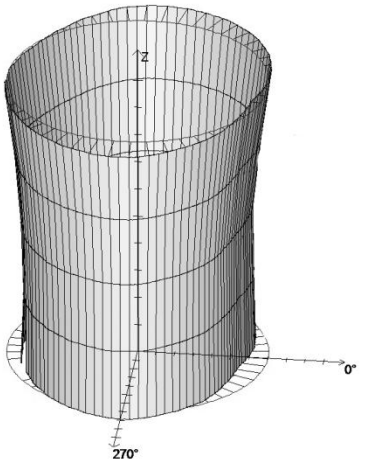

- Due to higher pushing forces increases the error in form for both tested materials
- Low tool material strength results in an adaption of the tool form with the workpiece form

Carrier material preconditioning

Aim: Substitution of blasting process by 3-step finishing process

Elektrostatic arranged

d_K = 30 µm Al_2O_3

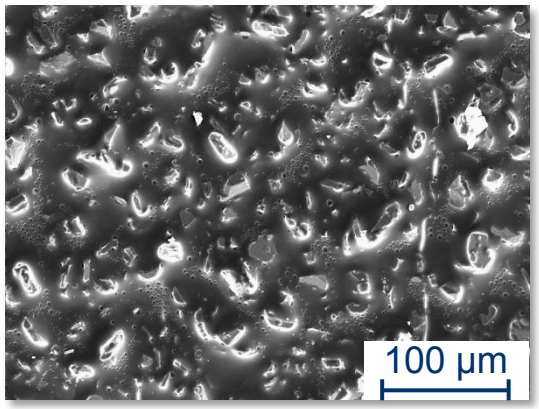

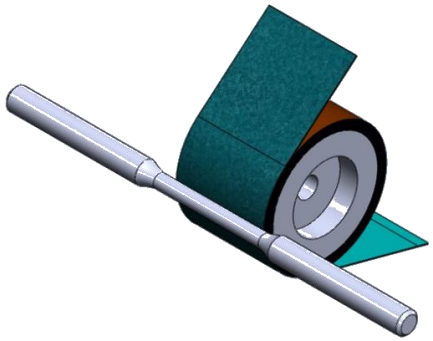

Carrier material
Rotation beding specimens
Material: 100Cr6
Hardness: 250 ± 10 HV0,1

3 process steps with different grain sizes

Muddled/slurry coated

d_K = 30 µm Al_2O_3

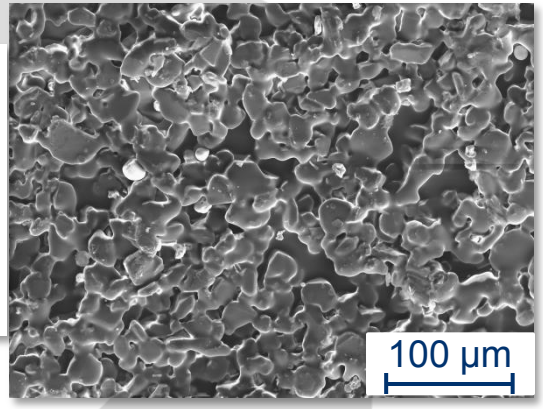

d_K = 9 µm Al_2O_3

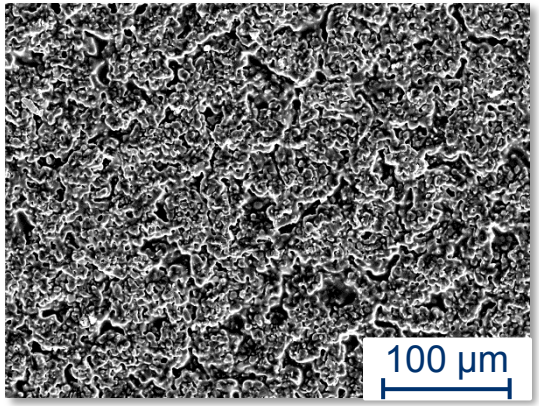

d_K = 3 µm Al_2O_3

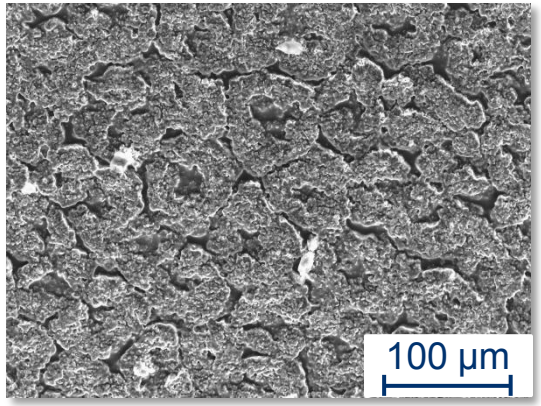

Surface quality carrier material

Material	Abrasive	Grain size	Force	Process time
100Cr6	Al_2O_3	d_K = 30; 9; 3 µm	F (30 µm) = 120 N F (9; 3 µm) = 60 N	t = 20 s t_{ges} = 60 s

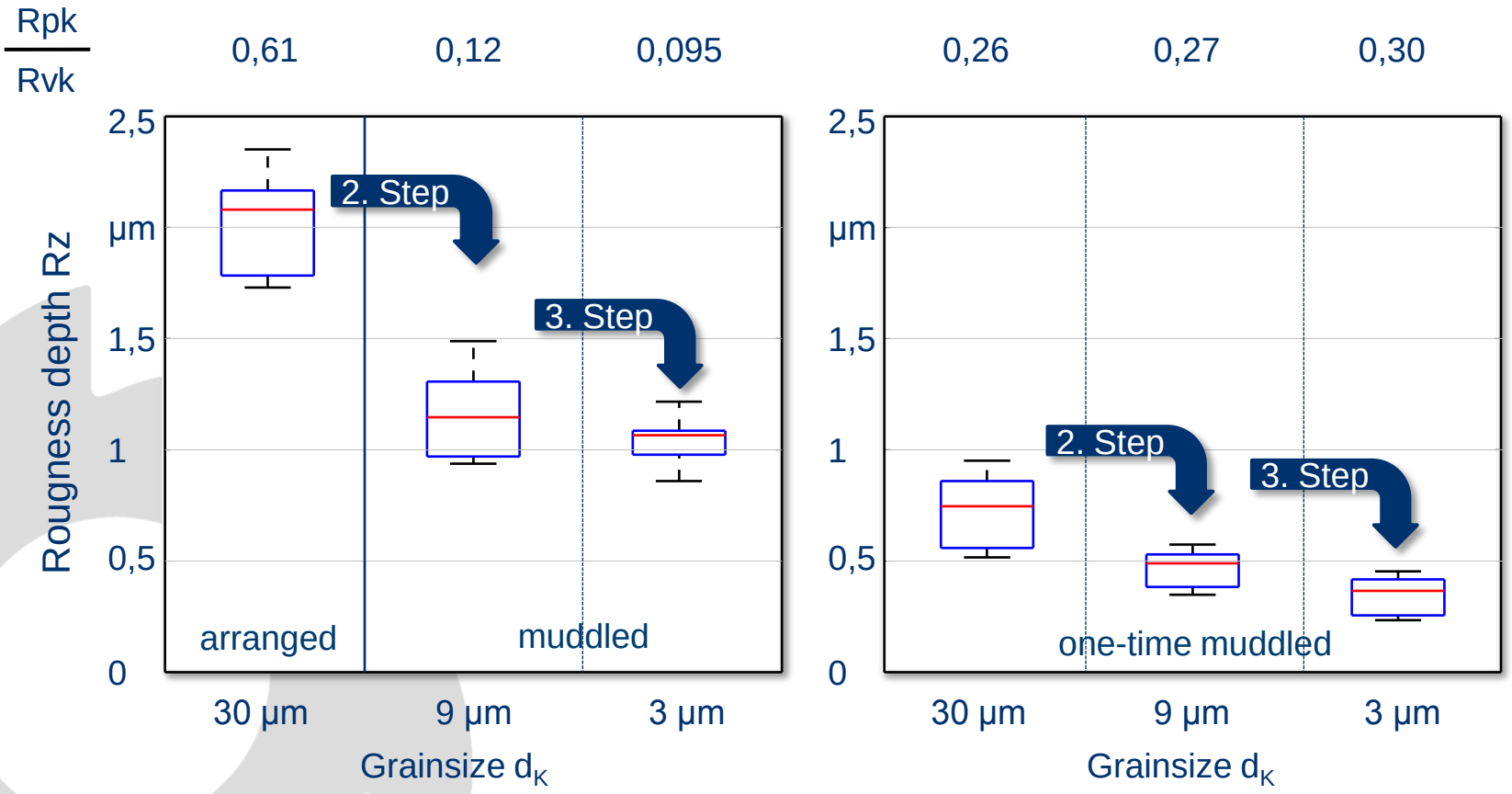

Surface roughness carrier material

Grinding

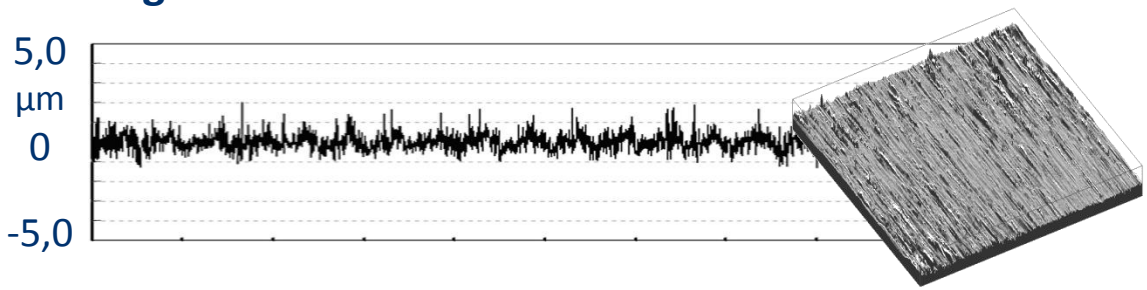

3-step finish process

first step with elektrostatic arranged finishbelt

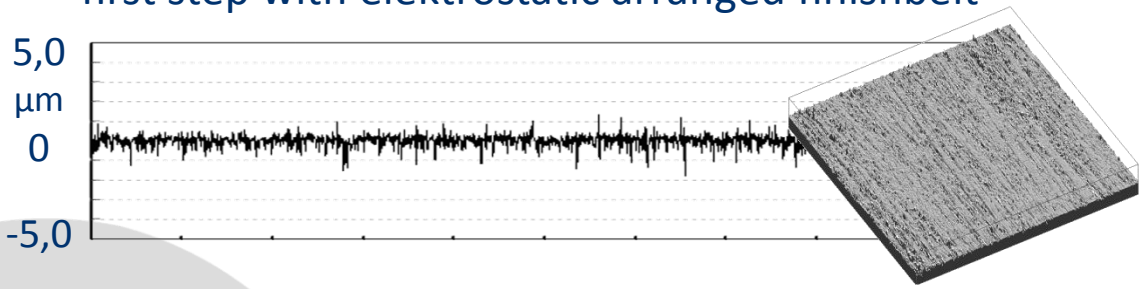

3-step finish process

first step with muddled finishbelt

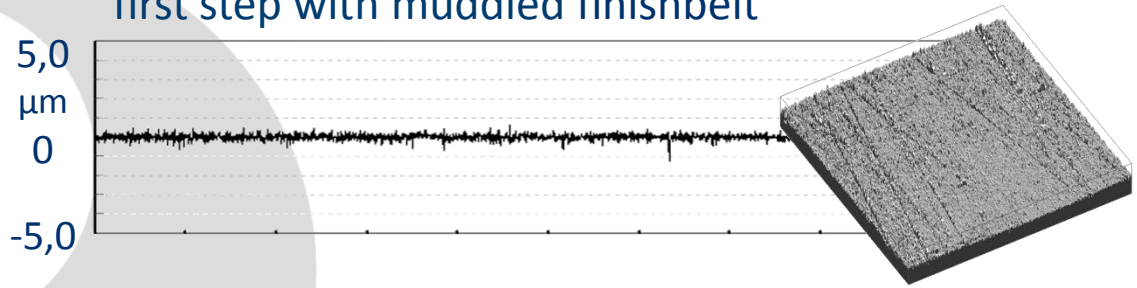

R-Profil

λ_c = 0,800 mm

L_t = 4,80 mm

Press roll

Vulkollan 50 Shore A

Force

F (30 µm) = 120 N

F (9 µm) = 60 N

F (3 µm) = 60 N

Tangential velocity

v_t = 10,2…20,4 m/min

Finish belt

30 – 9 – 3 µm Al_2O_3

Belt infeed: v_B = 45 mm/min

Oscillation

Frequency: f = 10 Hz

Amplitude: S = 5 mm

Interface carrier material-coating

Finished carrier material | Finished and coated | Blasting and coating

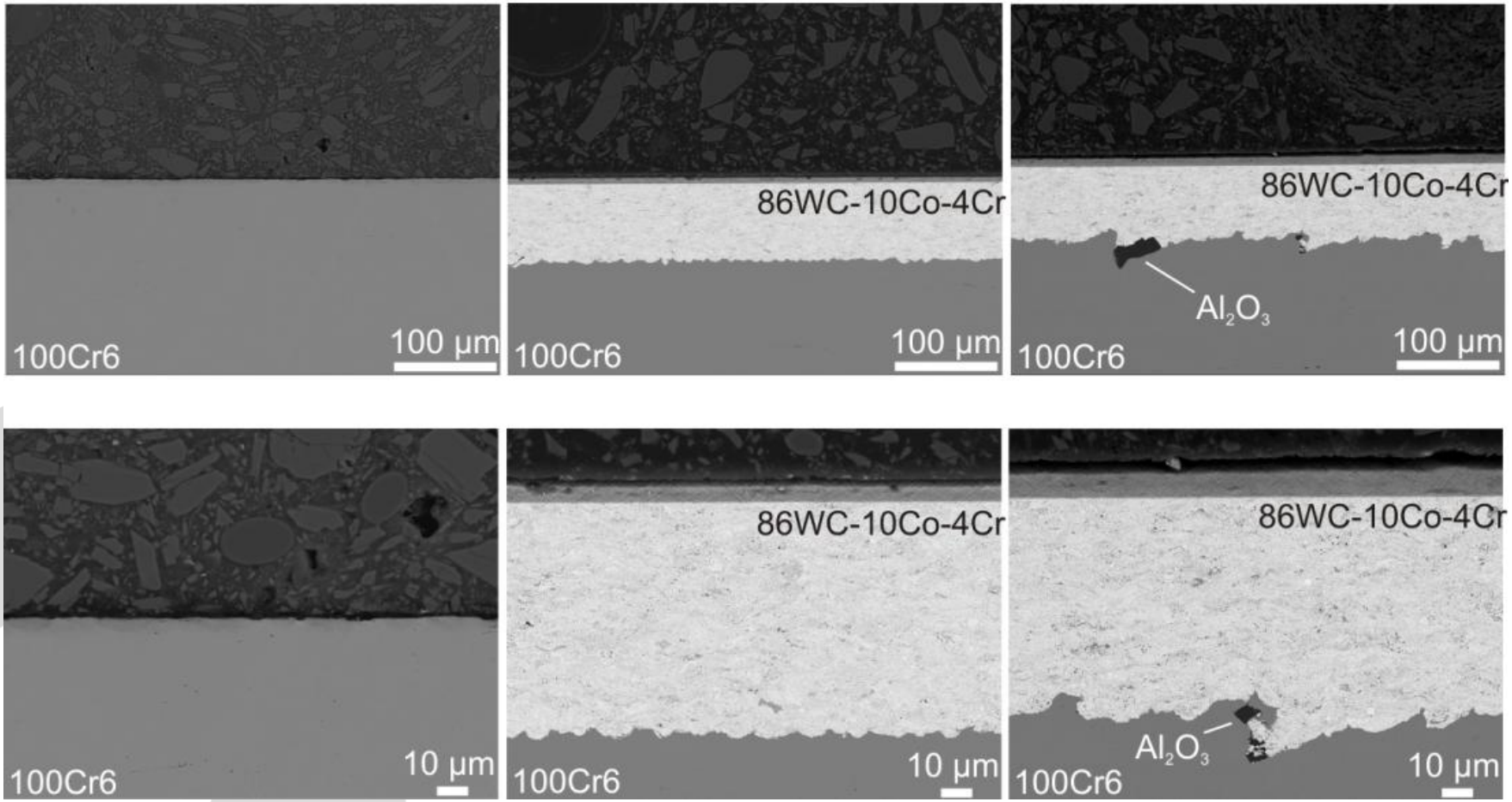

Rotating bending fatigue tests

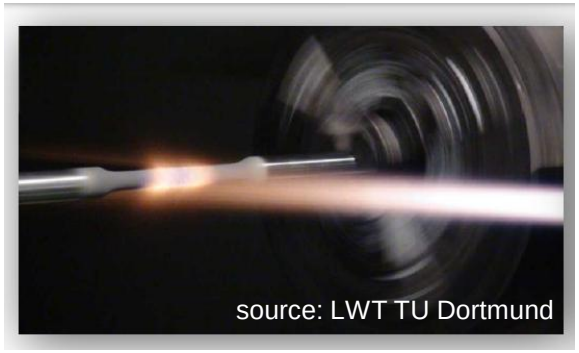

Wöhler-graph rotating bending fatigue test

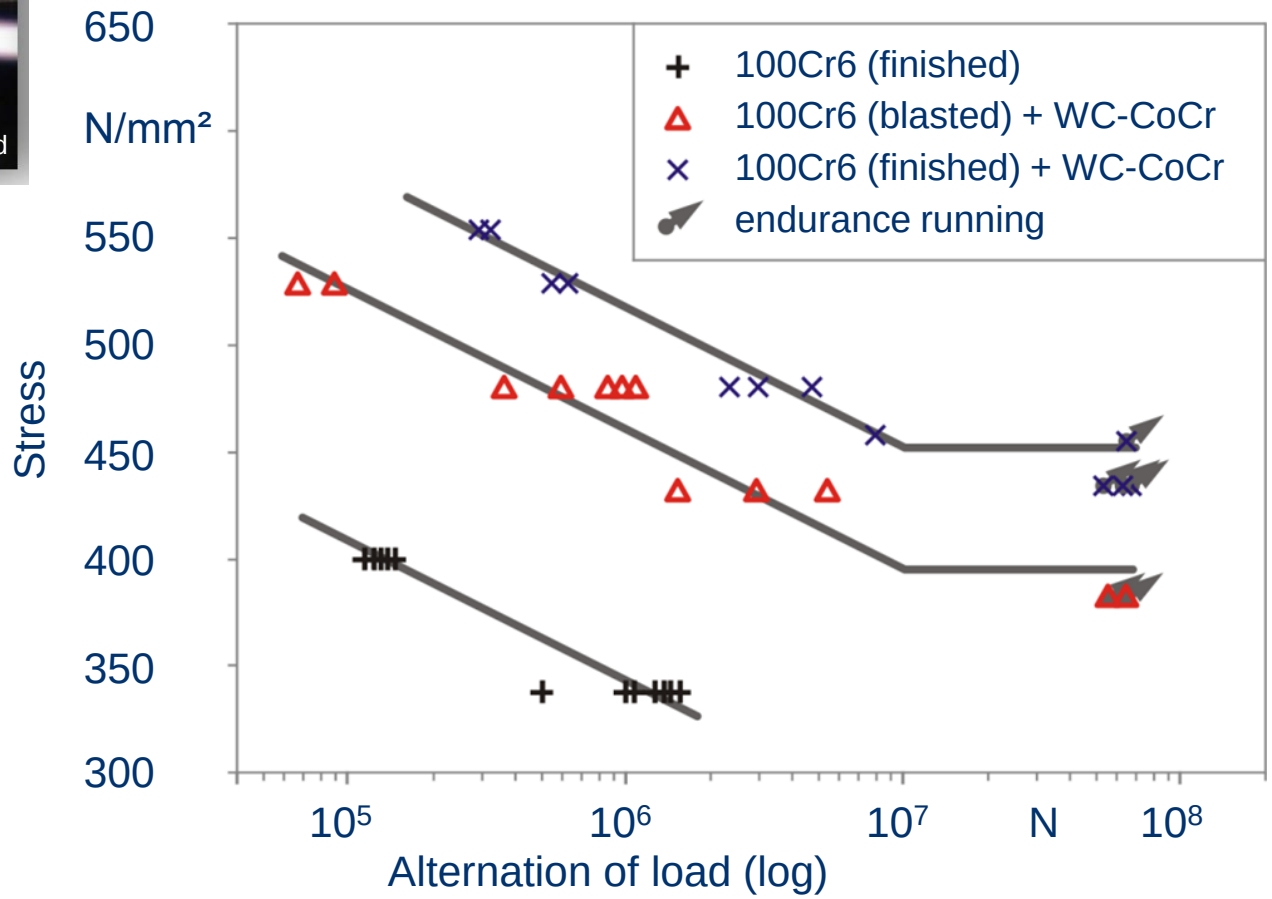

source: LWT TU Dortmund

Finishing of the coating

Material	Abrasive	Grain size	Force
86WC-10Co-4Cr	Diamond	d_K = 74; 30; 9; 3 µm	F = 120 N

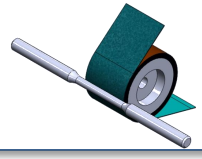

Elektrostatic oriented

d_K = 74 µm Diamant

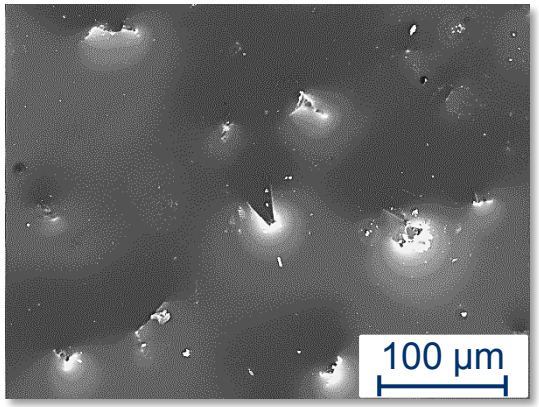

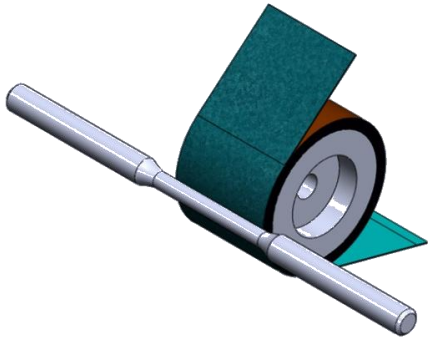

Wear resistant coating
Rotation bending specimens
Material: 86WC-10Co4Cr
Hardness: 1300 HV0,3

3 process steps with different grain sizes

Resin bonded

d_K = 30 µm diamond

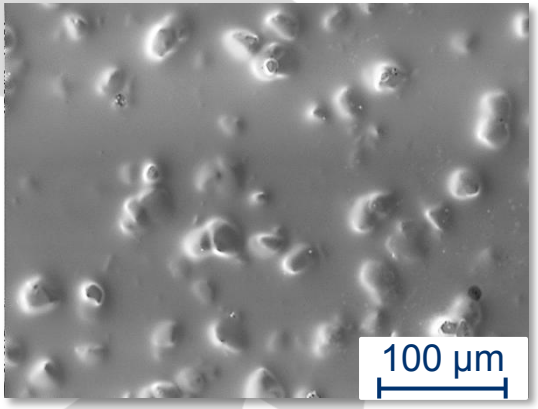

d_K = 9 µm diamond

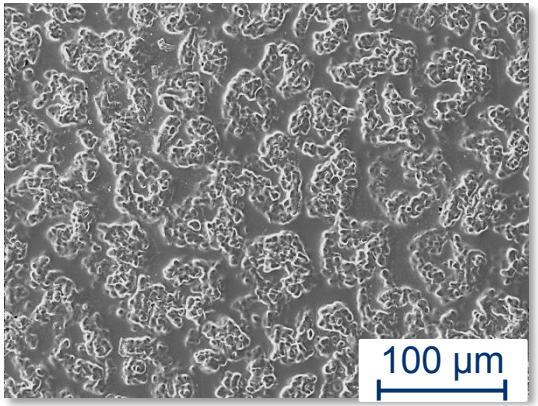

d_K = 3 µm diamond

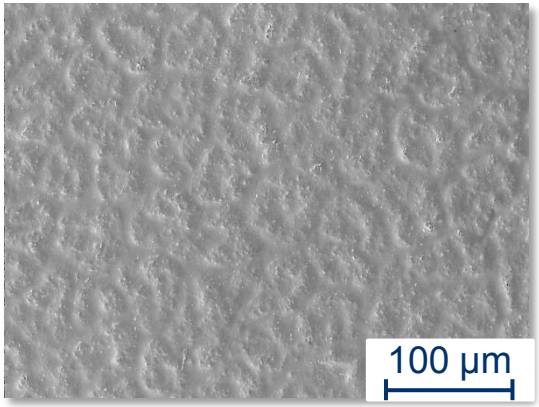

Surface topography coating

Material	Abrasive	Grain size	Force	Cutting speed v_c
86WC-10Co-4Cr	Diamond	d_K = 30; 9; 3 µm	F = 120 N	v_c = 21,2 m/min

Unfinished layer

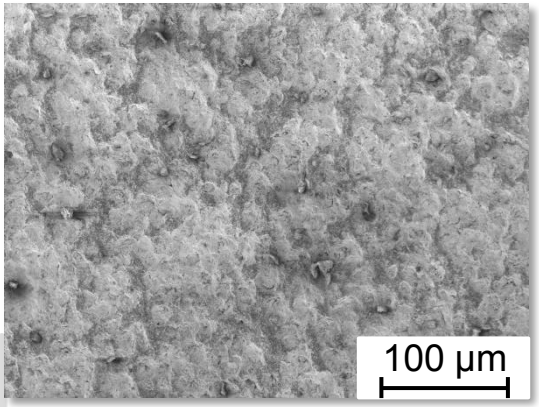

D30, insufficient prefinish

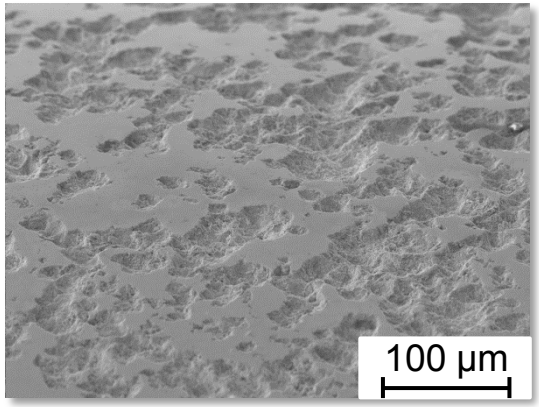

D30, t = 300 s

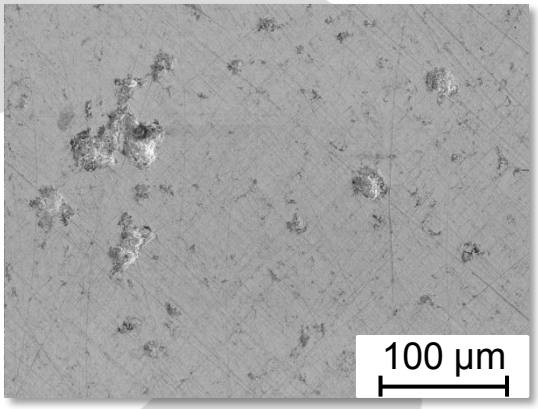

D30, D9, D3, t_{ges} = 660s

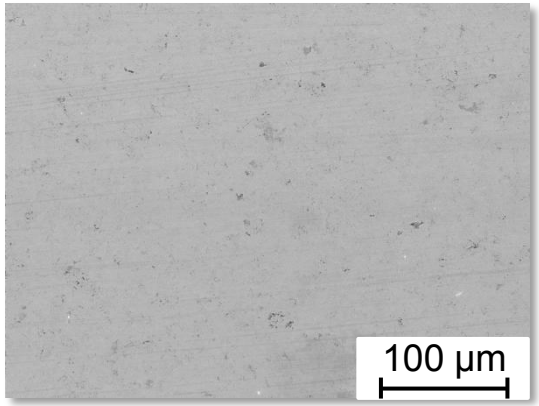

Layer thickness

Surface conditioning by the use of external shortstroke honing

- **Selective setup of the surface texture of the carrier material**

⇒Due to the adjustment of the single process steps, it is possible to reach selective surface texture parameters Rpk, Rk and Rvk and a surface quality Rz < 0,5 µm.

- **Machining of the wear resistance coating only with external shortstroke honing feasible**

⇒Surface qualities Rz < 0,5 on the coatings are achievable due to the usage of diamond-finishbelts.

Optimization of guide bars for BTA-drilling of high-alloyed steels

source: Shell

source: Kaiser Maschinenbau

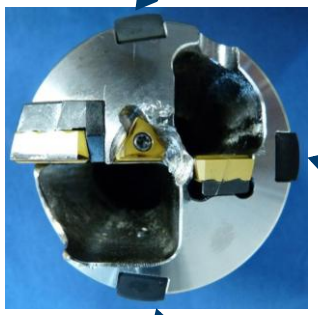

Optimization of guide bars for BTA-drilling of high-alloyed steels

Preparation of grinded guide bars through belt finishing

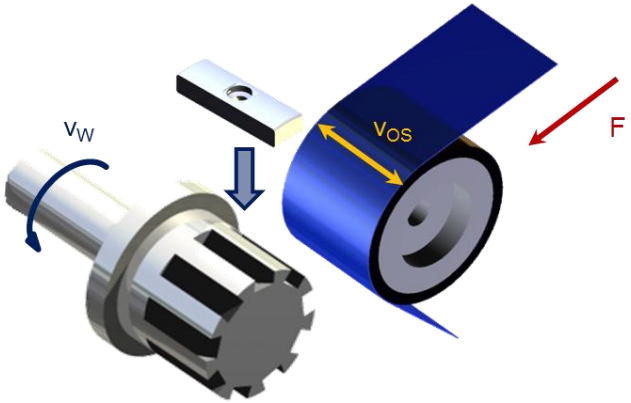

Improvement of the surface quality

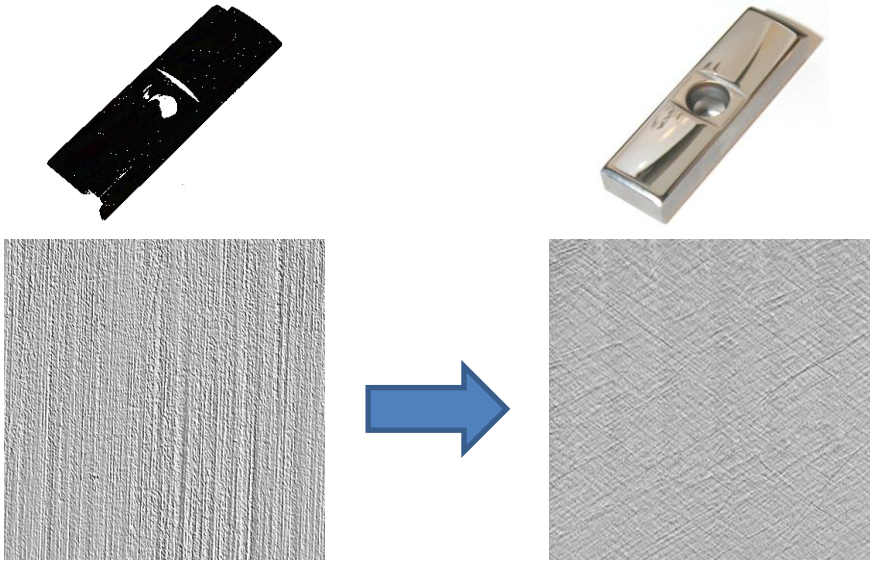

Rounding of shape transitions

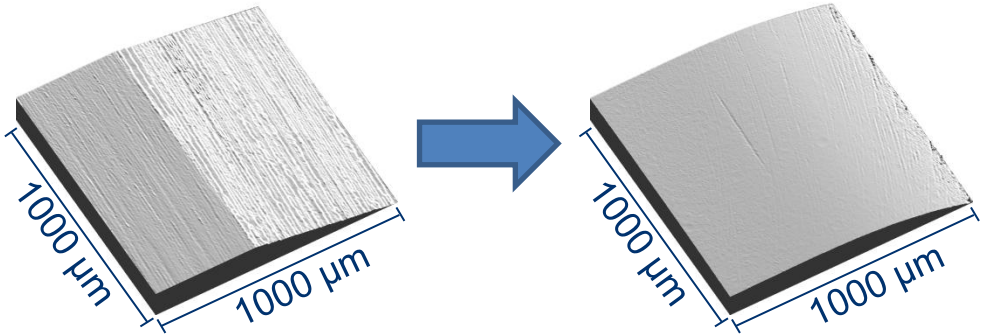

Optimization of guide bars for BTA-drilling of high-alloyed steels

grinding → micro-finishing → coating → micro-finishing

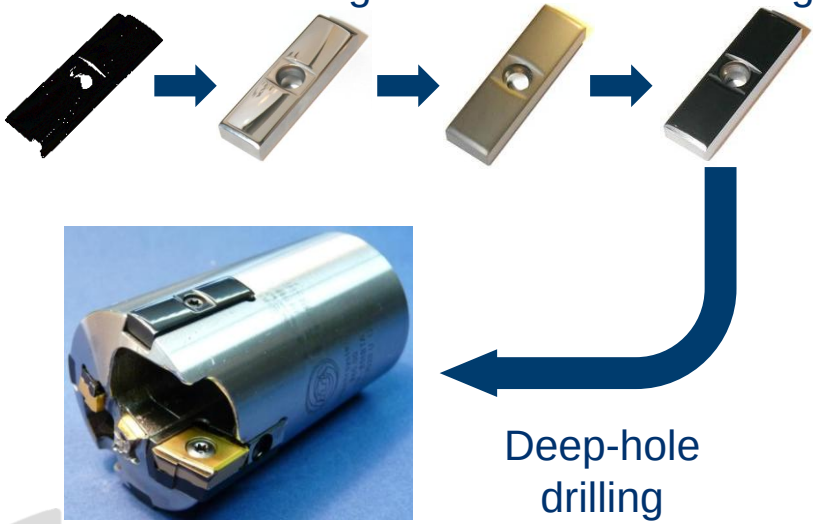

Deep-hole drilling

Bore hole quality

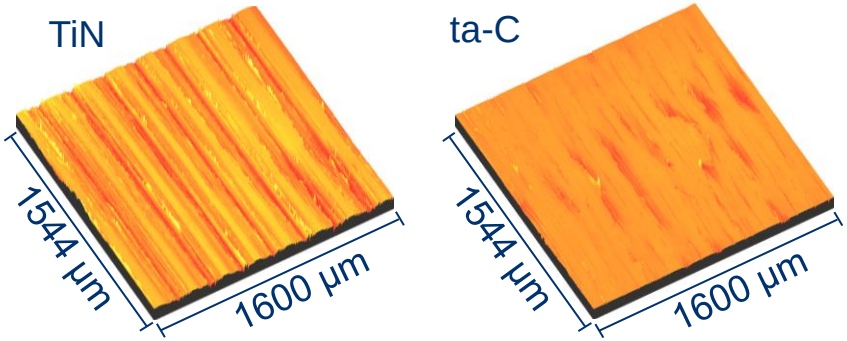

Conventional guide rod
(TiN-coated)

Optimized guide rod
(ta-C-coated; finished)

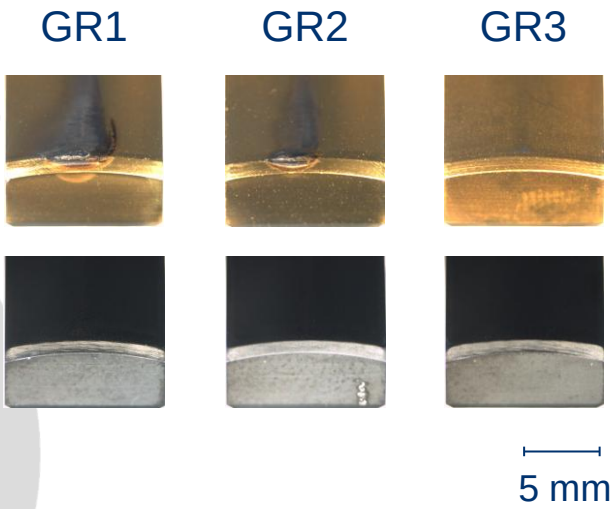

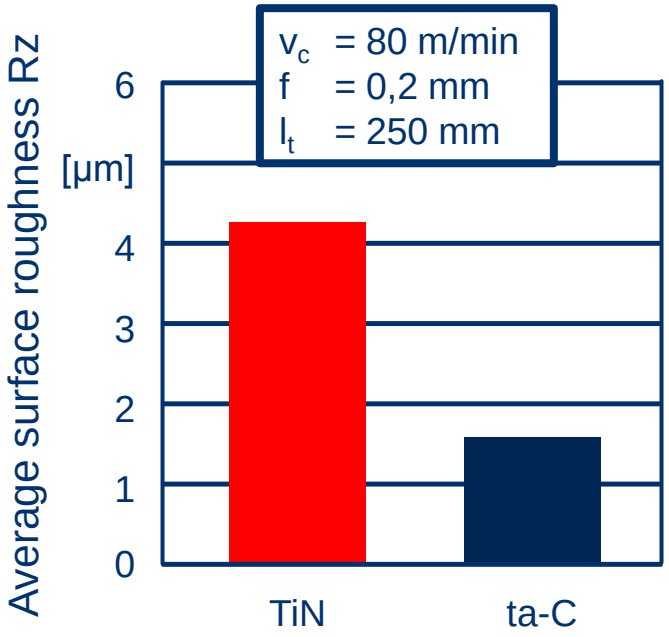

Overview

Introduction

Burr Minimization strategies in Machining Operations

Micro-finishing of hard coated parts

Detection of grinding burn and cracks by acoustic emission

FEM in Internal Traverse Grinding

Machining of low-sulfur steels

Influence of coated surfaces on friction coefficients

Machining of β-titanium alloys

Waviness reduction

Simulation strategies

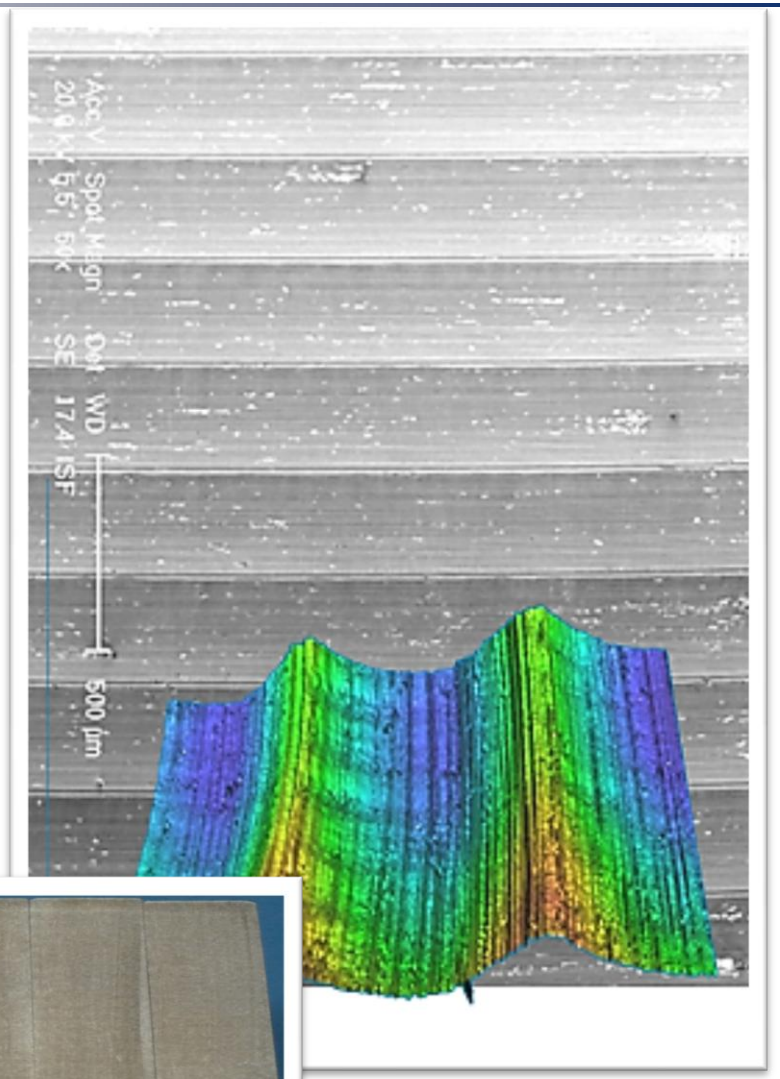

Experimental set up

- Flute grinding with and without coolant
- AE-Signal-Measurement with 4D-Optimizer Qass GmbH (f_{abt} = 25 MHz)

Lateral view set up

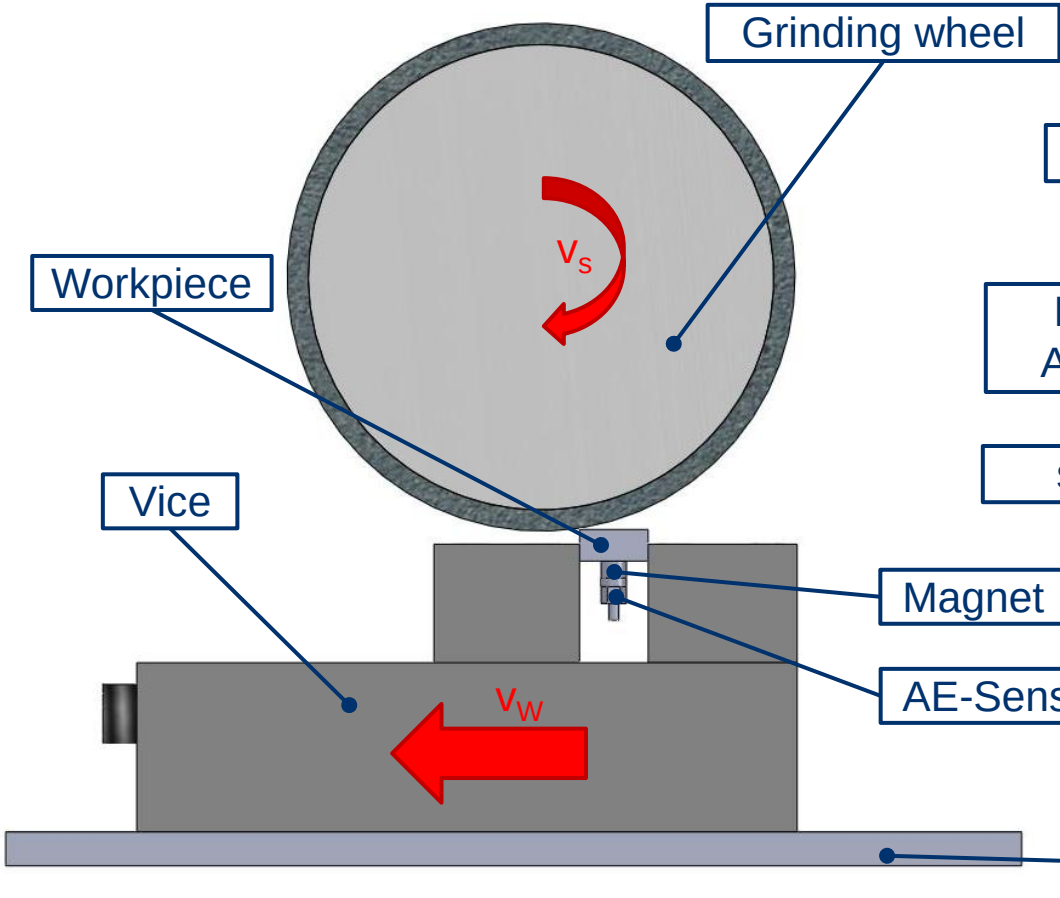

Top view on transparent workpiece

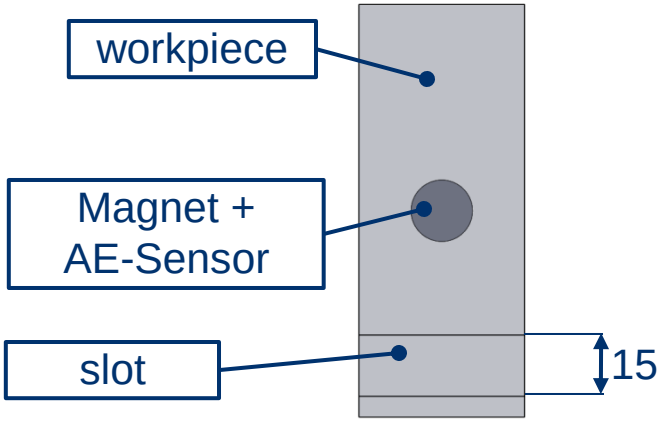

Material:
100Cr6 (62-63 HRC)

AE-Spectra: Face grinding / grinding burn

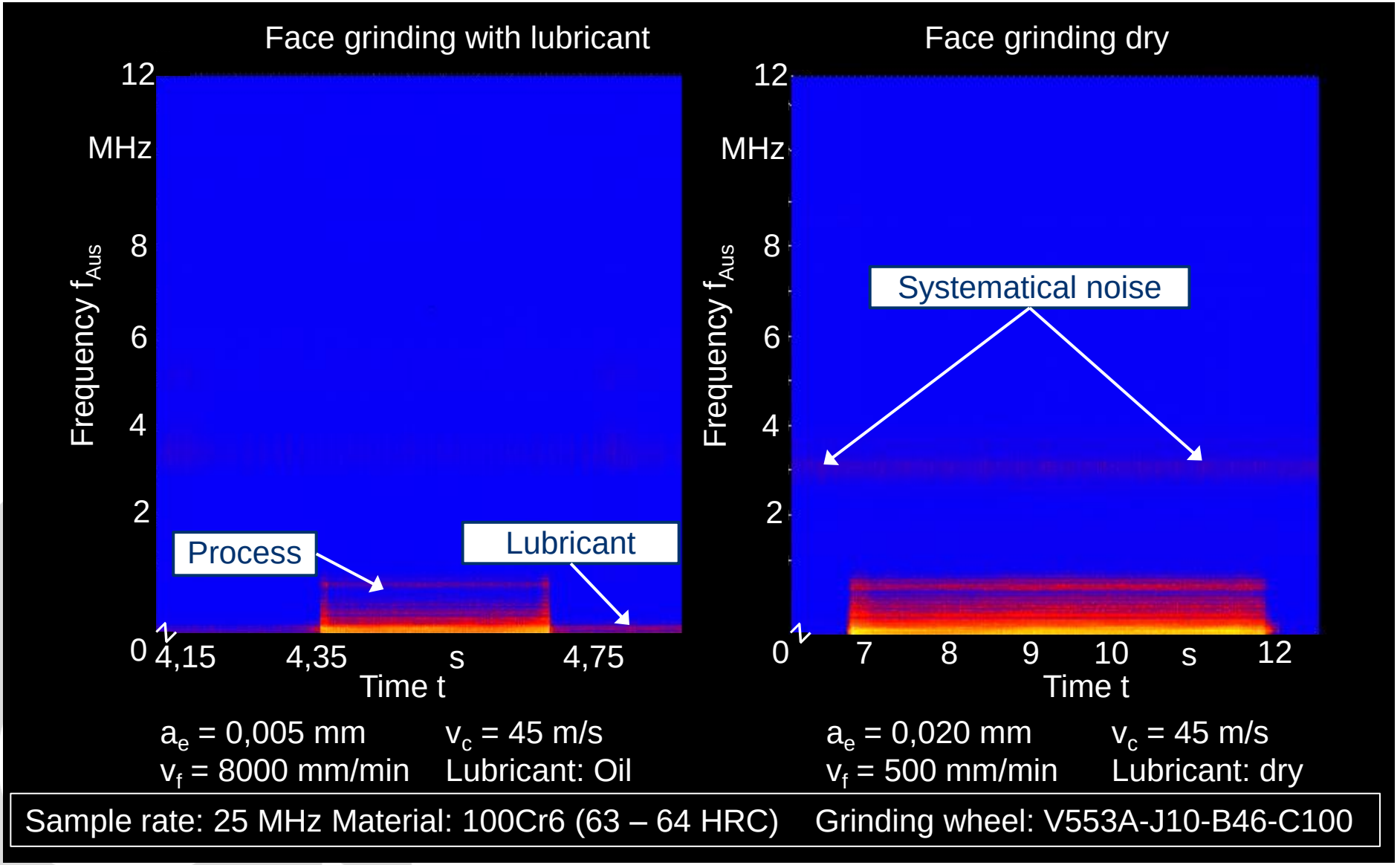

a_e = 0,005 mm v_c = 45 m/s
v_f = 8000 mm/min Lubricant: Oil

a_e = 0,020 mm v_c = 45 m/s
v_f = 500 mm/min Lubricant: dry

Sample rate: 25 MHz Material: 100Cr6 (63 – 64 HRC) Grinding wheel: V553A-J10-B46-C100

Nutenschleifen mit Rissen (dry)

AE-Spectrum

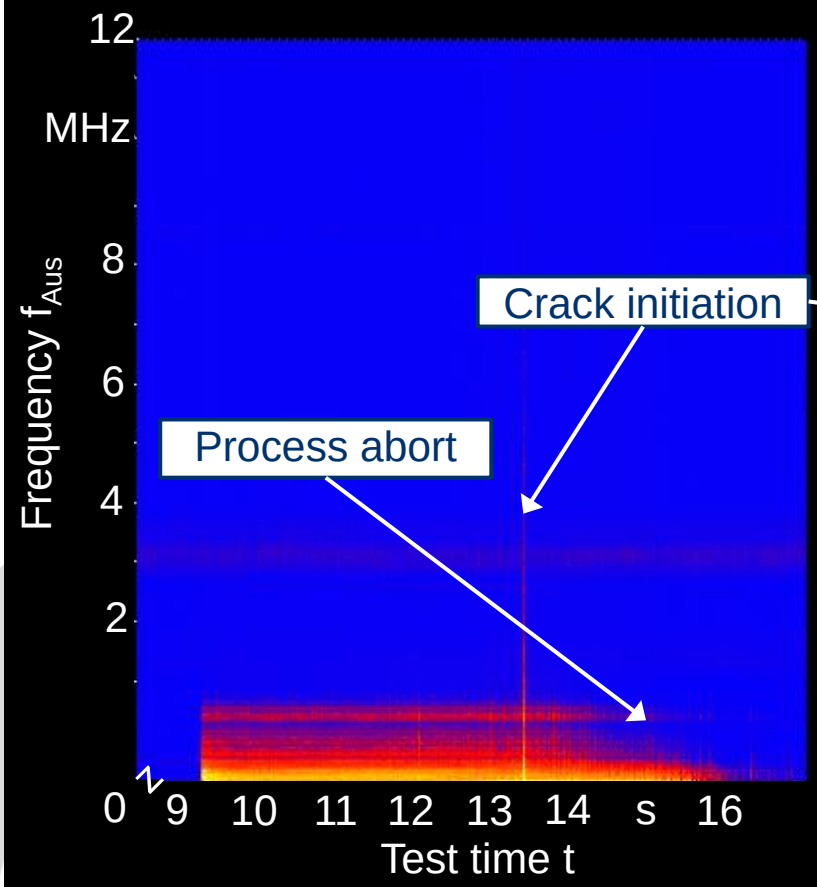

REM-pictures

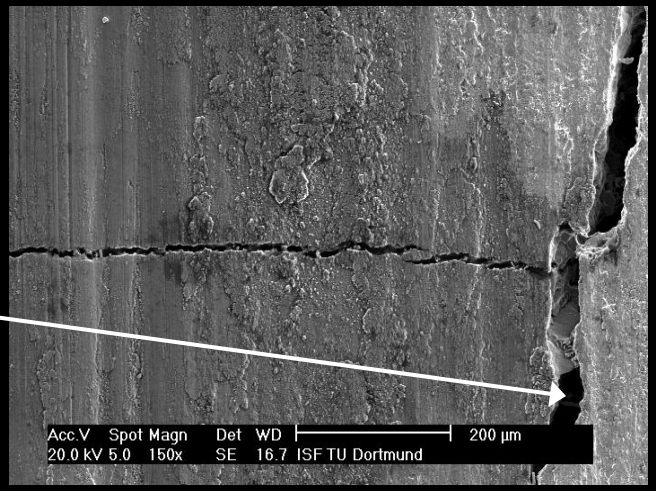

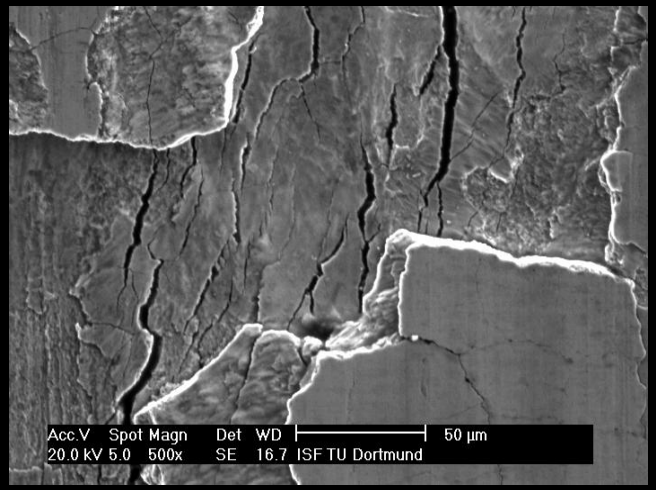

Sample rate: 25 MHz
Material: 100 Cr6 (63 – 64 HRC)
Grinding wheel: V553A-J10-B46-C10

a_e = 0,060 mm
v_c = 45 m/s
v_f = 500 mm/min
Coolant:
dry

Appearance of grindign burn

Grinding tests

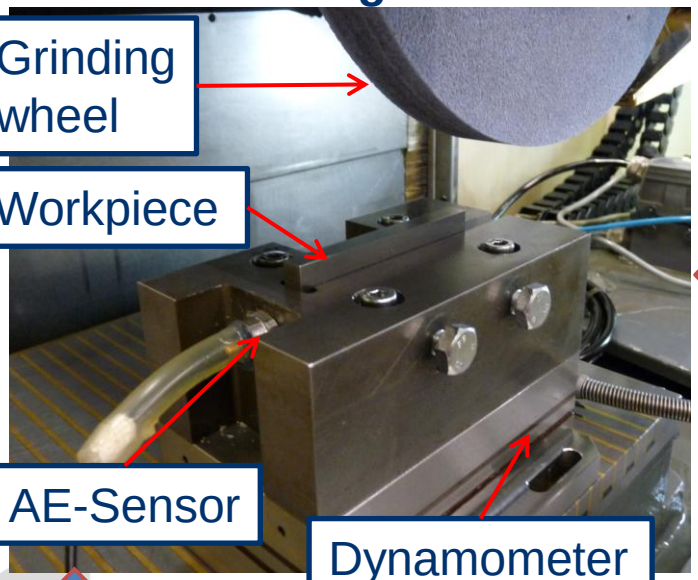

Comprehensive analysis of parameter space

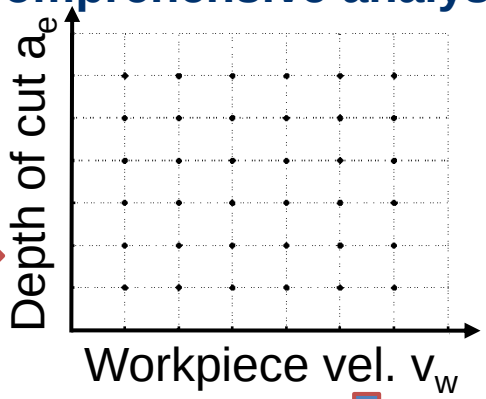

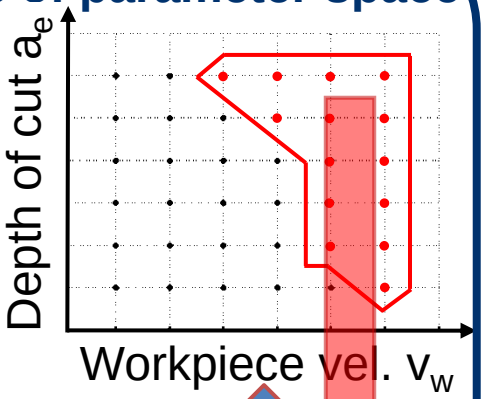

overheating
test point

Etching (Nital)

AE-Online-Measurement

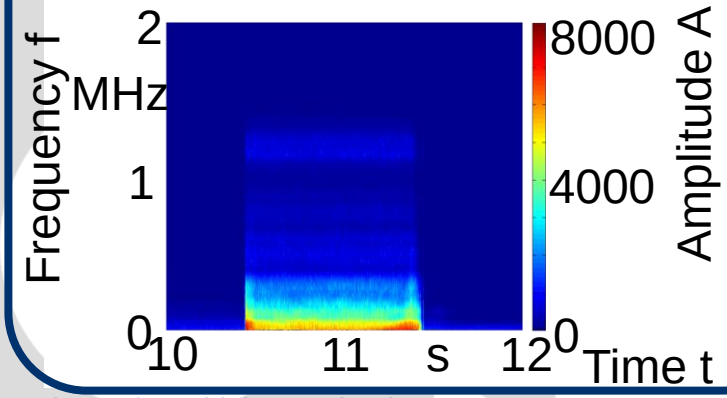

Metallographic microstructure / indentation hardness tests

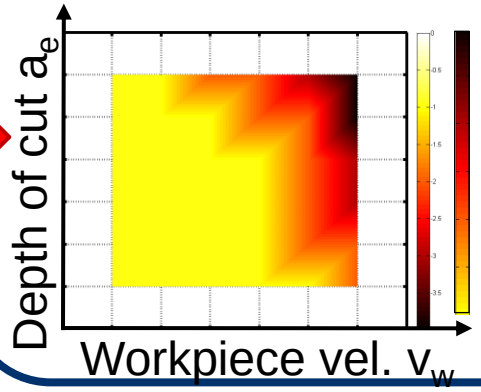

Influende of overheating

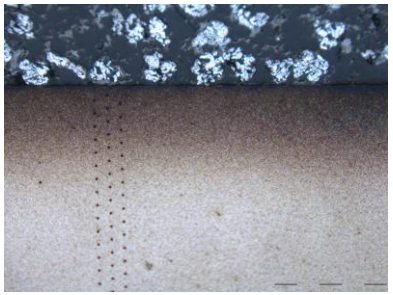

AE-Sensorik beim Schleifen: Schleifbrandentstehung III

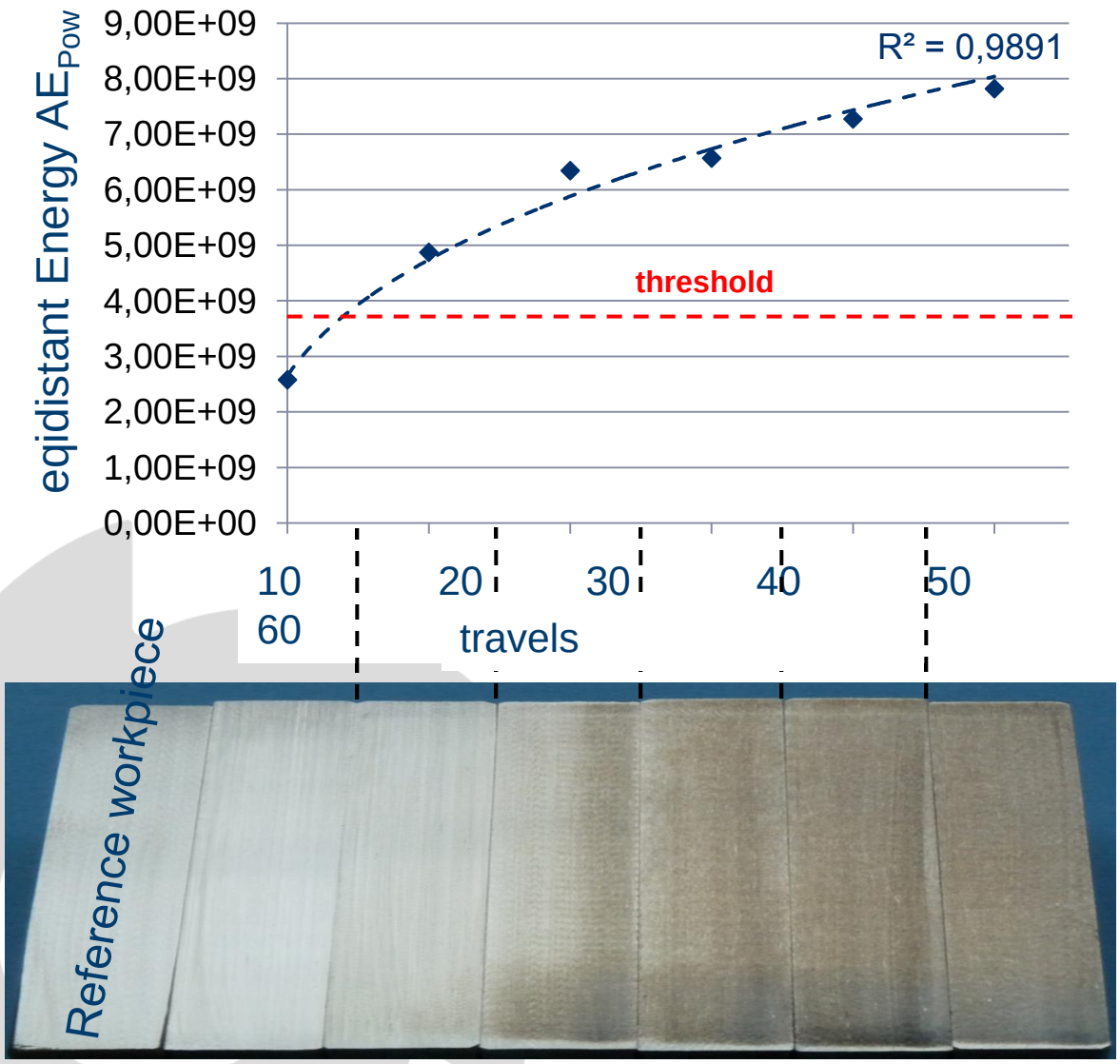

Conditions

process	: Face
grinding	: 100Cr6 (63-64 HRC)
Grinding wheel:	: A60VS6
Lubricantf:	: Oil

Grinding wheel velocity. v_s: 30 m/s
infeedg a_e: 0,1 mm
Workpiece velocityv_w: var.

Conclusion:

- **Fundamental correlation between overheating Foundation and AE signal**

→Comprehensive investigation of the parameter space

→ Microscopic observation of thermal damage

→ Observation / identification of the relevant frequency ranges

Overview

Introduction

Burr Minimization strategies in Machining Operations

Micro-finishing of hard coated parts

Detection of grinding burn and cracks by acoustic emission

FEM in Internal Traverse Grinding

Machining of low-sulfur steels

Influence of coated surfaces on friction coefficients

Machining of β-titanium alloys

Waviness reduction

Simulation strategies

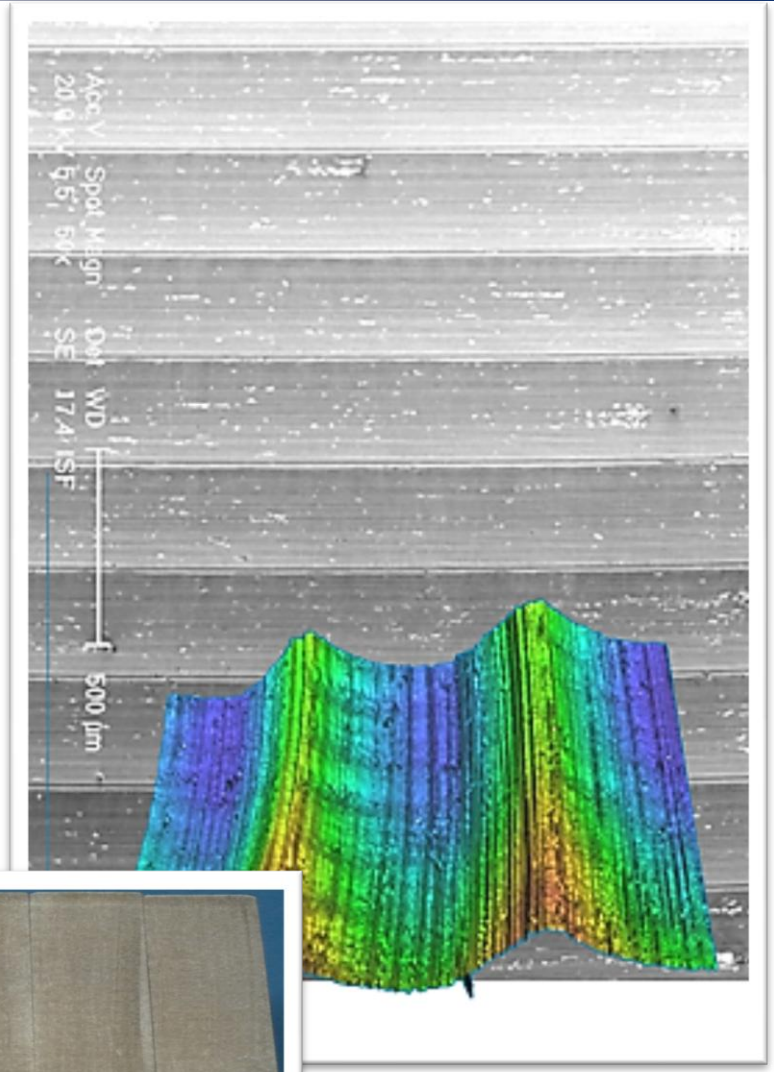

Comparison of Processes – „Infeed Grinding“ vs. „Internal Traverse Grinding“

Infeed Grinding

Internal Traverse Grinding (ITG)

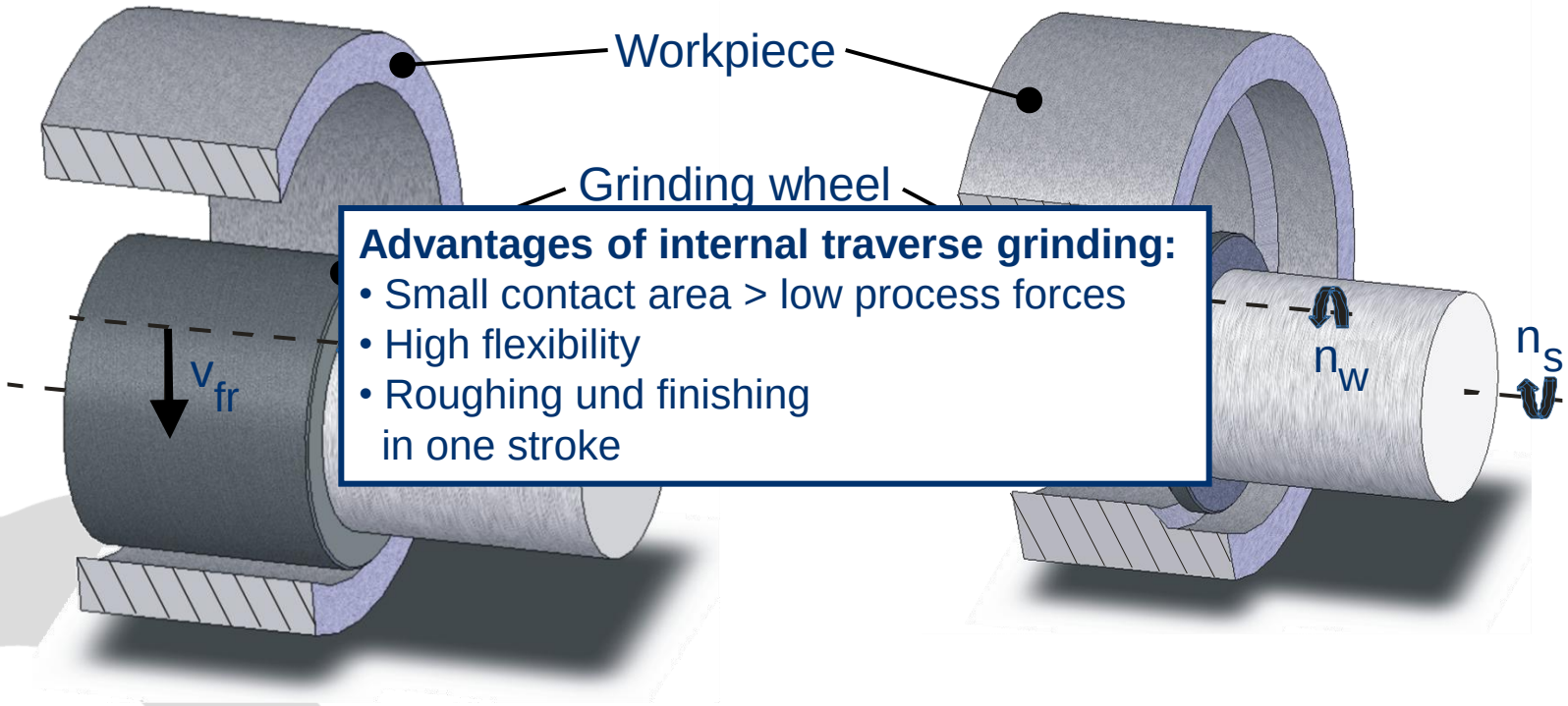

Advantages of internal traverse grinding:
- Small contact area > low process forces
- High flexibility
- Roughing und finishing in one stroke

n_w : Workpiece rpm
n_s : Grinding wheel rpm

v_{fa} : Axial feed velocity
v_{fr} : Radial feed velocity

Comparison of Processes – „Infeed Grinding“ vs. „Internal Traverse Grinding“

Infeed Grinding

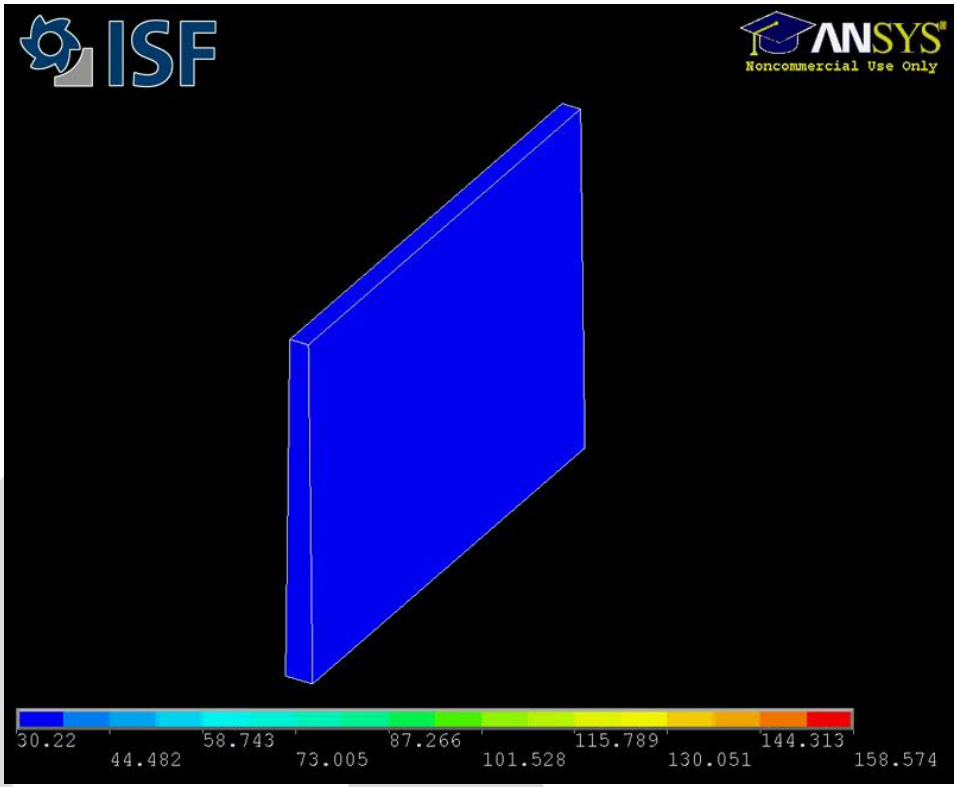

Internal Traverse Grinding (ITG)

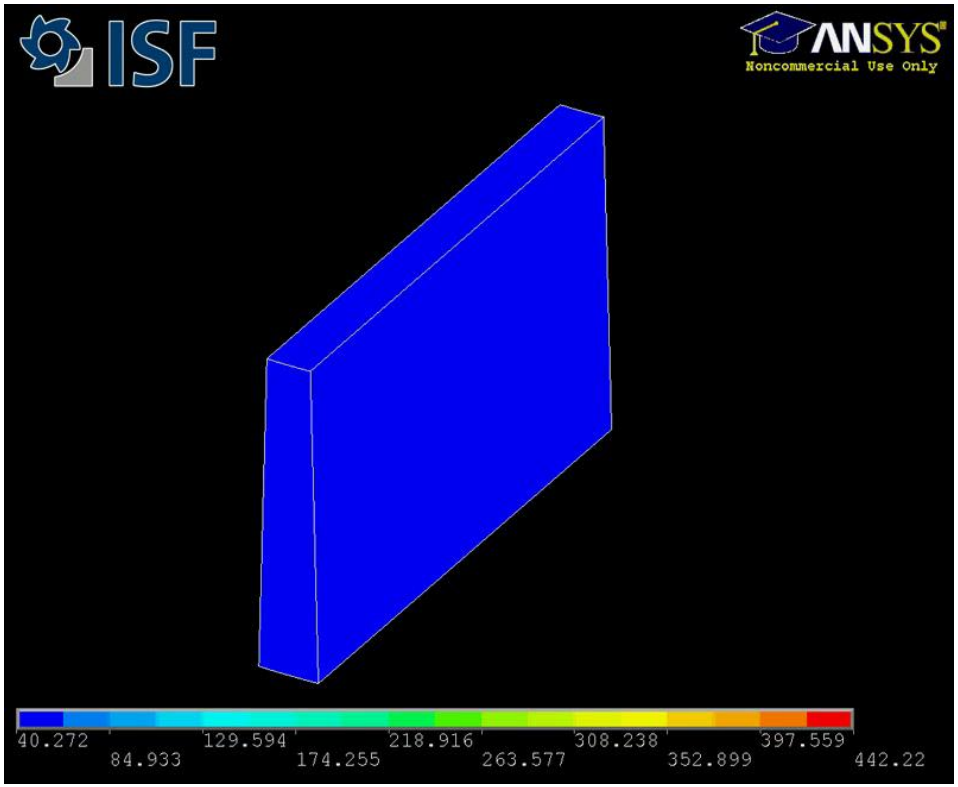

ITG - Problem and aim of research

Internal Traverse Grinding (ITG)

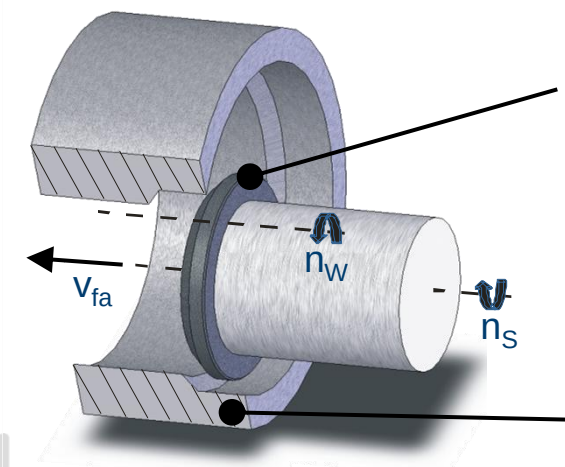

n_W : rpm of the workpiece
n_S : rpm of the grinding wheel

heat input in ITG- processes

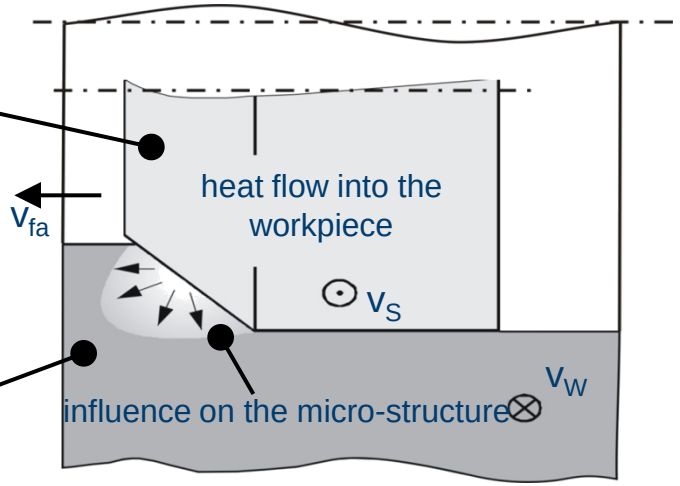

v_{fa} : axial feed rate
v_S : peripharel speed of the grinding wheel

Problem: Determination of the thermal loads on the workpiece in ITG- processes

Aim: Comprehension due to holistic simulation models

Internal Traverse Grinding (ITG)

Process Parameters: Q_w = 400 mm³/s, v_s = 133 m/s, v_w = 2 m/s

AE-Signal and Roughness in Relation to the Overall Dressing Infeed at the Finishing Zone

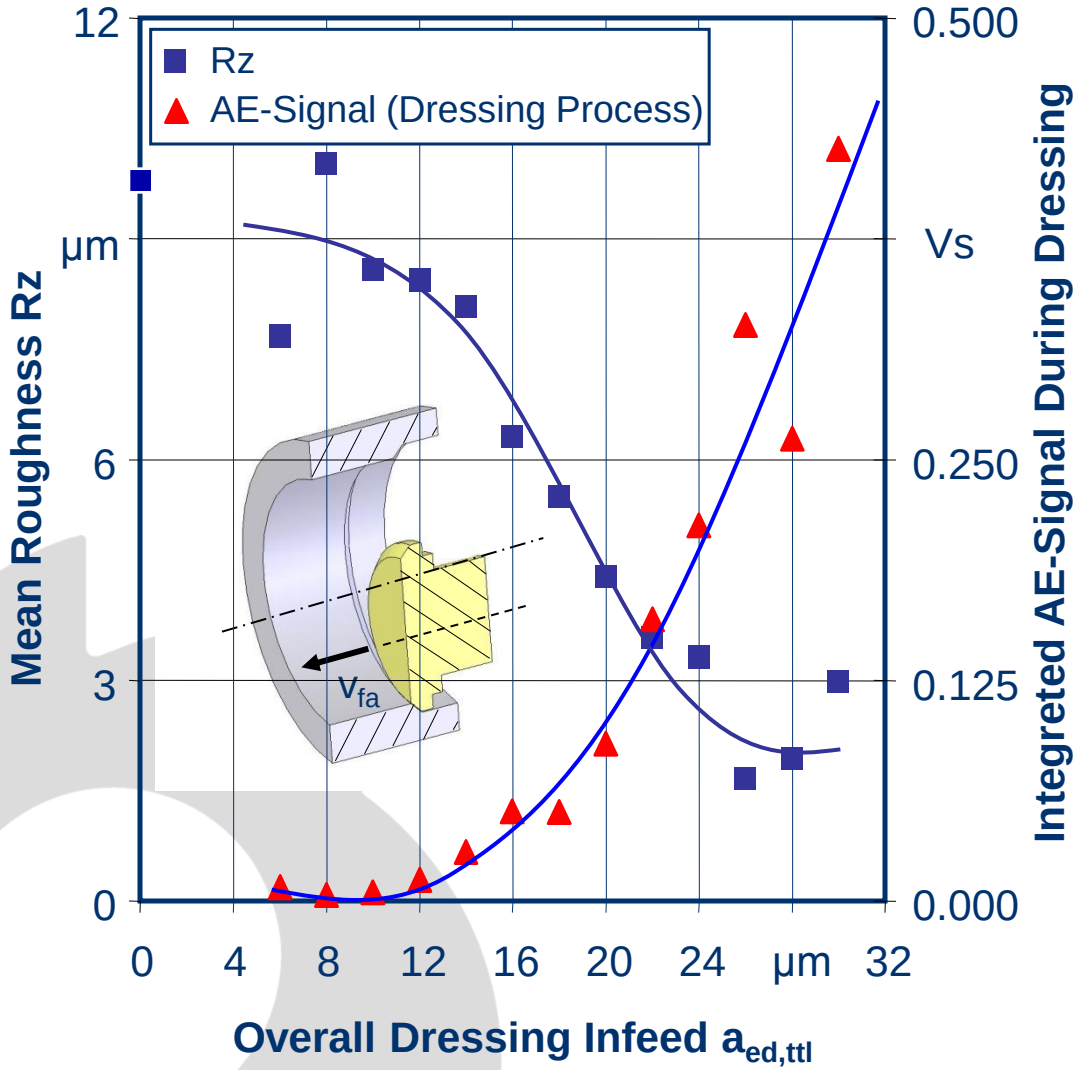

Workpiece:
90MnCrV 8, 63 ±1 HRC

Grinding Wheel:
B151 electroplated

Grinding:
v_s = 60 m/s, v_w = 2 m/s
$a_{e,ttl}$ = 0.15 mm
Q_w = 37.7 mm³/s

Dressing:
Fixed, a_{ed} = 2 µm
v_{fd} = 100 mm/min

Coolant:
Grinding oil
ν (40°C) = 4 mm²/s

Overview

Introduction

Burr Minimization strategies in Machining Operations

Micro-finishing of hard coated parts

Detection of grinding burn and cracks by acoustic emission

FEM in Internal Traverse Grinding

Machining of low-sulfur steels

Influence of coated surfaces on friction coefficients

Machining of β-titanium alloys

Waviness reduction

Simulation strategies

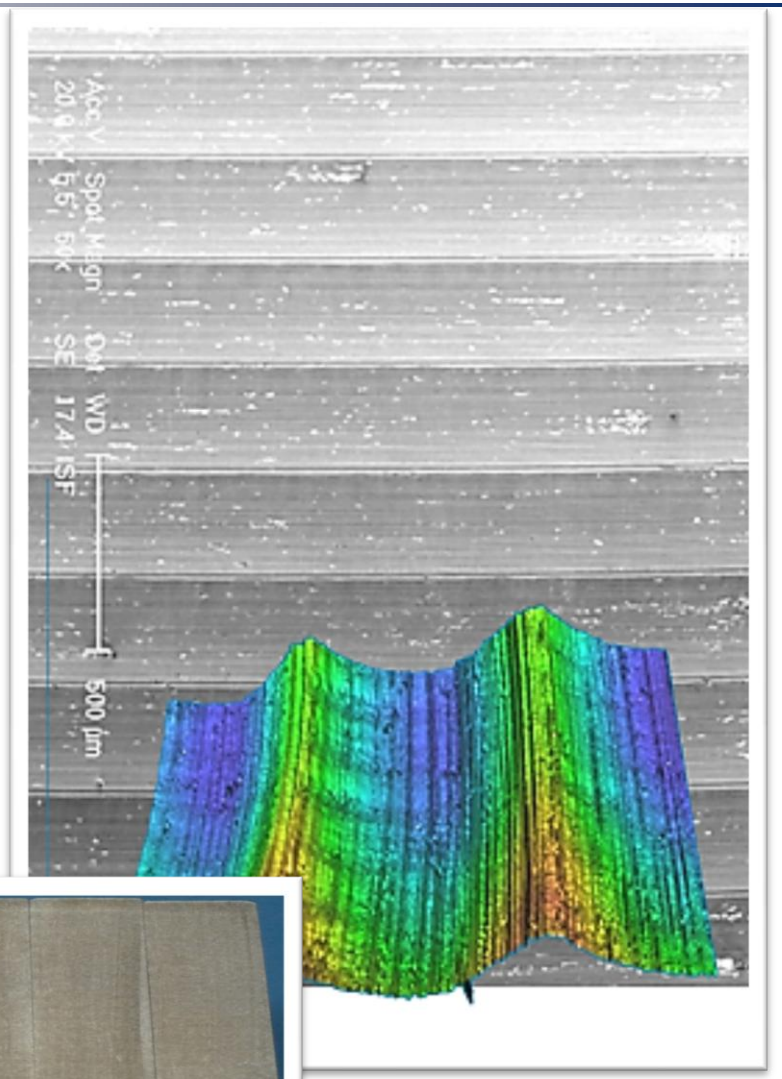

Turning of Low Sulfur Steels

Monforts RNC 602 Lathe

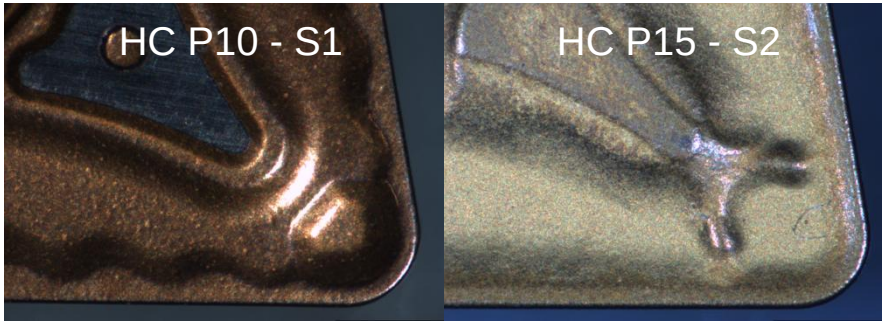

Cutting speed:	v_c = 250 - 350 m/min
Feed:	f = 0.2 - 0.4 mm
Depth of cut:	a_p = 2 mm
Tool:	CNMG120408
Material:	42CrMo4+QT
Volume removed:	V_z = 1000 cm³

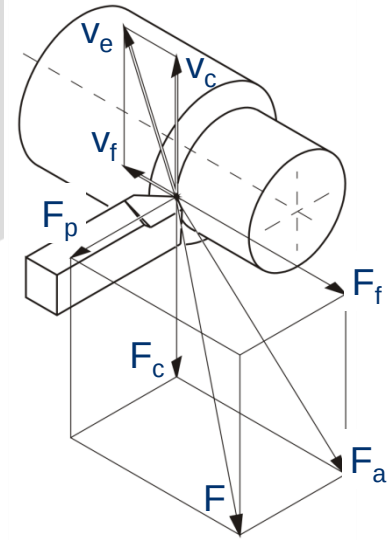

F_c: Cutting force
F_p: Passive force
F_f: Feed force
F_a: Active force
F : Resultant force

v_c : Cutting speed
v_e : Effective cutting speed
v_f : Feed velocity

3-Component Toolholder Dynamometer 9121

Measuring range
- F_x; F_y: -3 ... +3 kN
- F_z: -6 ... +6 kN

Sensitivity
- F_x; F_y: -7.9 pC/N
- F_z: -3.8 pC/N

Turning Quenched and Tempered Steel 42CrMo4 – Influence of Sulfur Content and Feed

Cutting speed:	v_c = 250 m/min	Material:	42CrMo4+QT
Feed:	f_1 = 0.2 mm; f_2 = 0.3 mm	Sulfur content:	S = 0.0110 % ; S = 0.0280 %
Depth of cut:	a_p = 2 mm	Coolant:	Dry machining
Tool:	CNMG120408-P10-S1		

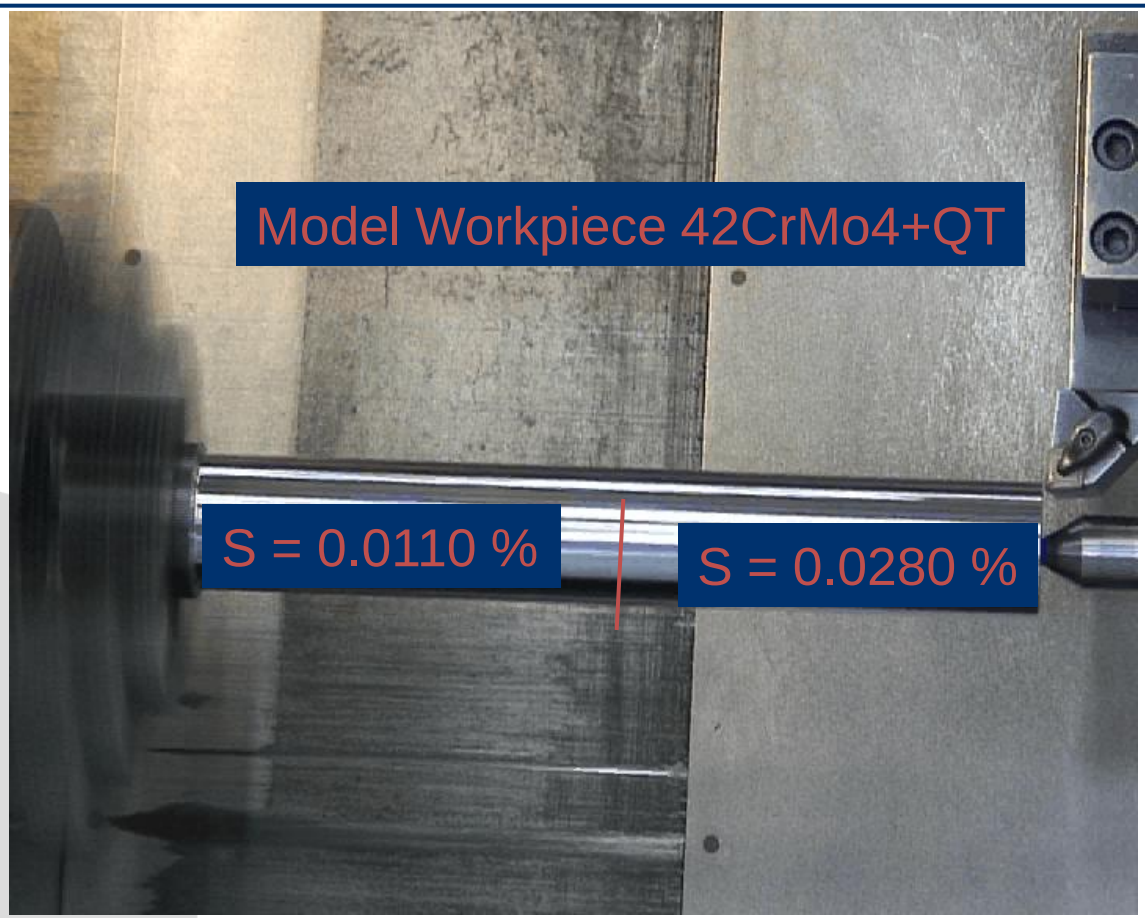

Turning Quenched and Tempered Steel 42CrMo4 – Influence of Chip Breaker Design on Chip Form

Cutting speed:	v_c = 250 m/min	Material:	42CrMo4+QT
Feed:	f = 0.2 mm	Sulfur content:	S = 0.0280 %
Depth of cut:	a_p = 2 mm	Coolant:	Emulsion
Tool:	CNMG120408 varied	Volume removed:	V_z = 1000 cm³

Tool

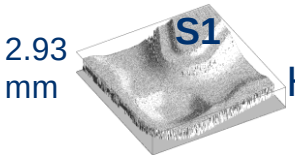

HC P10-S1

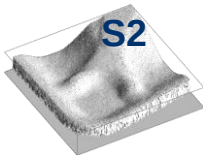

HC P15-S2

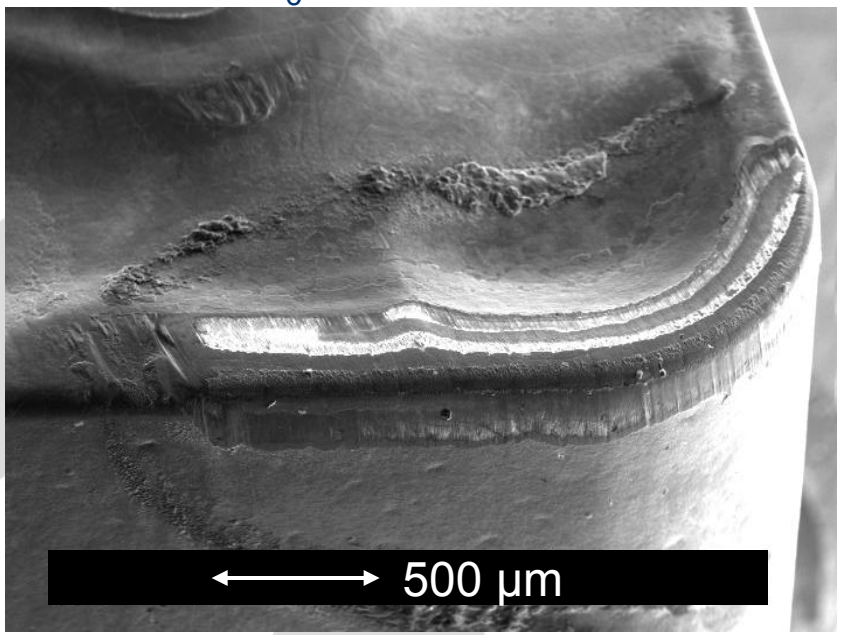

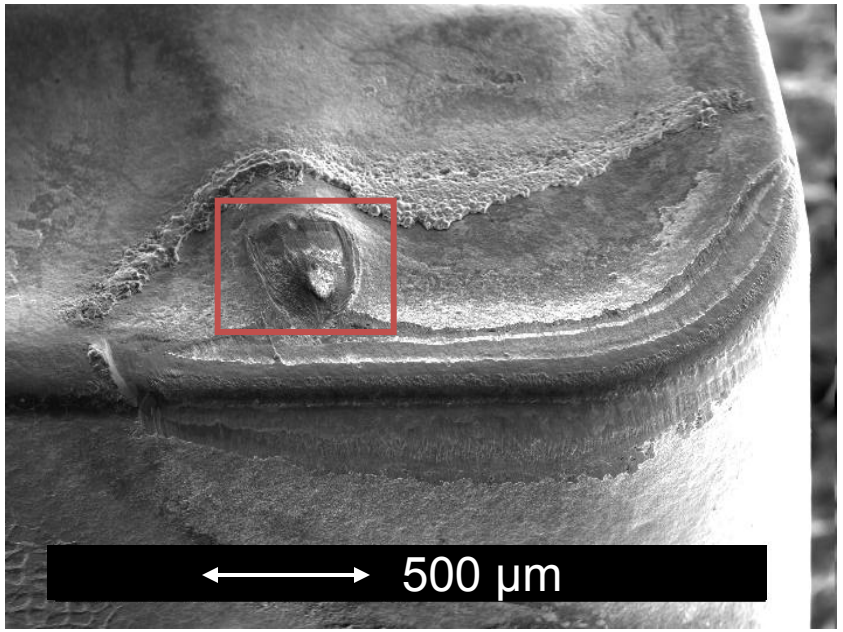

Turning Quenched and Tempered Steel 42CrMo4 – Influence of Cutting Speed and Sulfur Content on Tool Wear

Cutting speed:	v_c = 250 - 350 m/min	Material:	42CrMo4+QT
Feed:	f = 0.3 mm	Sulfur content:	S = 0.0110 %; S = 0.0280 %
Depth of cut:	a_p = 2 mm	Coolant:	Emulsion
Tool:	CNMG120408 P10-S1	Volume removed:	V_z = 1000 cm³

Cutting speed v_c

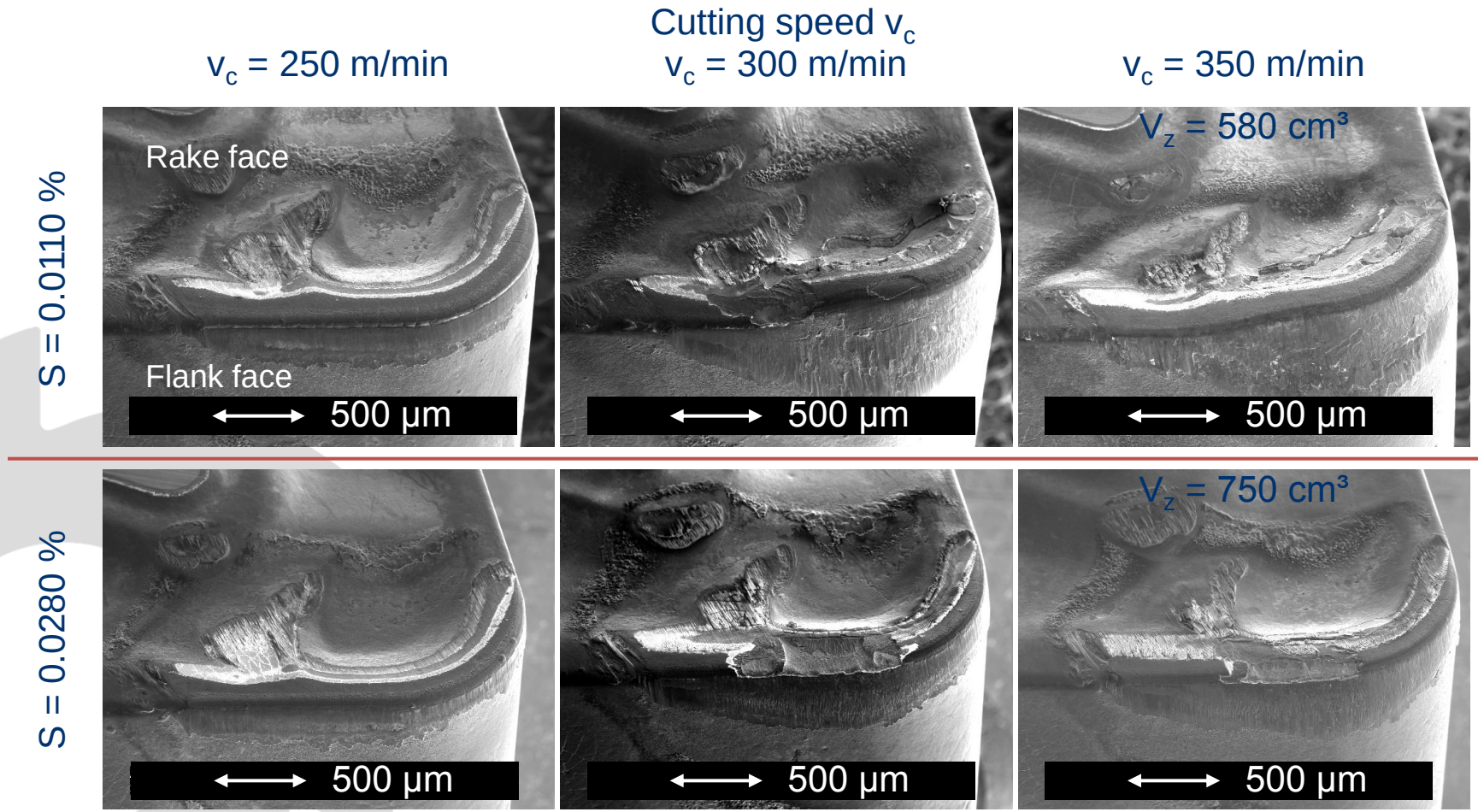

Turning Quenched and Tempered Steel 42CrMo4 – Influence of Chip Breaker Design on Chip Form

Cutting speed:	v_c = 250 m/min	Material:	42CrMo4+QT
Feed:	f = 0.2 mm	Sulfur content:	S = 0.0110 % ; S = 0.0280 %
Depth of cut:	a_p = 2 mm	Coolant:	Emulsion
Tool:	CNMG120408	Volume removed:	V_z = 250 cm³

Tool

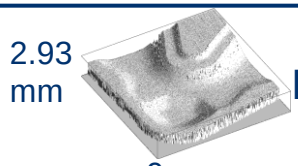

HC P10-S1

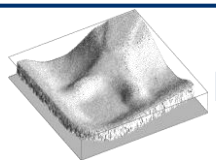

HC P15-S2

Sulfur content

S = 0.0280 %

S = 0.0110 %

50 mm

10 mm

Deep Hole Drilling of Low Sulfur Steels

Utilised tools

Single-lip drill (brazed)

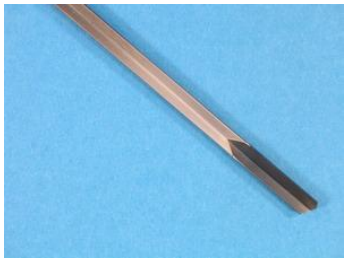

Single-lip drill (solid carbide)

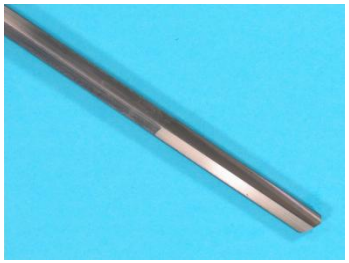

Twist drill (solid carbide)

Twist drill (solid carbide mod.)

Experimental setup

Drilling depth l = 150 mm

Tool diameter d = 5 mm

Emulsion

Pilot hole

Influencing factors

Feed

Cutting speed

Analysis

Tool wear

Mechanical tool loads

Bore-hole quality

Chip form

Burr formation

Deep Hole Drilling of Low Sulfur Steels

Grob BZ 600

Power:	64 kW
Torque:	204 Nm
Working area:	X-Axis: 800 mm
	Y-Axis: 700 mm
	Z-Axis: 630 mm
Velocities:	X / Y: 60,000 mm/min
	Z: 70,000 mm/min
Spindle speed:	45-12,500 min^{-1}
Coolant supply:	Inner and outer supply:
	25 l/min at 80 bar / MMS

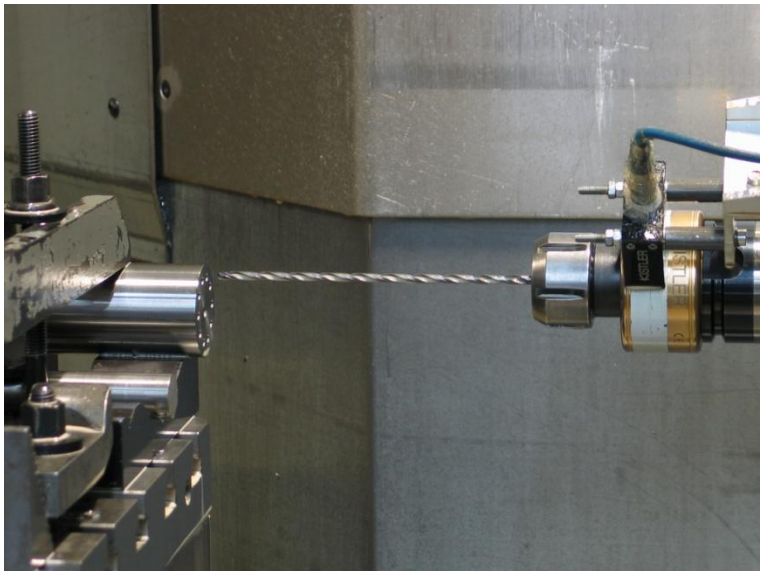

Deep hole drilling of quenched and tempered steel- opportunities to increase cutting parameters

Cutting speed:	v_c = 80 m/min	Material:	42CrMo4+QT ; R_m = 960 N/mm²
Feed:	f = 0,3 mm	Content of sulfur:	**S = 0,0110 %**
Tool:	Twist drill; d = 5 mm	Coolant / pressure:	emulsion / p = 25 bar
Cutting tool material:	HC-K30 + TiAlN	Drilling depth:	l = 150 mm

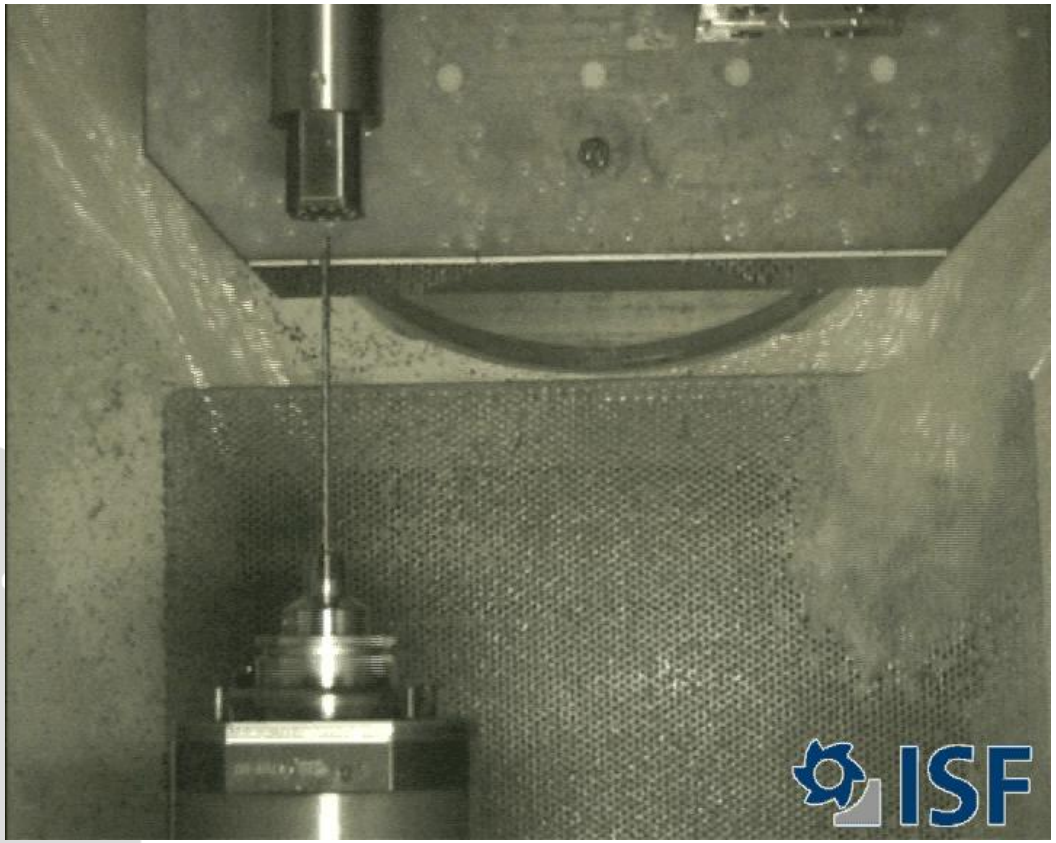

Deep Hole Drilling of Quenched and Tempered Steel 42CrMo4 – Influence of Sulfur Content on Tool Wear and Chip Form

Cutting speed:	v_c = 80 m/min	Material:	42CrMo4+QT
Feed:	f = 0.02 mm	Sulfur content:	S = 0.0110 % ; S = 0.0280 %
Tool:	Single-lip drill	Coolant / Pressure:	Emulsion / p = 60 bar
Cutting material:	HW-K15	Drilling length:	L_f = 5.1 m

Part of the tool

Sulfur content	Tool tip	Cutting edge corner	Chip form
S = 0.0110 %	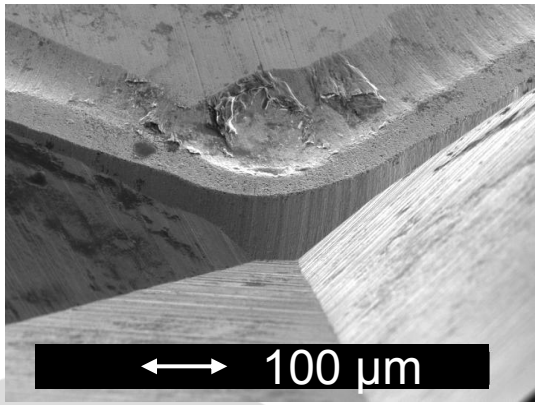	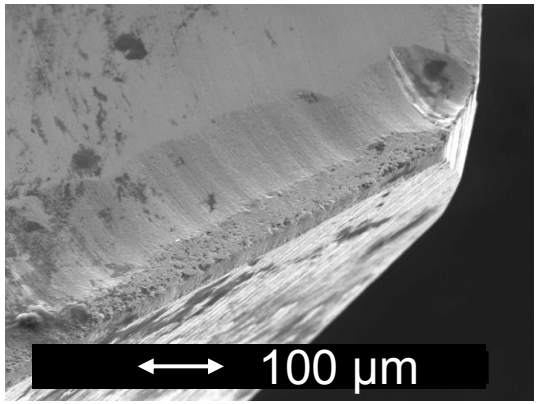	
S = 0.0280 %	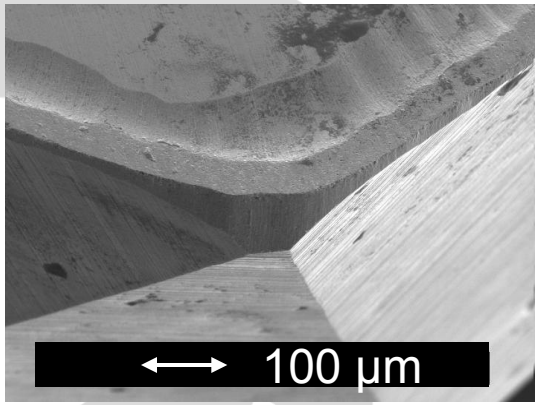	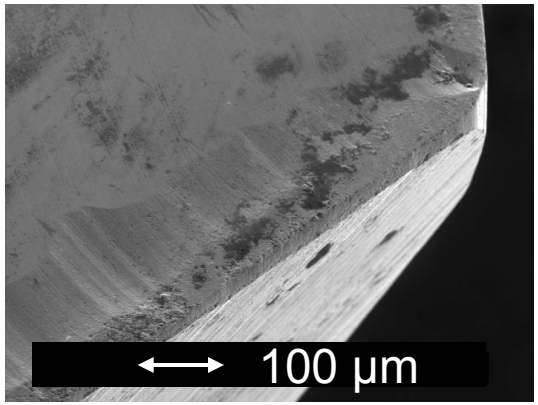	

10 mm

Deep Hole Drilling Quenched and Tempered Steel 42CrMo4 – Influence of Chip Flute Surface on Chip Form

Cutting speed:	v_c = 80 m/min		Material:	varied
Feed:	f = 0.2 mm		Sulfur content:	varied
Tool:	Twist drill		Coolant / Pressure:	Emulsion / p = 20 bar
Cutting material:	HC-K30F + TiAlN		Drilling length:	L_f = 5.1 m

Material / Sulfur content

18CrNiMo7-6 S = 0.0010 %	20MnCr5 S = 0.0063 %	42CrMo4+QT S = 0.0076 %	42CrMo4+QT EVA S = 0.0110 %

Tool wear

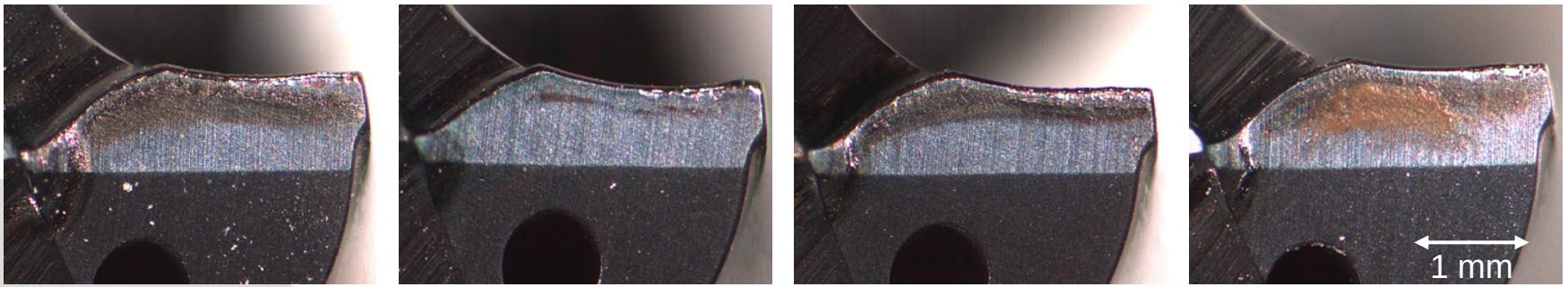

Chip form

Deep Hole Drilling Quenched and Tempered Steel 42CrMo4 - Influence of Cutting Data on Chip Form

Cutting speed:	v_c = 60 - 100 m/min	Material:	42CrMo4+QT
Feed:	f = 0.15 - 0.25 mm	Sulfur Content:	**S = 0.0076 %**
Tool:	Twist drill	Coolant / Pressure:	Emulsion / p = 20bar
Cutting material:	HC-K30F + TiAlN	Drilling length:	L_f = 5.1 m

Cutting speed v_c

v_c = 60 m/min | v_c = 80 m/min | v_c = 100 m/min

Feed f

f = 0.15 mm

f = 0.2 mm

f = 0.25 mm

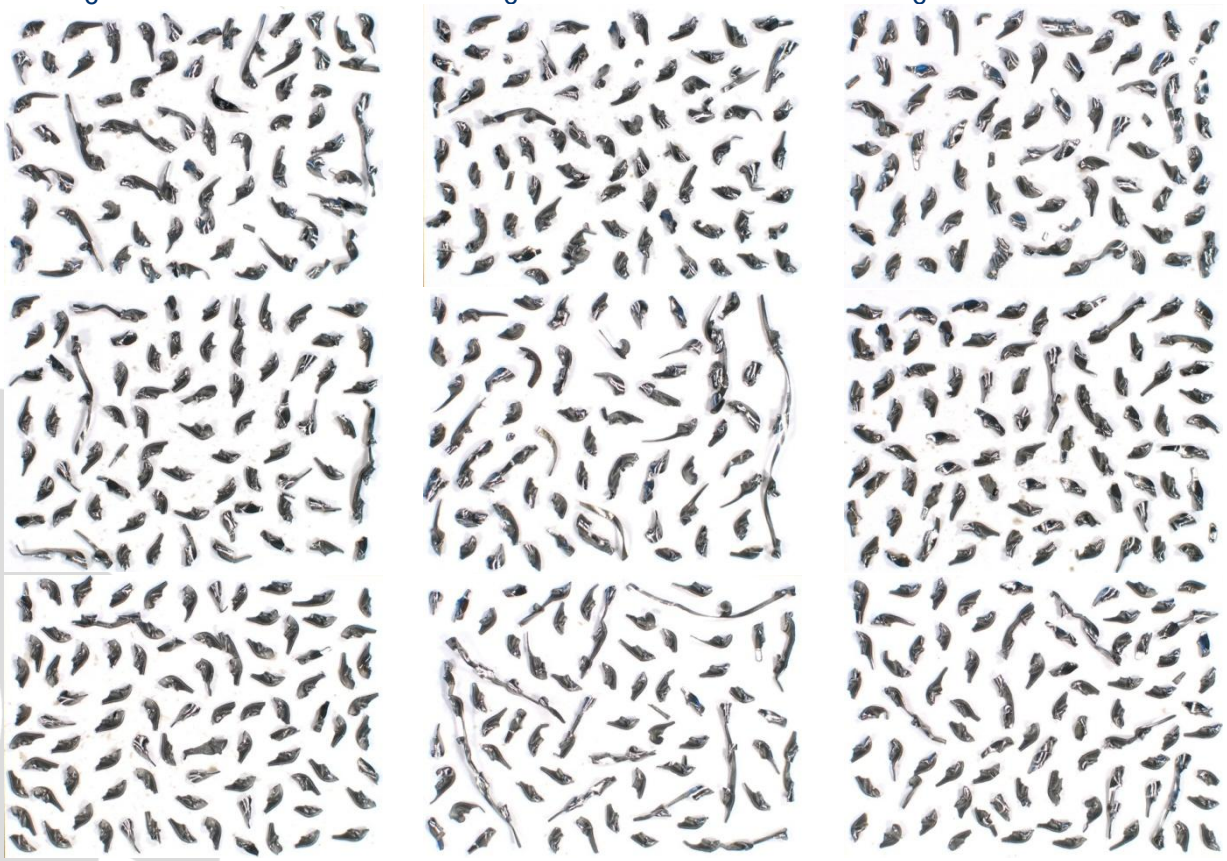

↔ 1 cm

Summary

Turning

- The sulfur content of steel has an influence on chip formation and tool wear.
- It is possible to compensate the influence of the sulfur content by adapting the chip breaker design and the cutting data.

Deep Hole Drilling

- Deep hole drilling of low sulfur steels increases the risk of tool breakages.
- Very good drill hole quality can be produced by using single-lip drills.
- High feed rates are attainable by using twist drills.
- Polished flutes improve chip formation.

Conclusion

An efficient process design for the machining of low sulfur steels is possible.

Overview

Introduction

Burr Minimization strategies
in Machining Operations

Micro-finishing of hard coated parts

Detection of grinding burn and cracks by acoustic emission

FEM in Internal Traverse Grinding

Machining of low-sulfur steels

Influence of coated surfaces on friction coefficients

Machining of β-titanium alloys

Waviness reduction

Simulation strategies

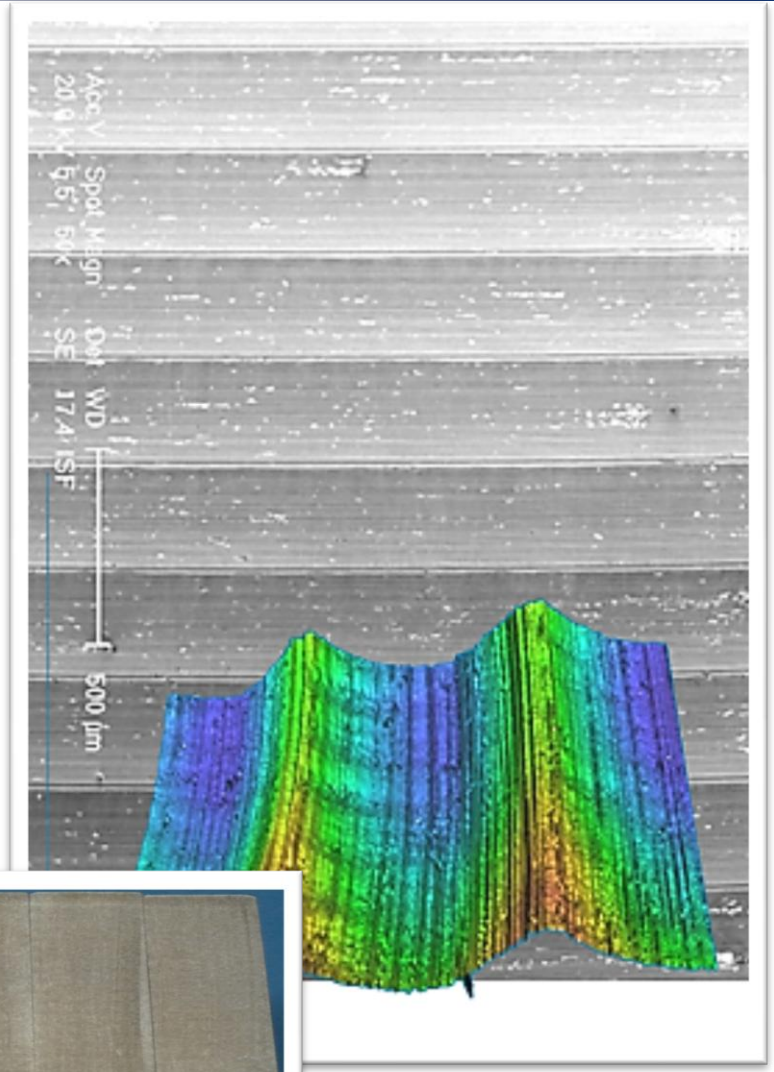

Experimental investigations

process parameters

layer system:	**Libo**	**HVOF**
cutting speed v_c:	10 m/s	10 m/s
process kinematic:	synchron/asynchron	synchron
feed velocity v_f:	500 - 2000 mm/min	200 - 800 mm/min
depth of a cut a_e:	0,02 - 0,04 mm	0,01 - 0,02 mm
width of a cut a_p:	2,4 - 4,8 mm	2 - 3,2 mm

target variables

process forces:	F_t, F_a, F_n
roughness:	Rz, Ra, Rv, Rp, Rmax

tools

material:	CBN, Diamant
grain size:	91, 126, 181
bonding:	ceramik, epoxy, metall, galvanic
shape:	cylindrical grinding tips (d = 10 - 15 mm)

Experimental set up

grinding of flat samples

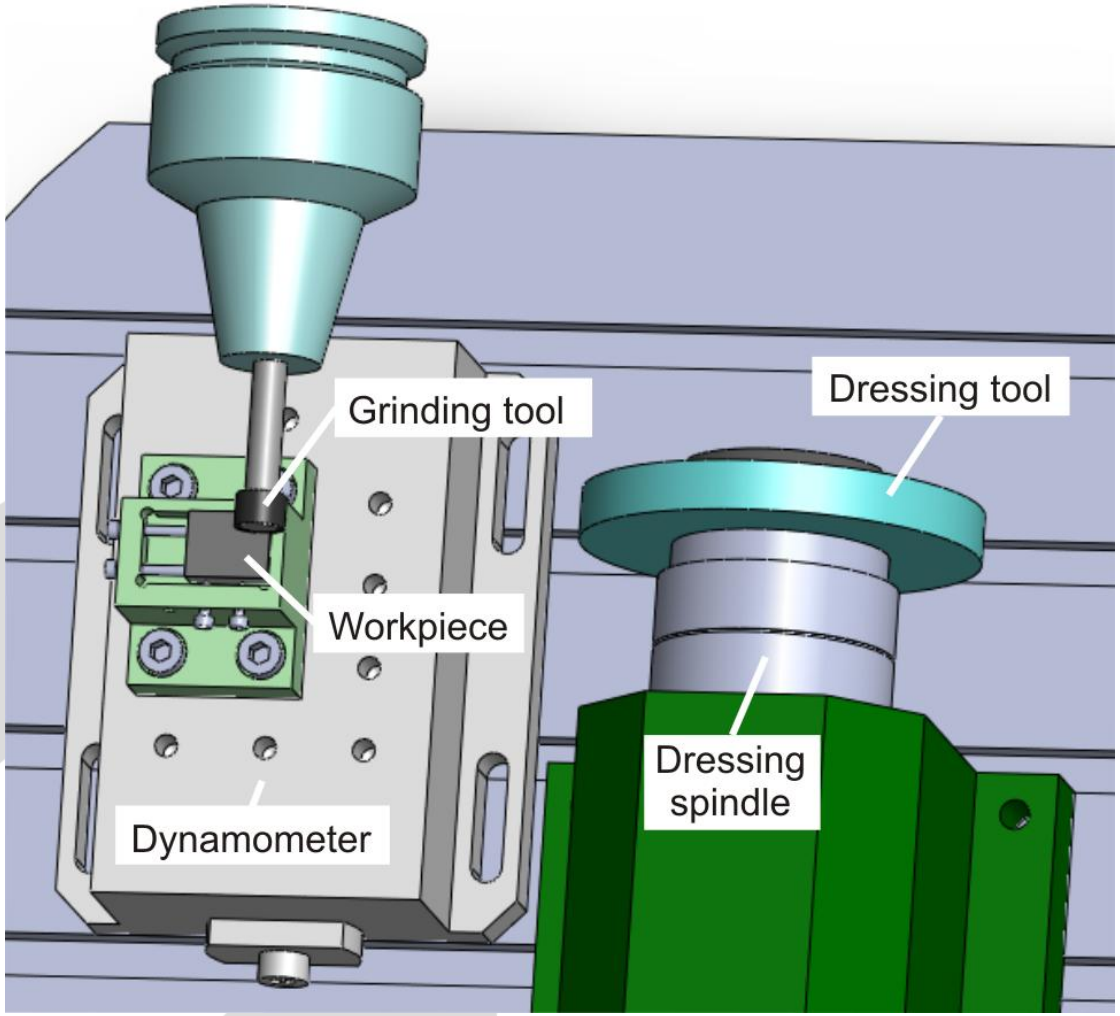

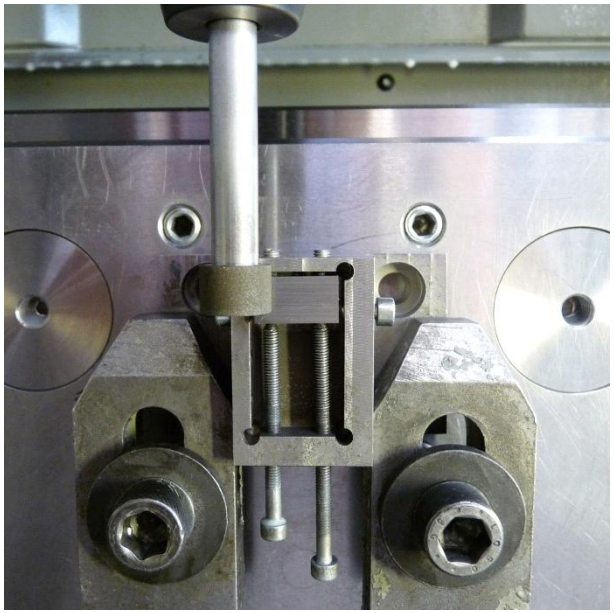

Surface quality (Libo)

unprocessed

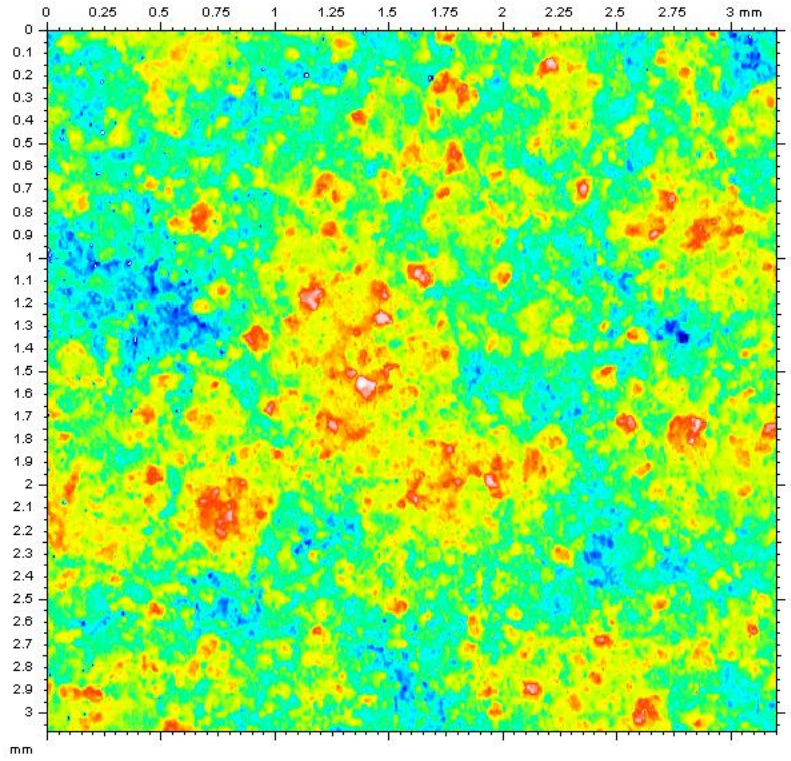

ground

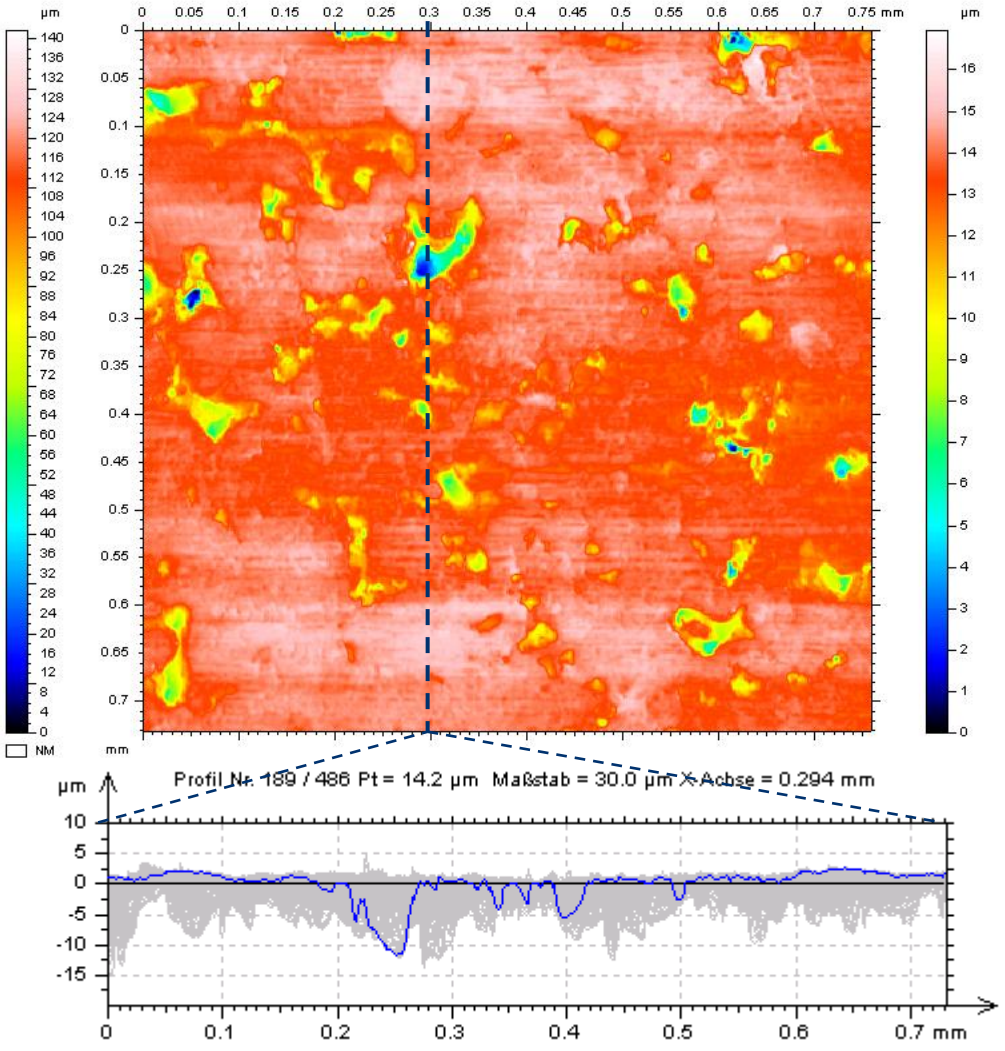

Rz after grinding:

→ Rz = 4,7 - 13,6 µm

Surface quality (HVOF)

unprocessed

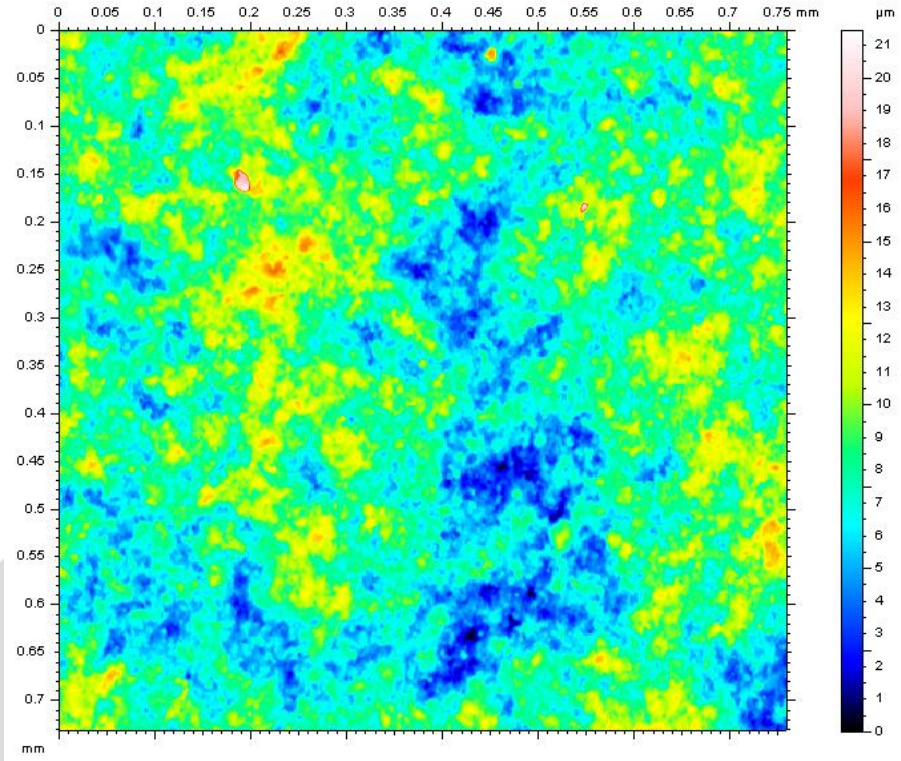

ground

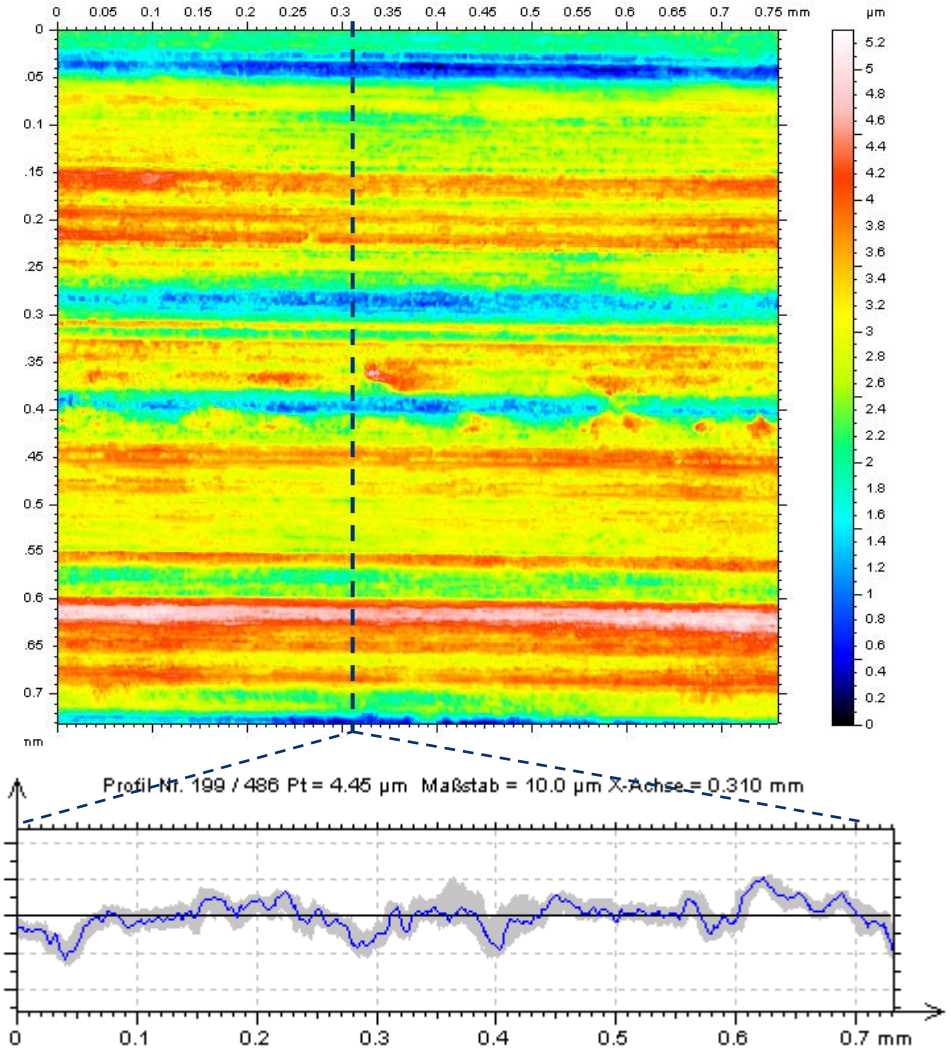

Rz after grinding :

→ Rz = 3,6 - 4,2 µm

Determination of friction coefficients

grinding

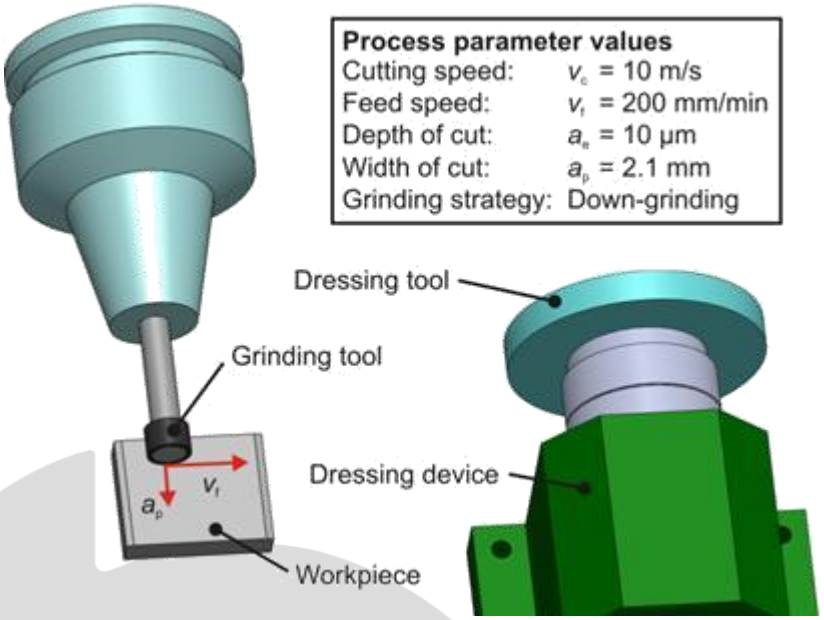

smooth rolling

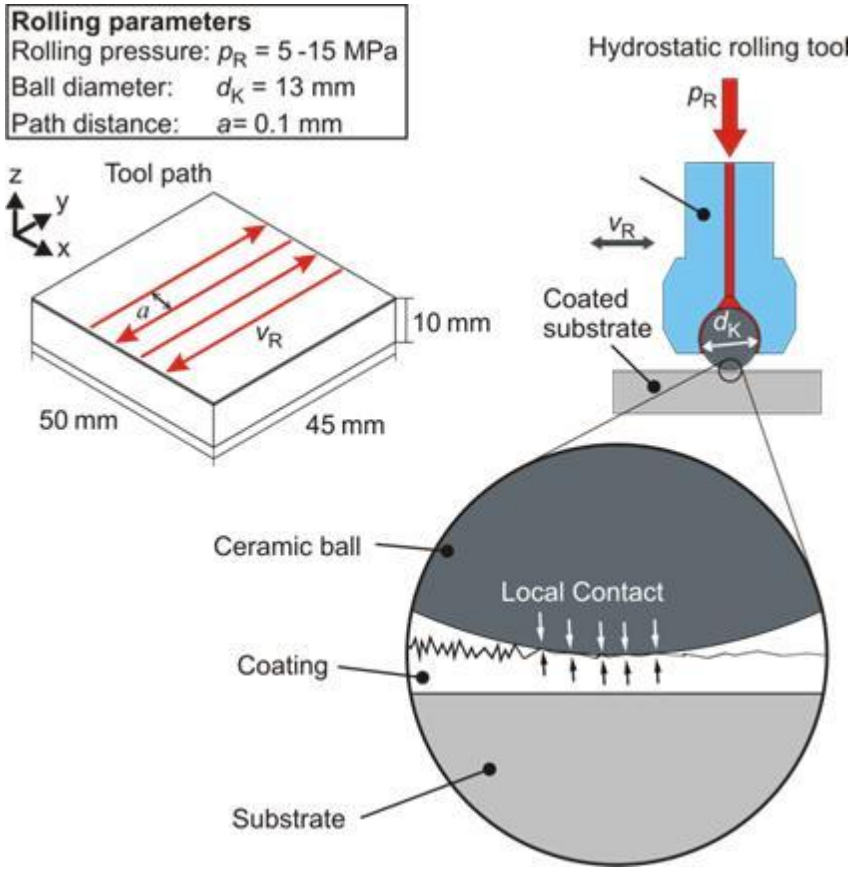

Determination of friction coefficients

strip drawing test

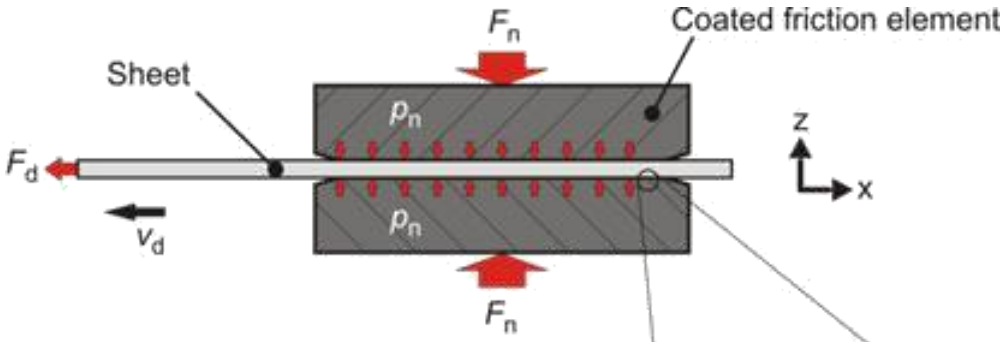

F_n : Normal contact force
p_n : Normal contact pressure
F_d : Drawing force
v_d : Drawing velocity
A_n : Nominal contact area (=1800 mm^2)

Calculation of contact pressure: $p_n = \frac{F_n}{A_n}$

friction element	processing	sheet
T1	unprocessed	S1
T2	grinded in drawing direction	S2
T3	smooth rolling after grinding (p_r = 5Mpa)	S3
T4	smooth rolling after coating (p_r = 5Mpa)	S4
T5	smooth rolling after coating(p_r = 15Mpa)	S5
T6	cross grinded to drawing direction	S6
T7	reference workpiece (C60 steel)	S7
-	reference sheet	S0

Determination of friction coefficients

topography of the friction element

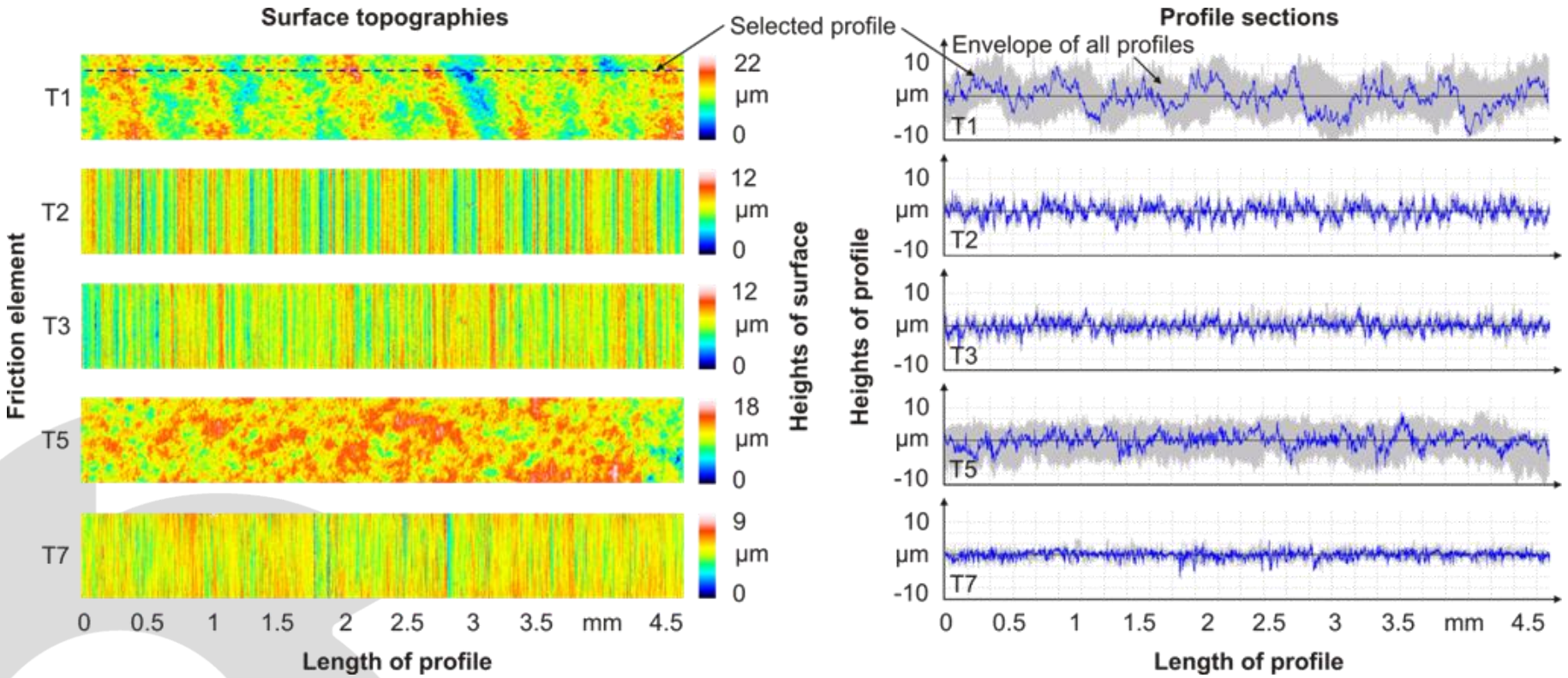

Determination of friction coefficients

topography of the sheet strips

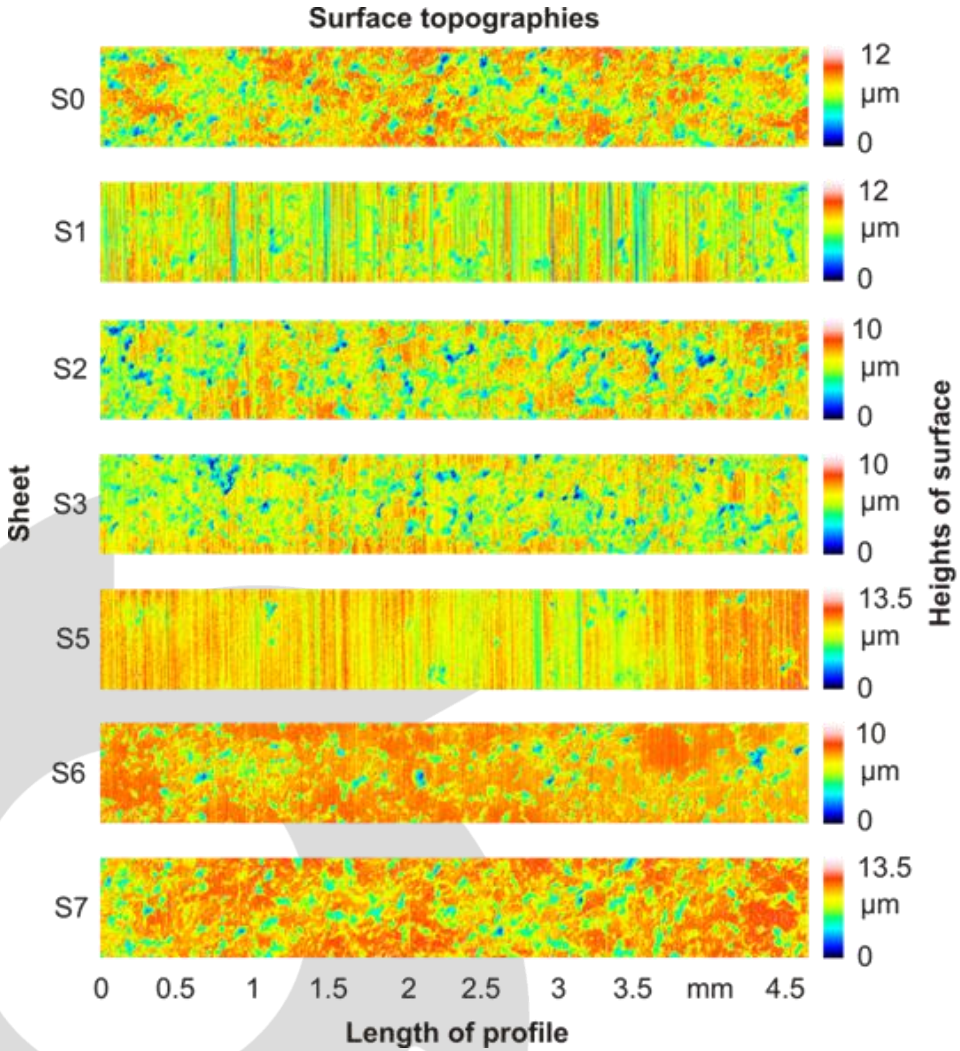

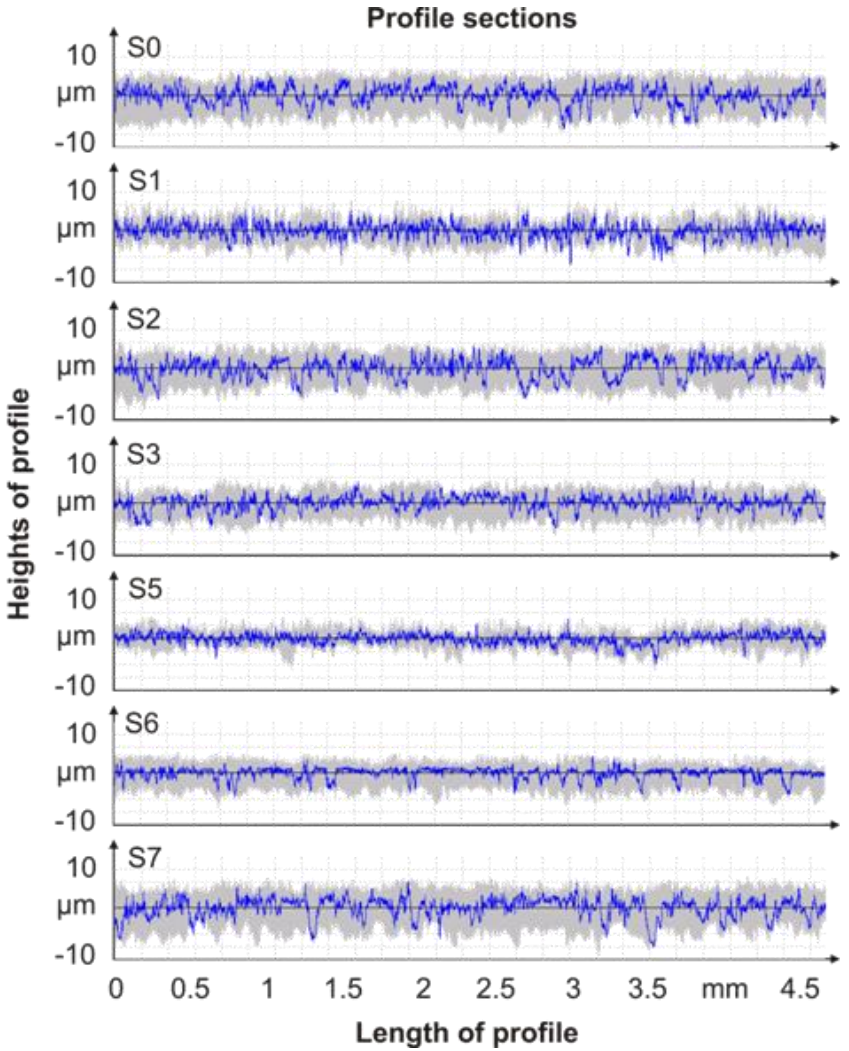

Determination of friction coefficients

roughness of the friction elements

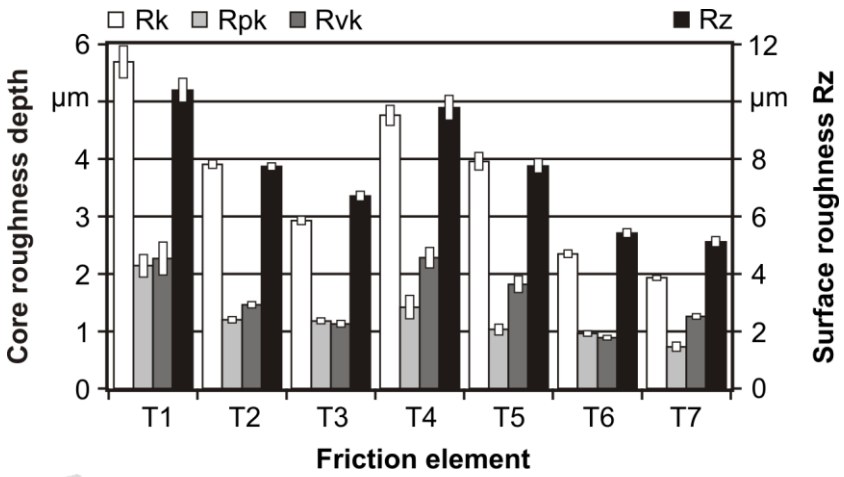

roughness of the sheet strips

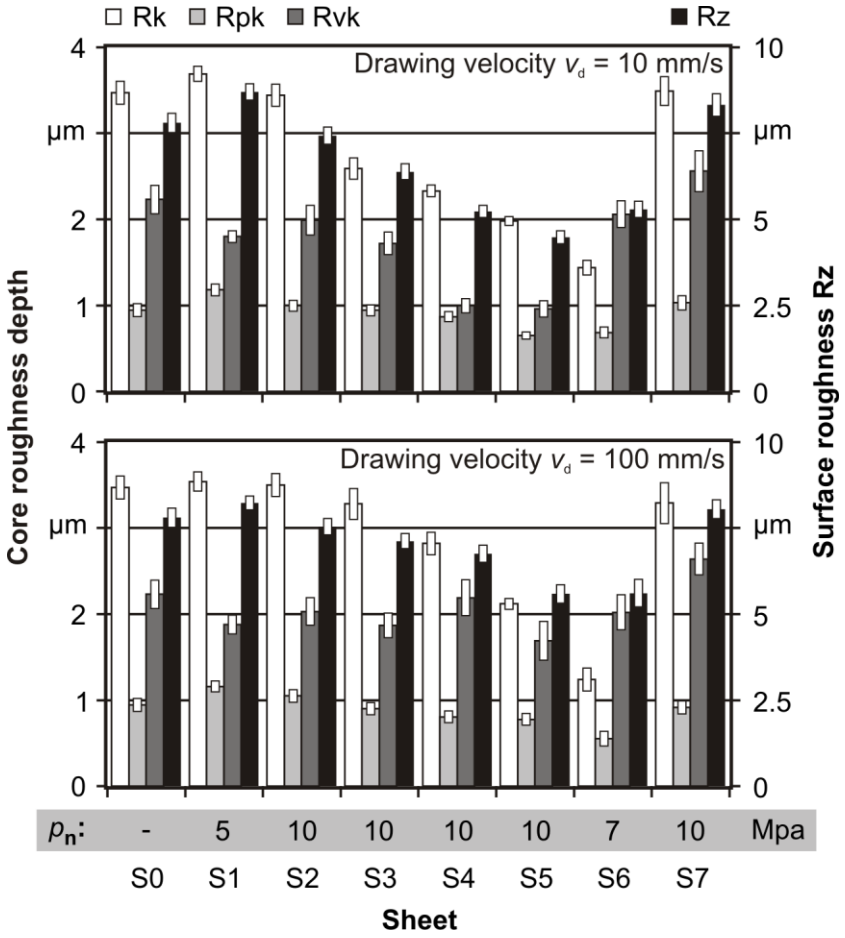

Determination of friction coefficients

friction coefficients

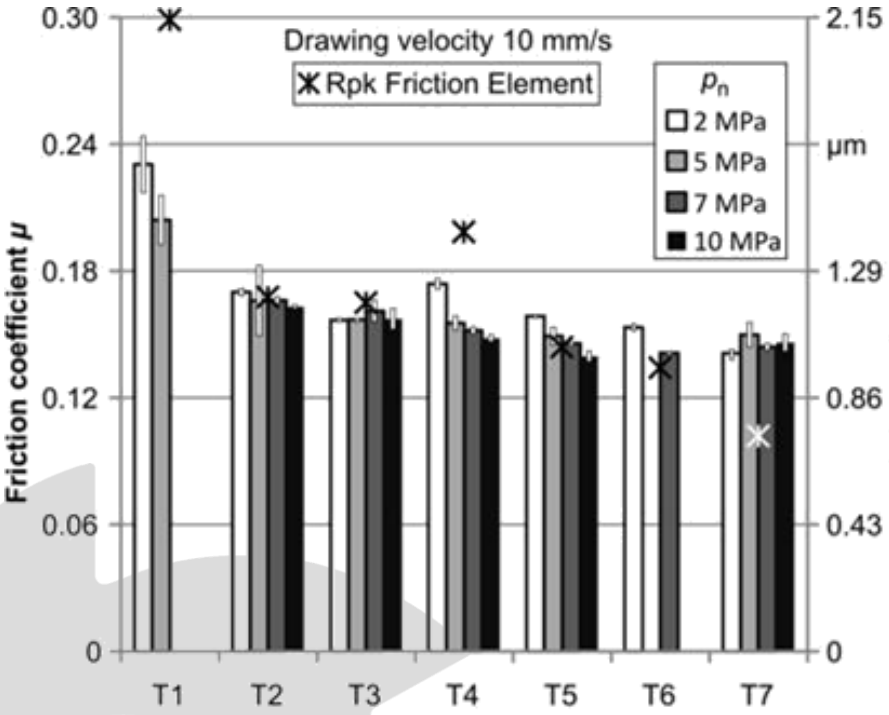

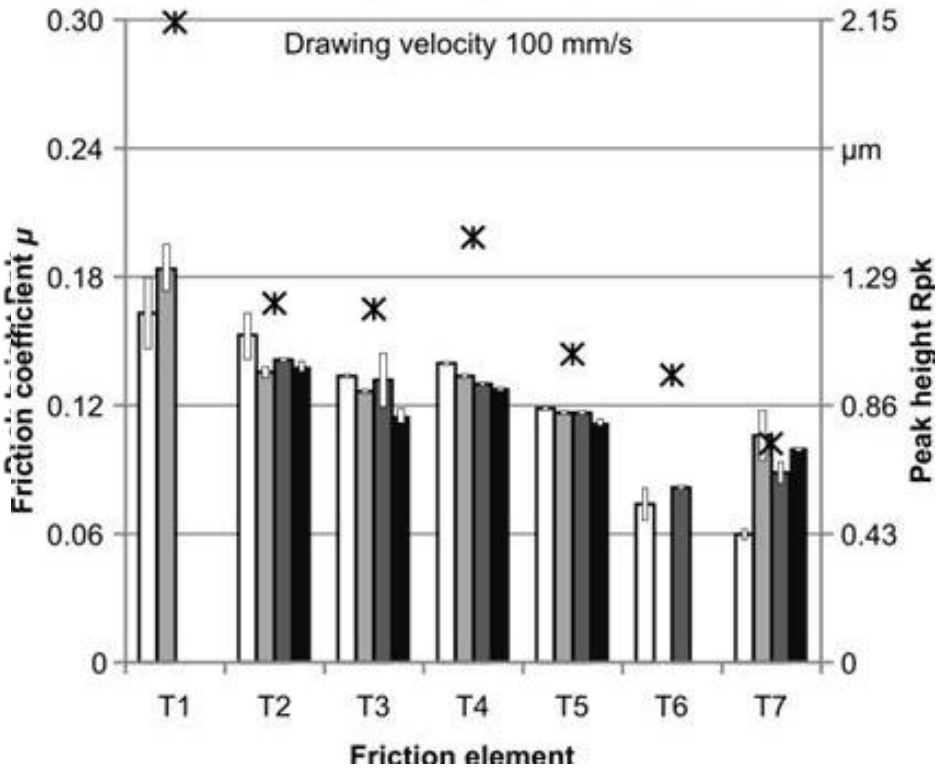

Overview

Introduction

Burr Minimization strategies in Machining Operations

Micro-finishing of hard coated parts

Detection of grinding burn and cracks by acoustic emission

FEM in Internal Traverse Grinding

Machining of low-sulfur steels

Influence of coated surfaces on friction coefficients

Machining of β-titanium alloys

Waviness reduction

Simulation strategies

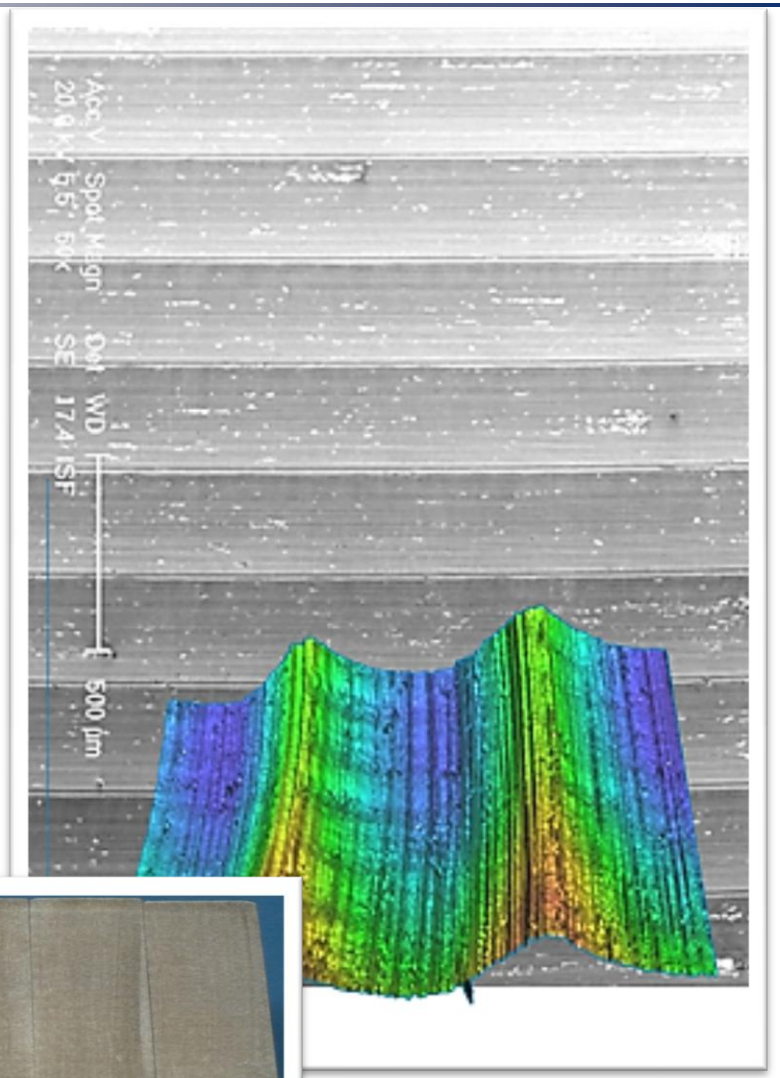

Investigations on the machining of β-titanium alloys

Examples of use

mechanical properties

Material	Ti-10-2-3
Composition	Ti-10V-2Fe-3Al
Young‘s modulus	106 GPa
Density ρ	4.65 g/cm^3
Tensile strength R_m	965-1195 MPa
Yield point $R_{p0.2}$	895-1105 MPa
Fracture strain A	4-8 %

Machining characteristics

Material accumulations on the cutting edge

Snarled chip formation

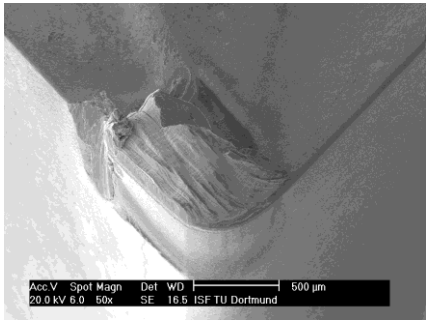

High pressure lubrication supply : influence on the chip form and surface integrity

Material:	Ti-10V-2Fe-3Al, sta
Cutting speed:	v_c = 100 m/min
Feed rate:	f = 0.1 mm
Depth of cut:	a_p = 0.3 mm
Lubrication:	Emul.; p, $\dot{V}$ = Varied

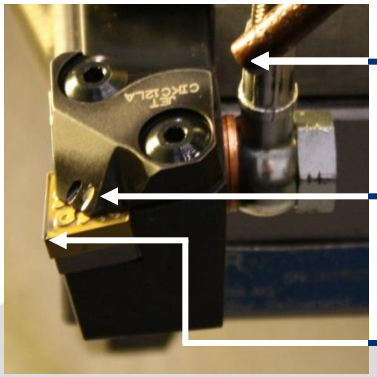

Conventional flood lubrication

p = 2.5 bar
$\dot{V}$ = 40 l/min

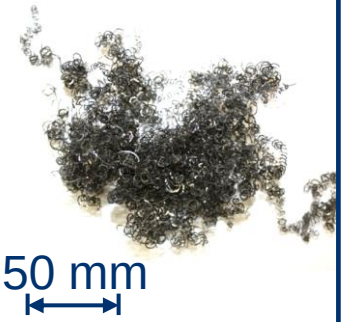

High pressure cooling (emulsion)

p = 65 bar
$\dot{V}$ = 25.8 l/min

High pressure cooling (CO_2)

p = 65 bar

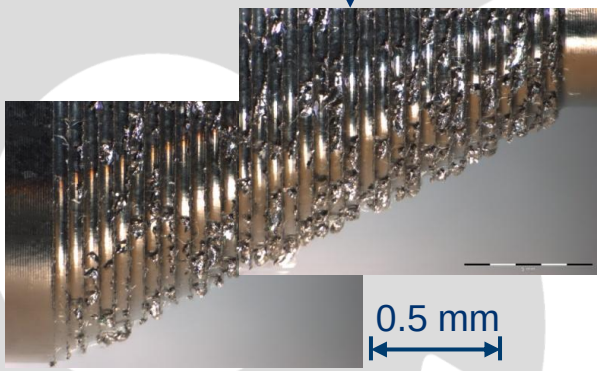

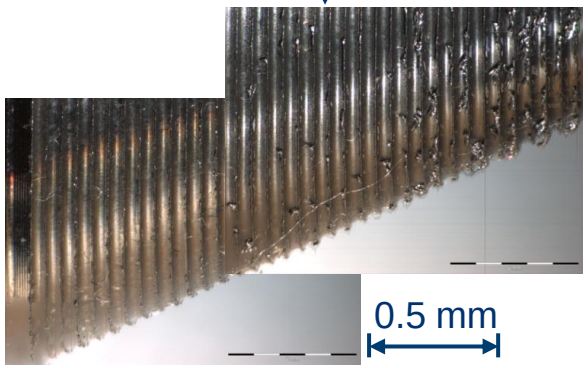

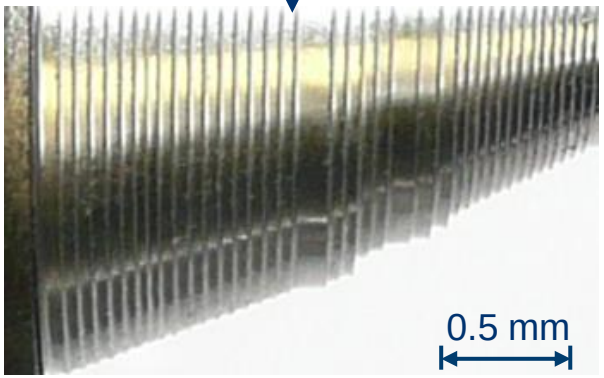

CO_2-high pressure cooling

Working room conditions after the process

- Sublimation of CO_2 and ice crystals
- Sample purification of lubrication residua not necessary

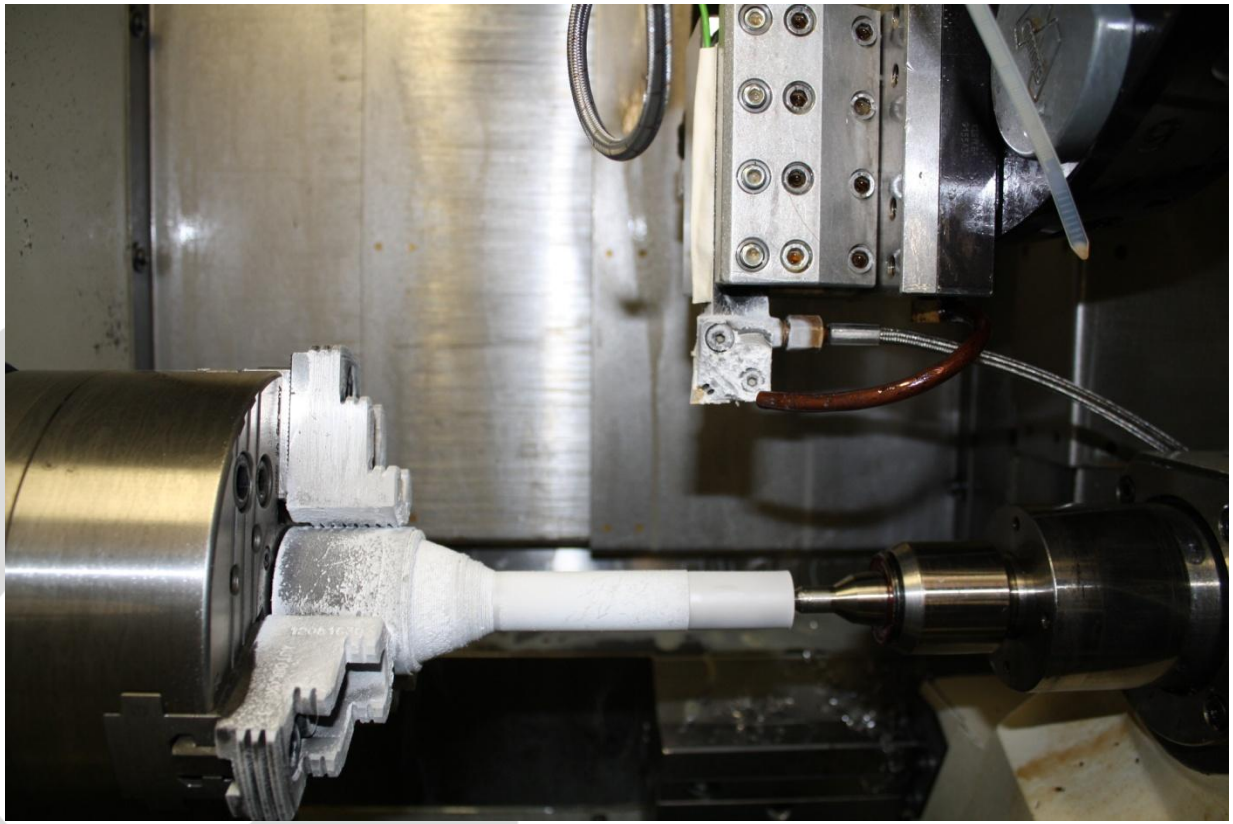

High pressure cooling CO_2

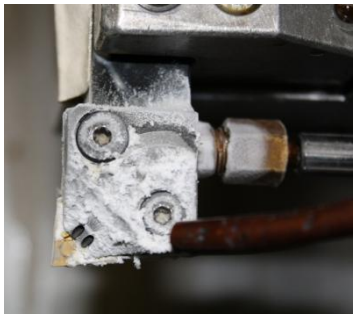

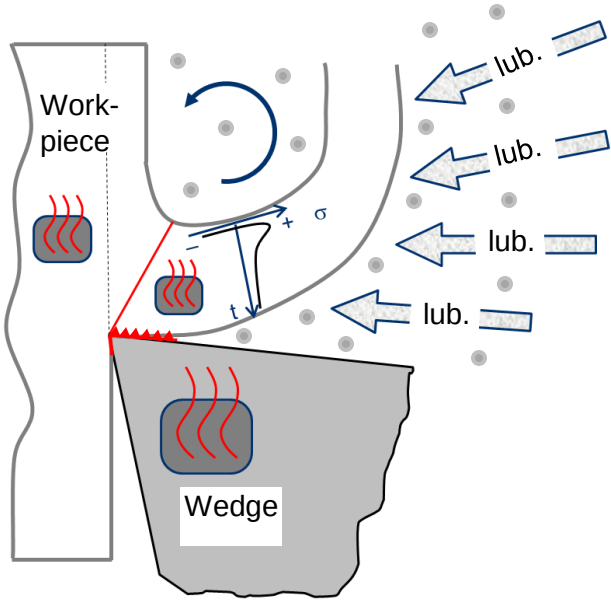

CO_2-high pressure cooling

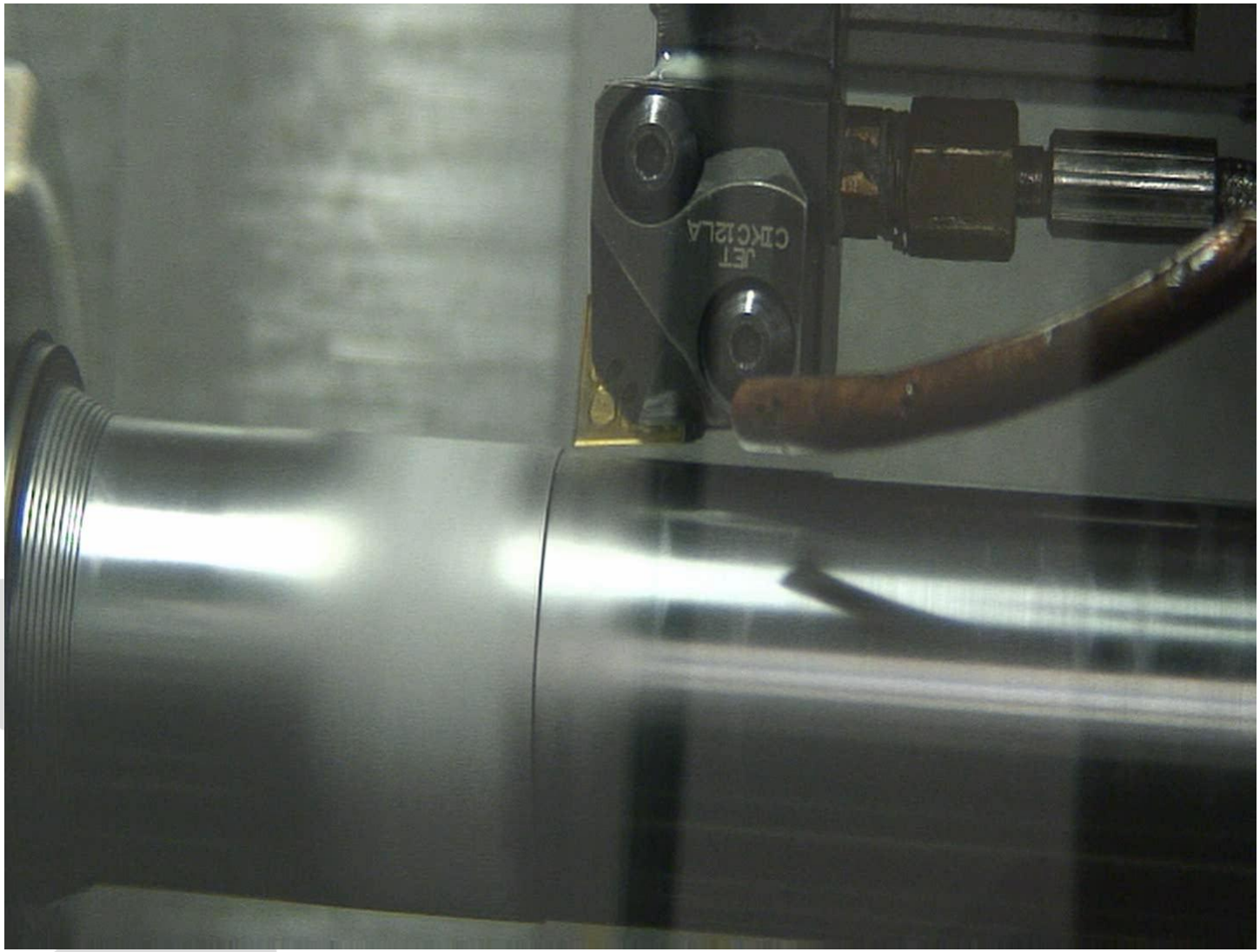

Influence of the lubrication concept on the tool wear

Material:	Ti-10V-2Fe-3Al	**Cutting speed:**	v_c = 100 m/min
Heat treatment:	lös. + ausgelagert (sta)	**Feed:**	f = 0.1 mm
Tool:	CNMG120404-MF4	**Depth of cut:**	a_p = 0.3 mm
Cutting tool mat.:	HC, (Ti,Al)N	**Lub. concept:**	Variable

0.5 mm

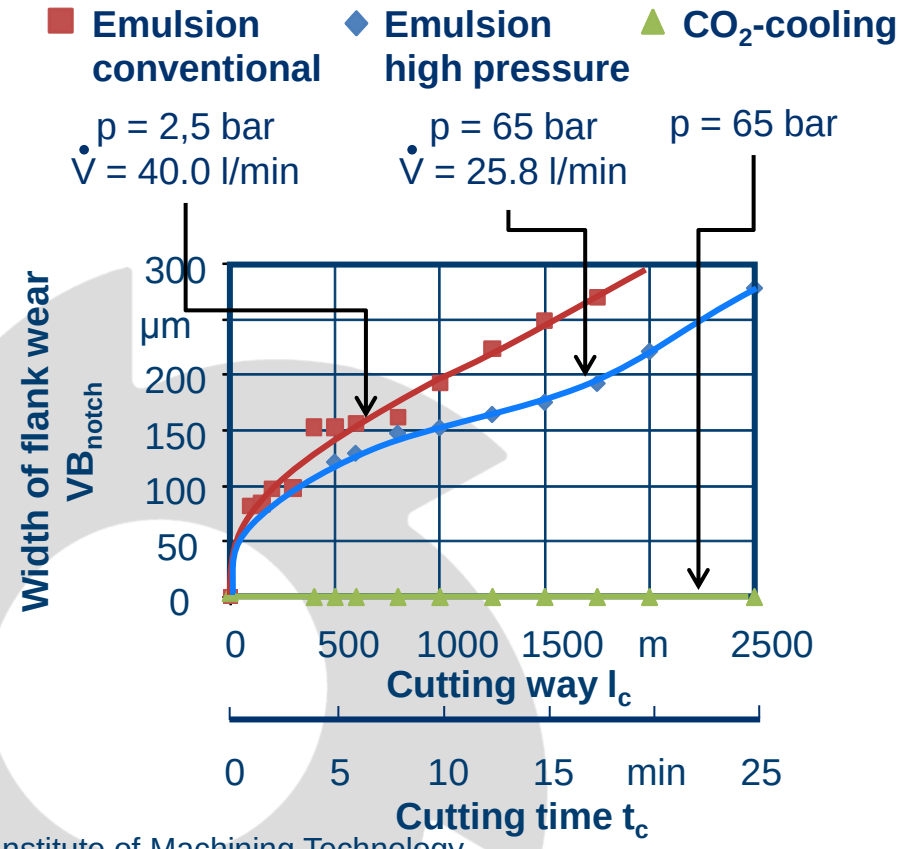

l_c = 1000 m — **Tool life**

Emulsion conventional

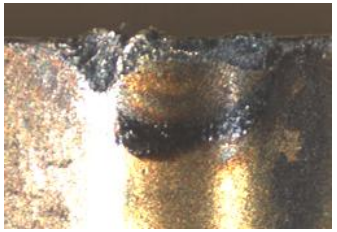

l_c = 1750 m
t_c = 17.5 min
$\overline{VB}$ = 140 µm
VB_n = 270 µm

Emulsion high pressure

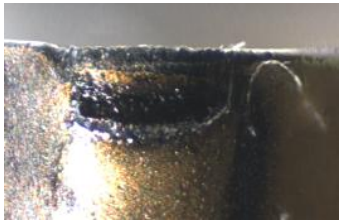

l_c = 2500 m
t_c = 25.0 min
$\overline{VB}$ = 159 µm
VB_n = 258 µm

CO_2-cooling

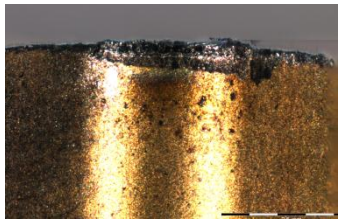

l_c = 2500 m
t_c = 25.0 min
$\overline{VB}$ = 99 µm
VB_n = 0 µm

Overview

Introduction

Burr Minimization strategies in Machining Operations

Micro-finishing of hard coated parts

Detection of grinding burn and cracks by acoustic emission

FEM in Internal Traverse Grinding

Machining of low-sulfur steels

Influence of coated surfaces on friction coefficients

Machining of β-titanium alloys

Waviness reduction

Simulation strategies

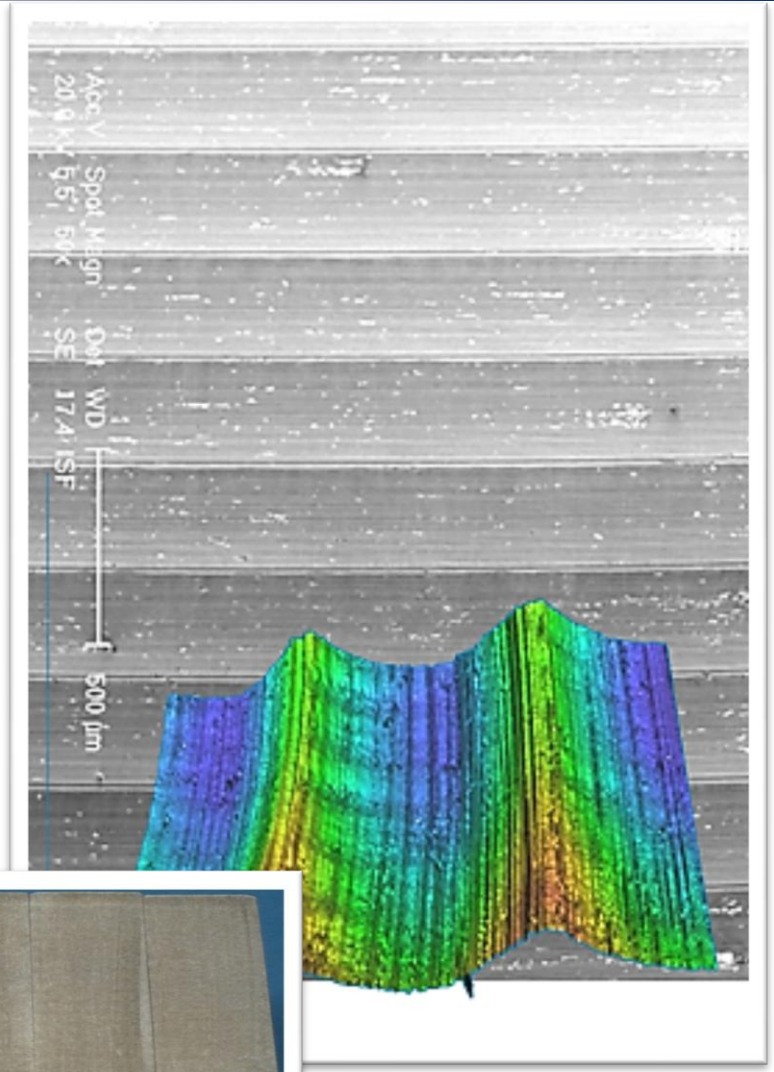

Influence of phase shifting onto the workpiece surface

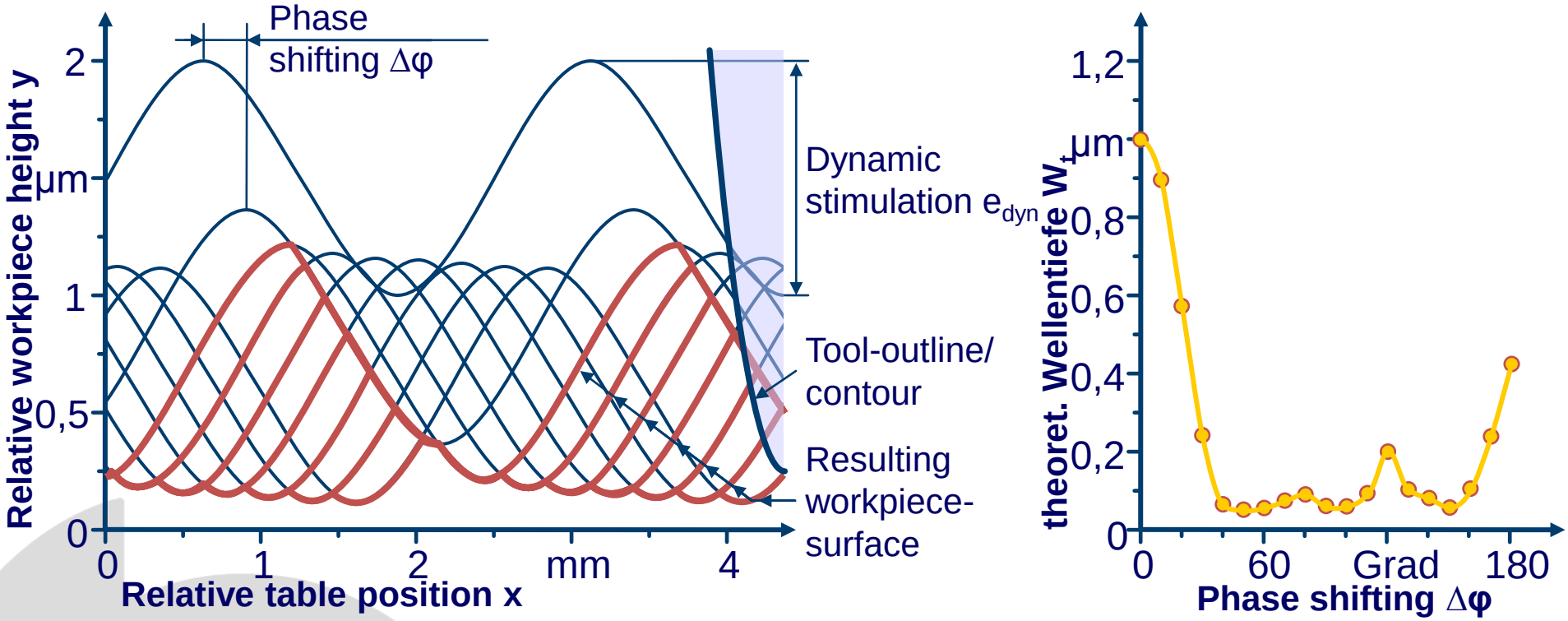

Model assumptions:

Tangential feed	f_t = 3 mm
Depth of cut	a_e = 0,014 mm
Resilience while spark out	calculated with normal-grinding-force
Diameter of tool	d_s = 280 mm
Dynamic stimulation	e_{dyn} = 1 µm
Process configuration	10 spark out strokes

Surface pattern while flat grinding with vertical feed

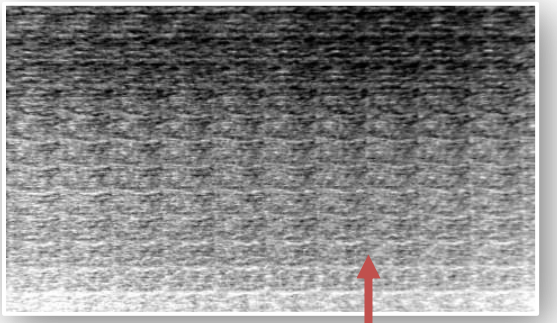

$\Delta\varphi = 0° \rightarrow \lambda_f = 0°$

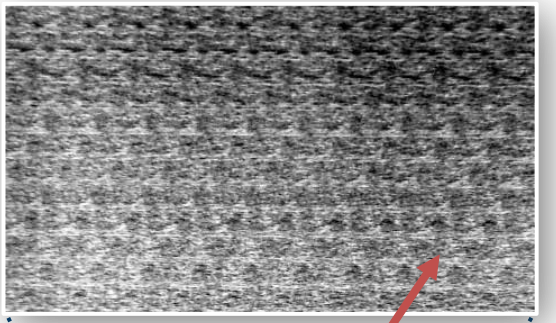

$\Delta\varphi = 120° \rightarrow \lambda_f = 30°$

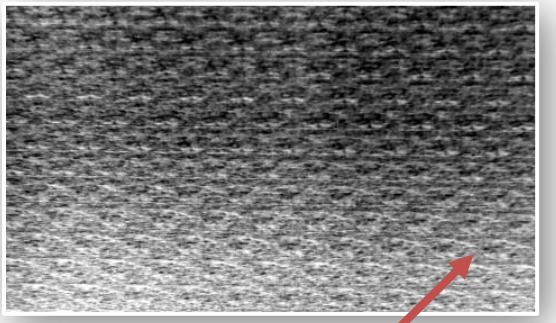

$\Delta\varphi = 180° \rightarrow \lambda_f = 45°$

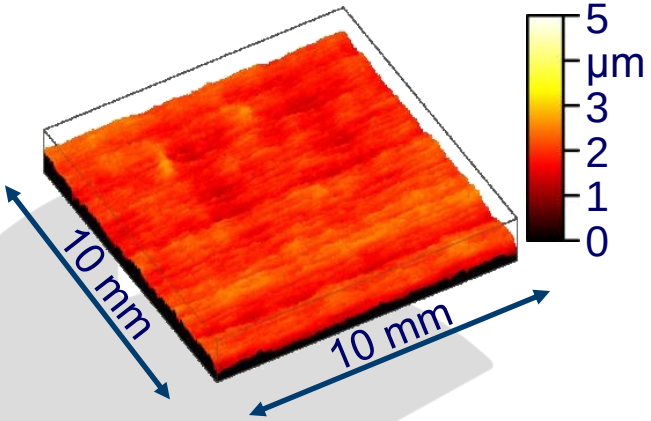

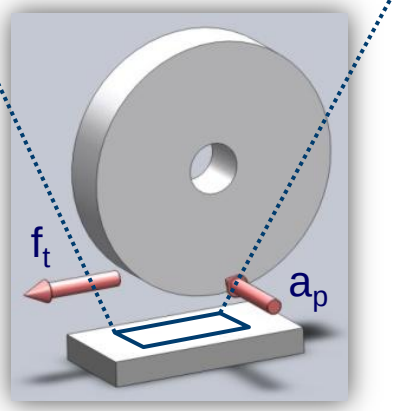

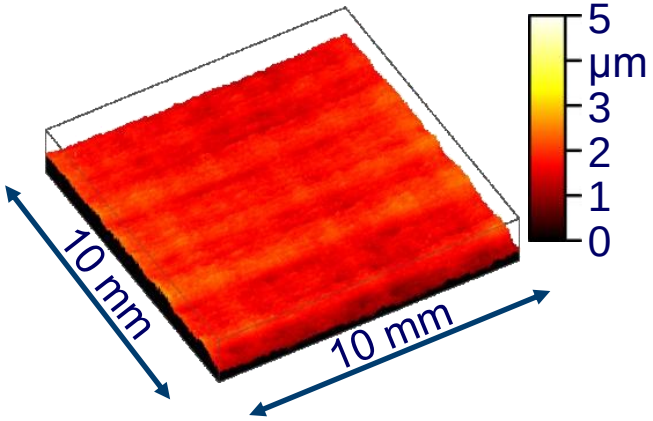

Tool	sintered corundum grinding wheel 3A 54 G/H 162 V635
Workpiece	X210CrW12, ca. 62 HRC, 80 mm x 40 mm
Cutting speed	v_c = 30 m/s
Tangential feed	f_t = 4 mm
Line distance	a_p = 2 mm

Surface pattern while flat grinding

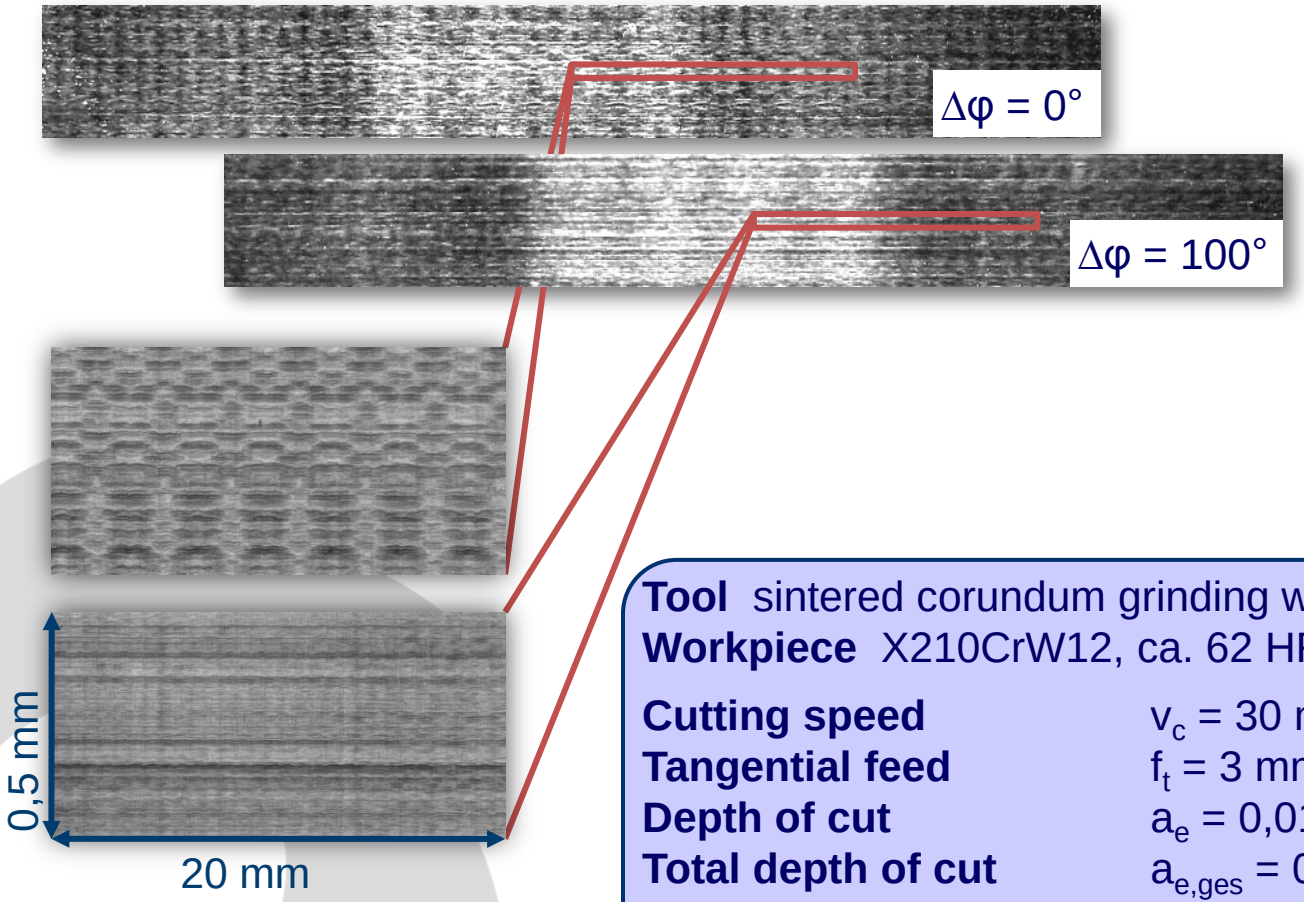

Tool sintered corundum grinding wheel 3A 54 G/H 162 V635
Workpiece X210CrW12, ca. 62 HRC, 80 mm x 10 mm

Cutting speed	v_c = 30 m/s
Tangential feed	f_t = 3 mm
Depth of cut	a_e = 0,014 mm
Total depth of cut	$a_{e,ges}$ = 0,210 mm
Process configuration	10 spark out strokes, varied phase shifting

„first impression“ of workpiece surfaces

$$\text{Brightness} \sim \frac{\text{Reflection}}{\text{Scattering}}$$

$$\text{sensation magnitude: } S_0 = k\frac{\Delta_{q\,rough}}{\Delta_{q\,fine}} \sim S_1 = \frac{W\Delta q \,/\, (W\Delta q_{max} \in W\Delta q_i)}{R\Delta q \,/\, (R\Delta q_{max} \in R\Delta q_i)}$$

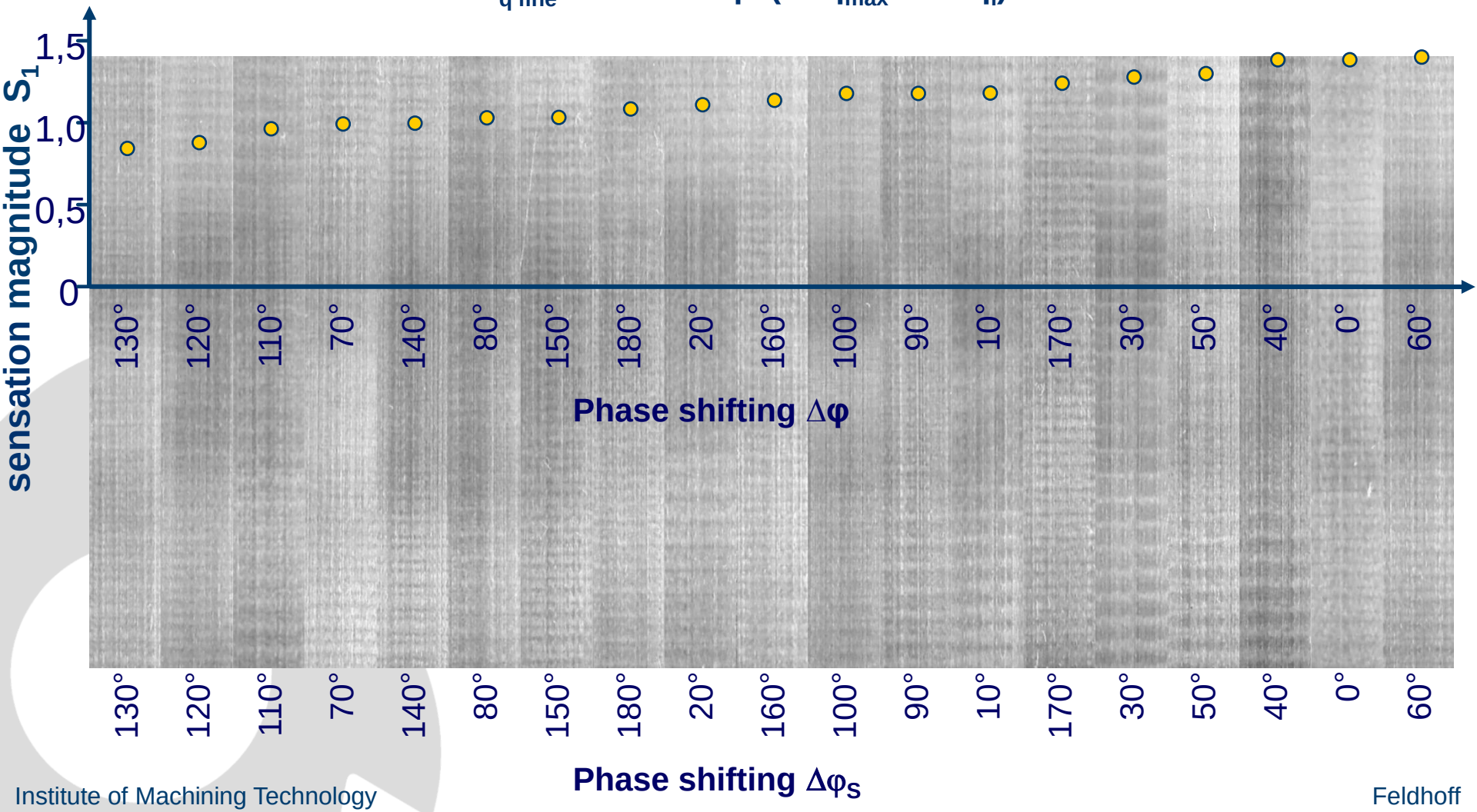

Dynamic process characteristics

Tool	sintered corundum grinding wheel 3A 54 G/H 162 V635
Workpiece	X210CrW12, ca. 62 HRC, 80 mm x 10 mm
Cutting speed	v_c = 28 m/s
Feed velocity	v_f = 30 m/min
Depth of cut	a_e = 0,003 mm
Total depth of cut	$a_{e,ges}$ = 0,300 mm
Process configuration	varied phase shifting

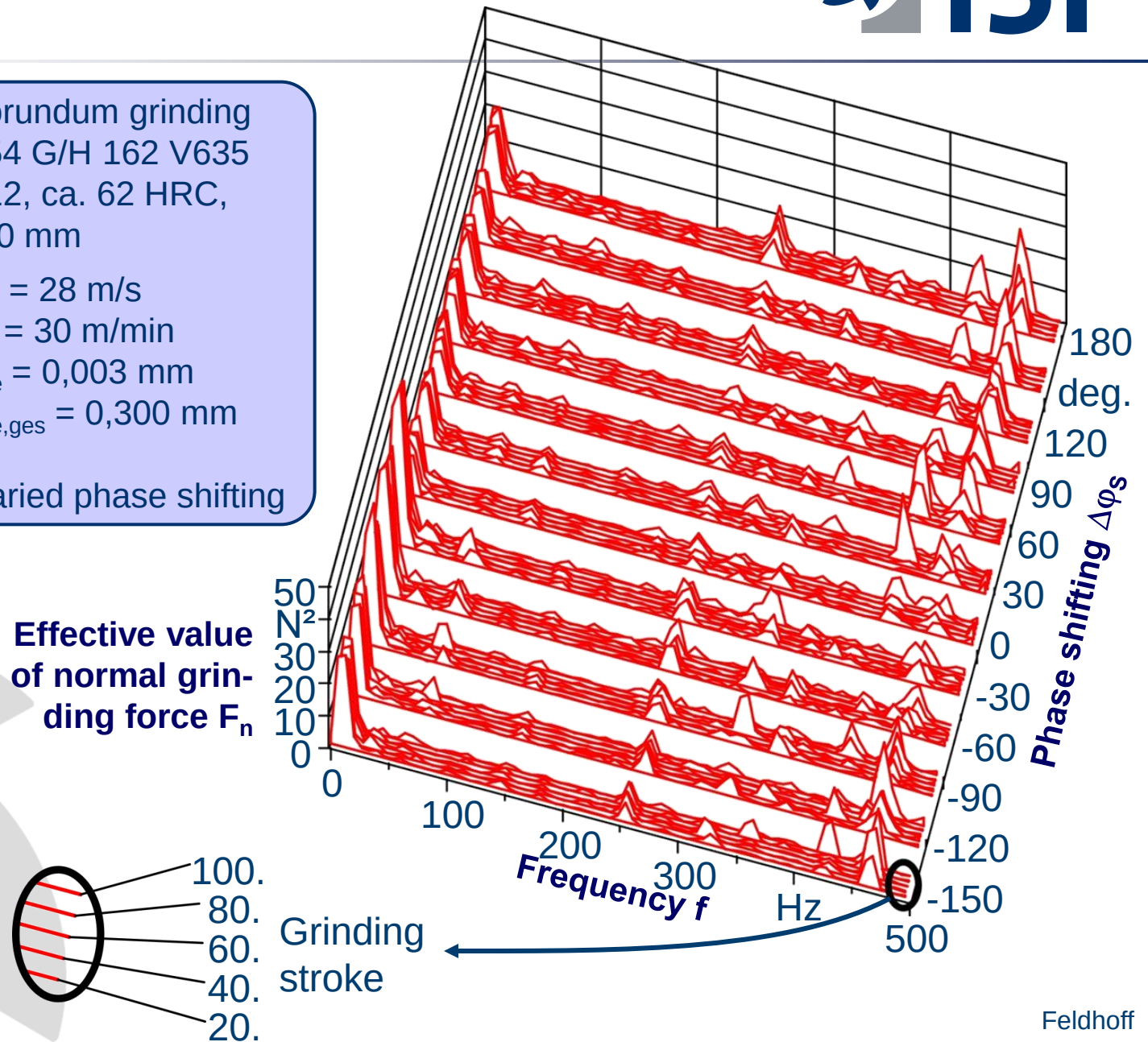

Modification of contact stiffness

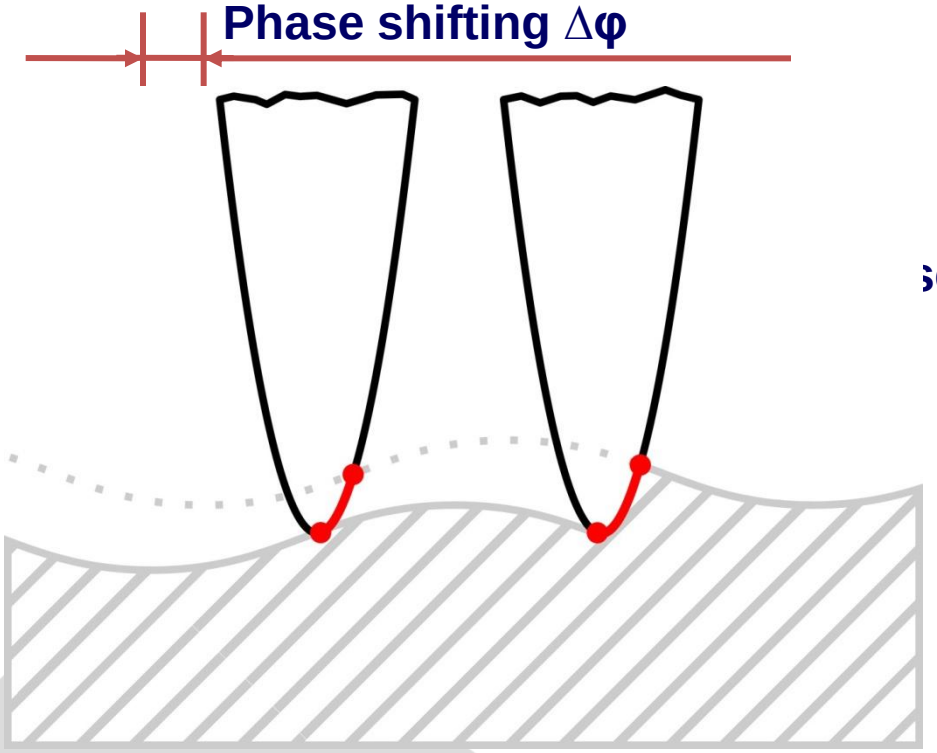

Phasenverschiebung Δφ = 30°

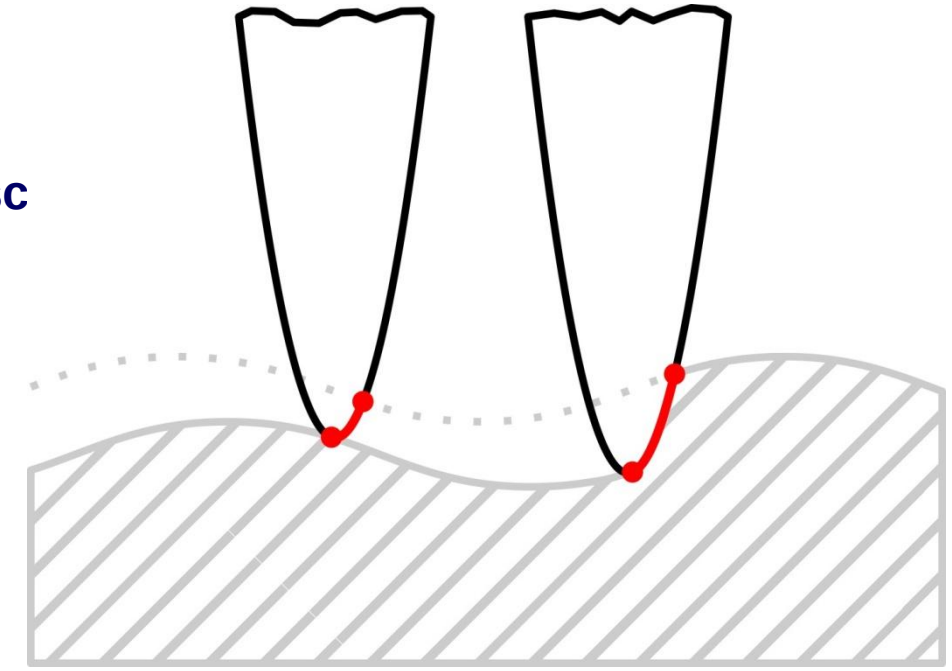

Phasenverschiebung Δφ = -30°

Real Engangement situation while testing (Heights 500 times magnified)

Tool sintered corundum grinding wheel 3A 54 G/H 162 V635
Workpiece X210CrW12, ca. 62 HRC, 80 mm x 40 mm

Cutting speed	v_c = 28 m/s
Tangential feed	f_t = 15 mm
Depth of cut	a_e = 0,003 mm
Total depth of cut	$a_{e,ges}$ = 0,300 mm

Influence of dynamic stimulation

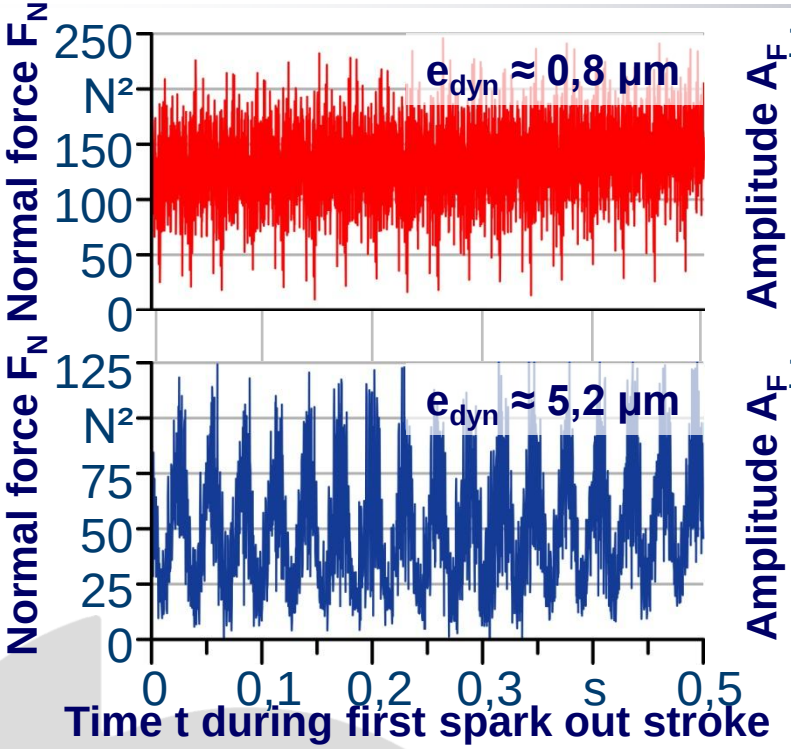

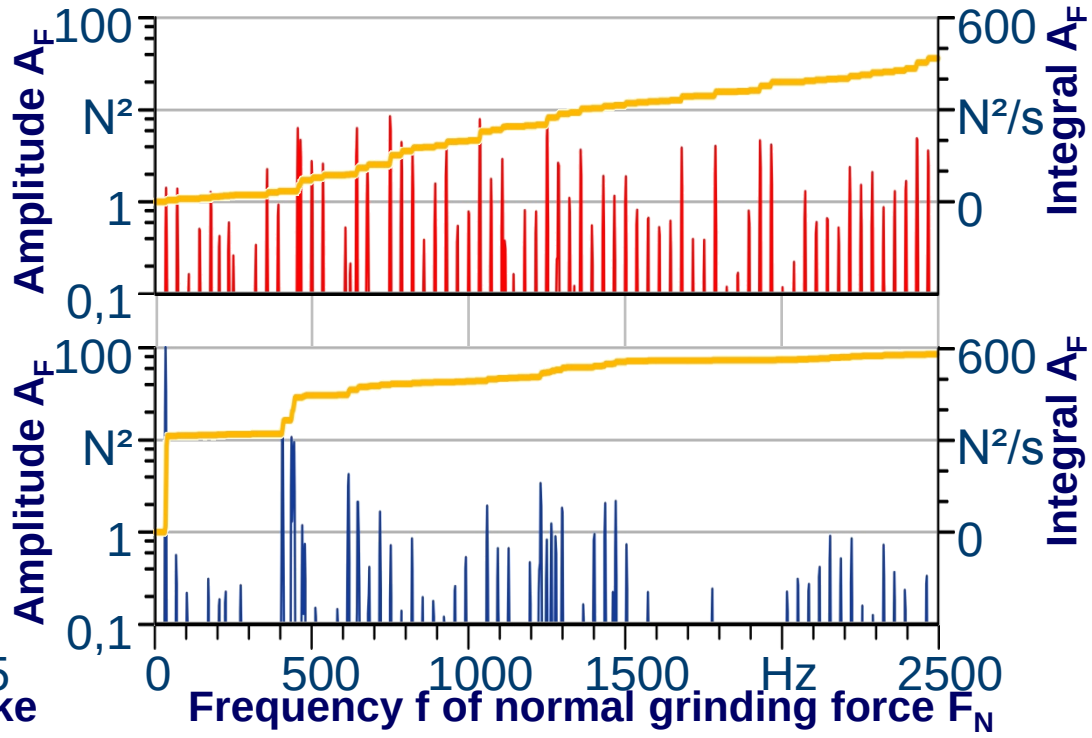

Cutting speed	v_c = 30 m/s
Feed velocity	v_f = 6,5 m/min
Depth of cut	a_e = 0,014 mm
Total depth of cut	$a_{e,ges}$ = 0,210 mm
Process configuration	8 spark out strokes, Δφ = -70°

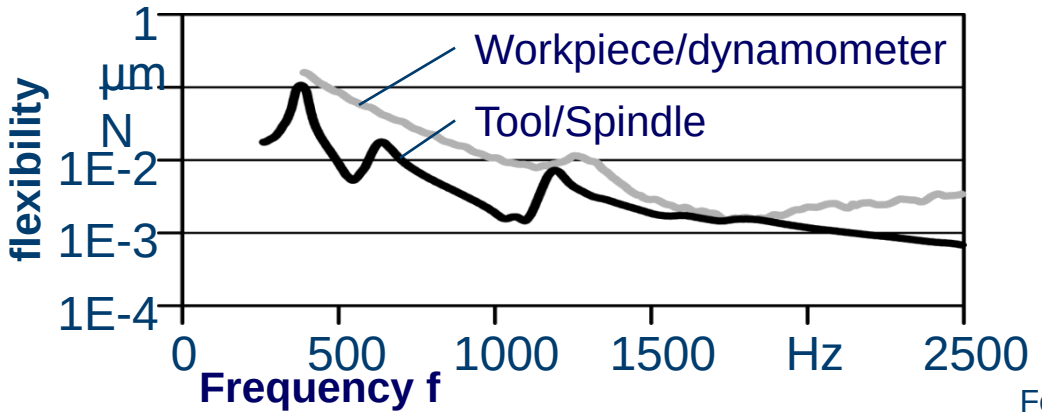

Overview

Introduction

Burr Minimization strategies in Machining Operations

Micro-finishing of hard coated parts

Detection of grinding burn and cracks by acoustic emission

FEM in Internal Traverse Grinding

Machining of low-sulfur steels

Influence of coated surfaces on friction coefficients

Machining of β-titanium alloys

Waviness reduction

Simulation strategies

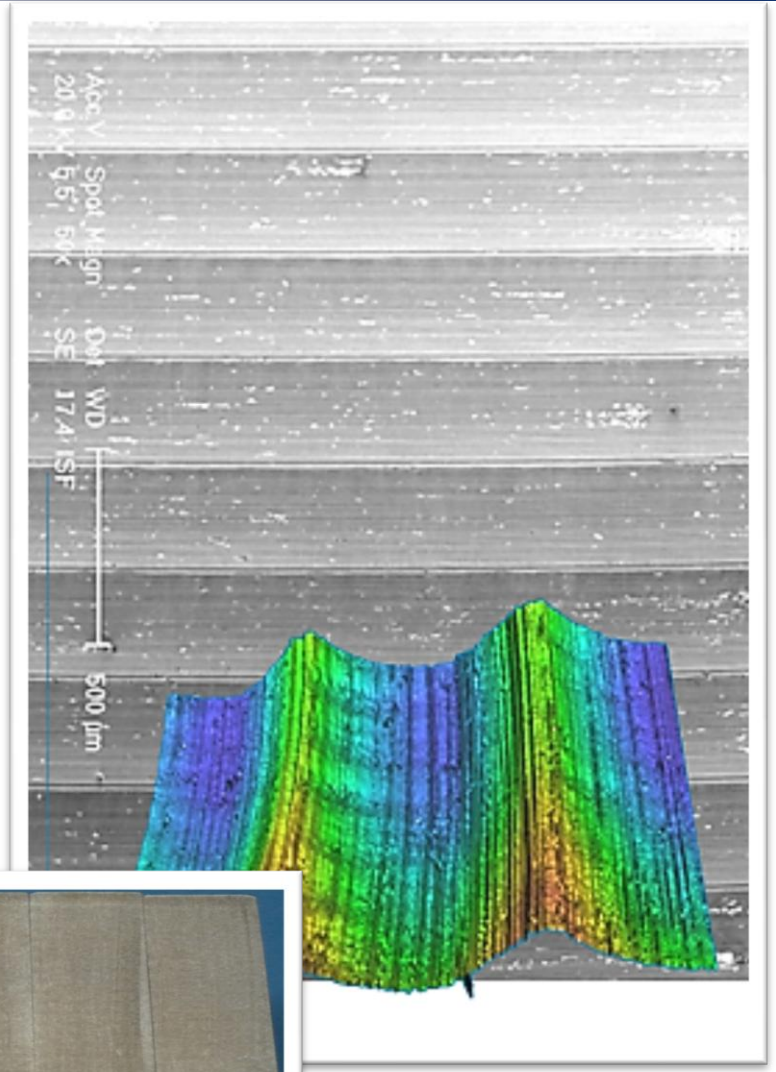

Simulation (Example Height Model/Dexel Model)

Height model/dexel model

Characteristics (height model):

- Surface defined by height values over two-dimensional grid
- Suited for 3-axis simulation
- Not suited for undercuts

Characteristics (dexel model):

- Surface defined by one or more value pairs over two-dimensional grid
- Pairs of values define entry into and exit out of material
- Suited for 5-axis simulation
- Suited for undercuts

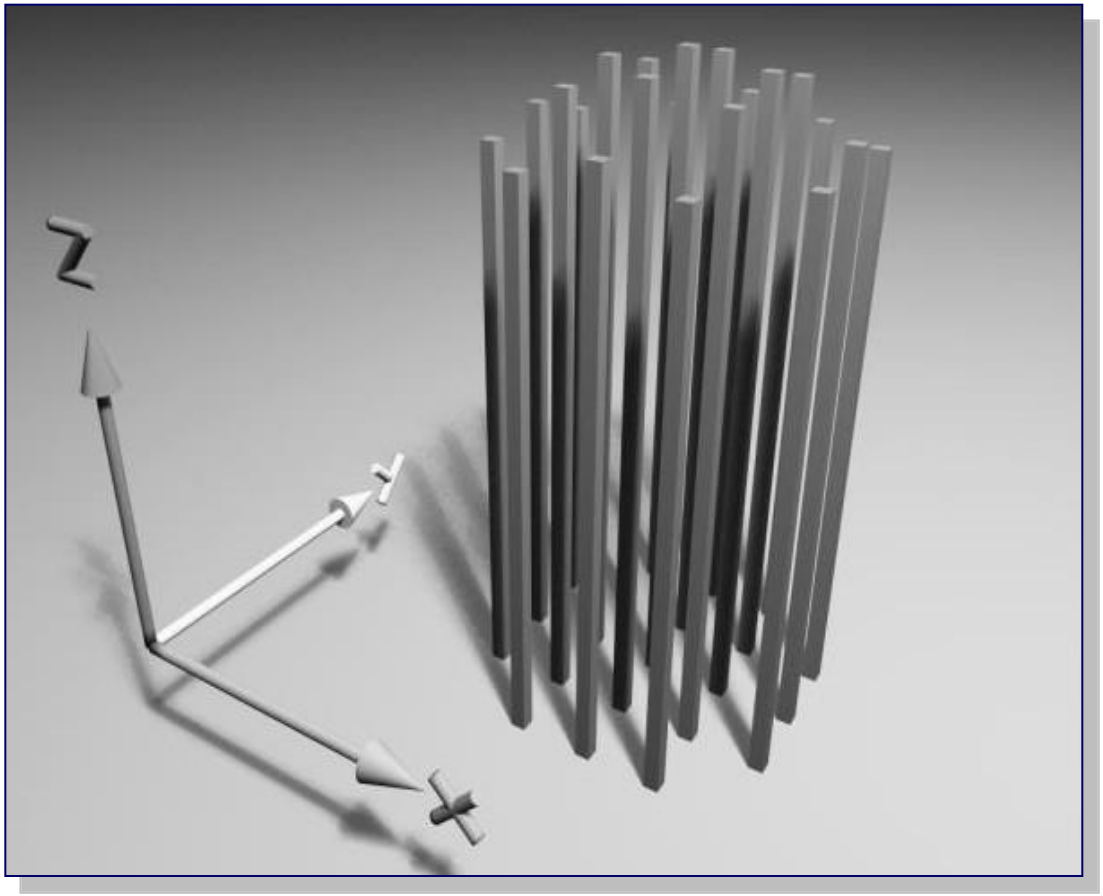

Simulation (Example Height Model/Dexel Model)

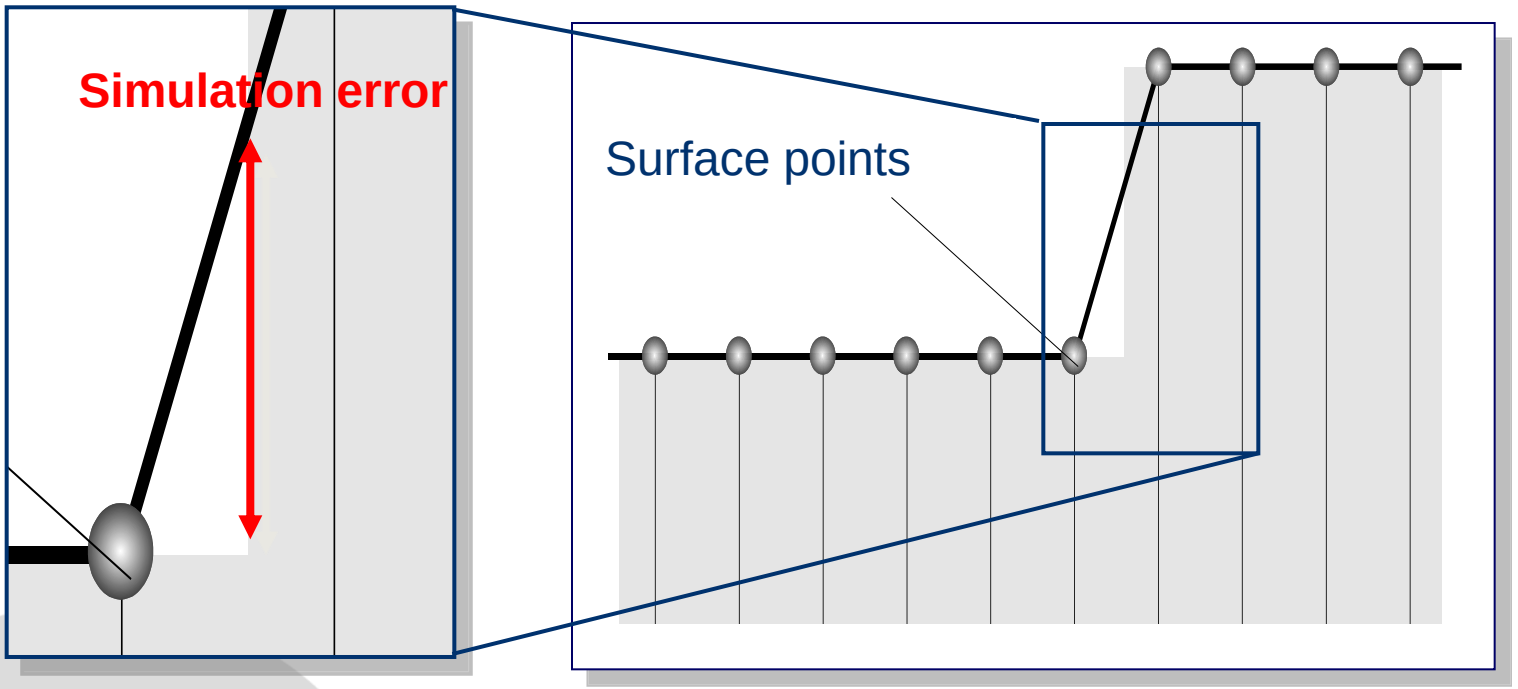

The reconstructed surface is inaccurate for steep slopes which are almost parallel to z-direction.

Solution:
Multi-dexel model

Simulation (Example Height Model/Dexel Model)

Two-dimensional model

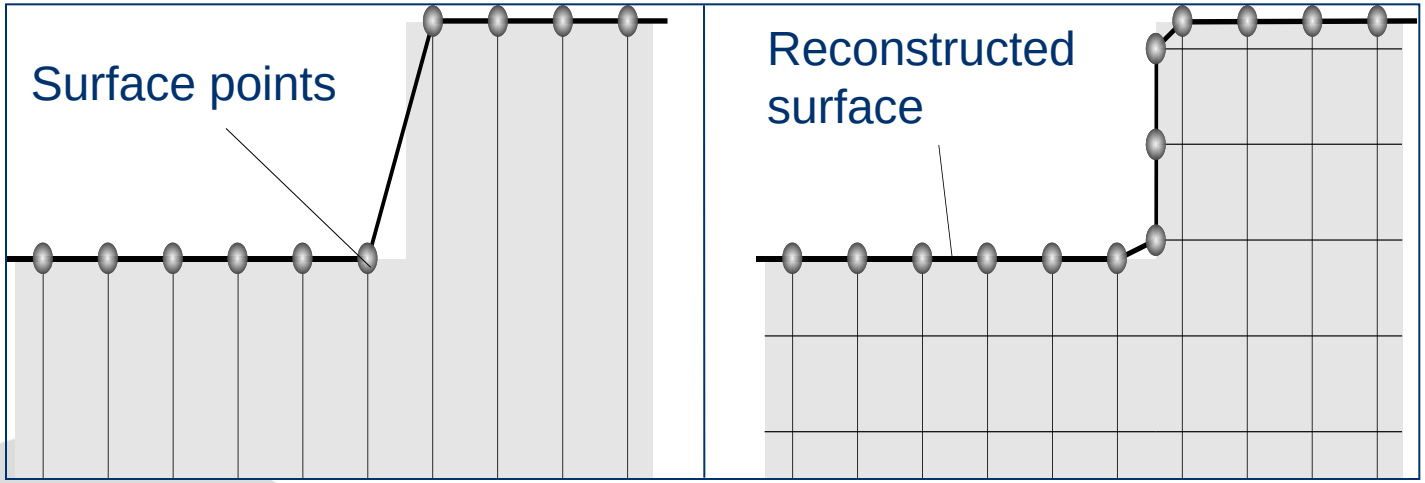

Reduction of the contour error of the dexel model (left) by using a multi-dexel model (right)

Simulation (Example Height Model/Dexel Model)

Three-dimensional model

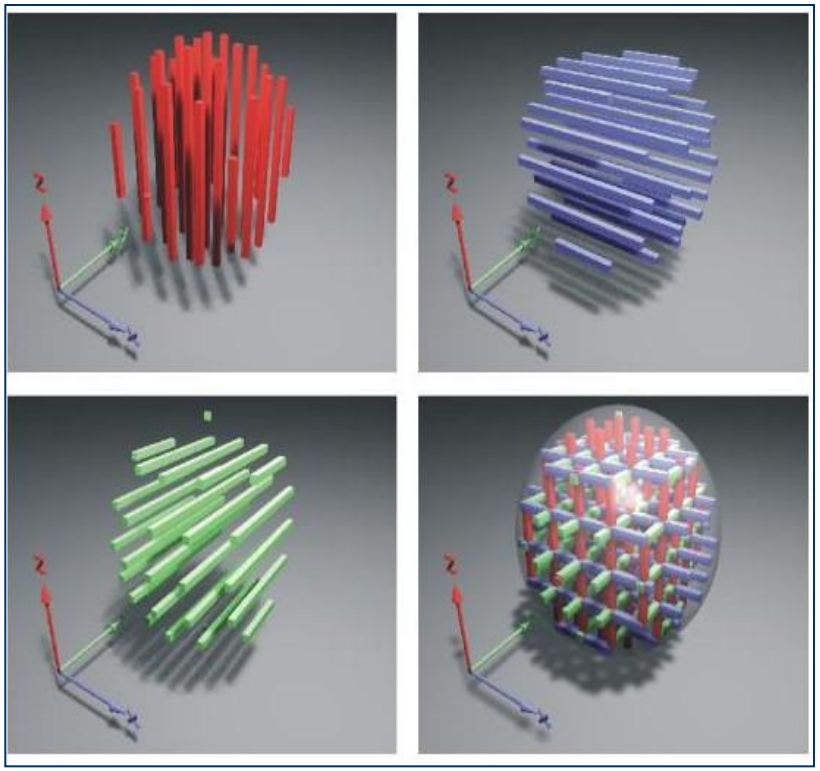

Representation of a sphere as a multi-dexel model (ru), which is defined by three single dexel models

Simulation example

Simulation tests

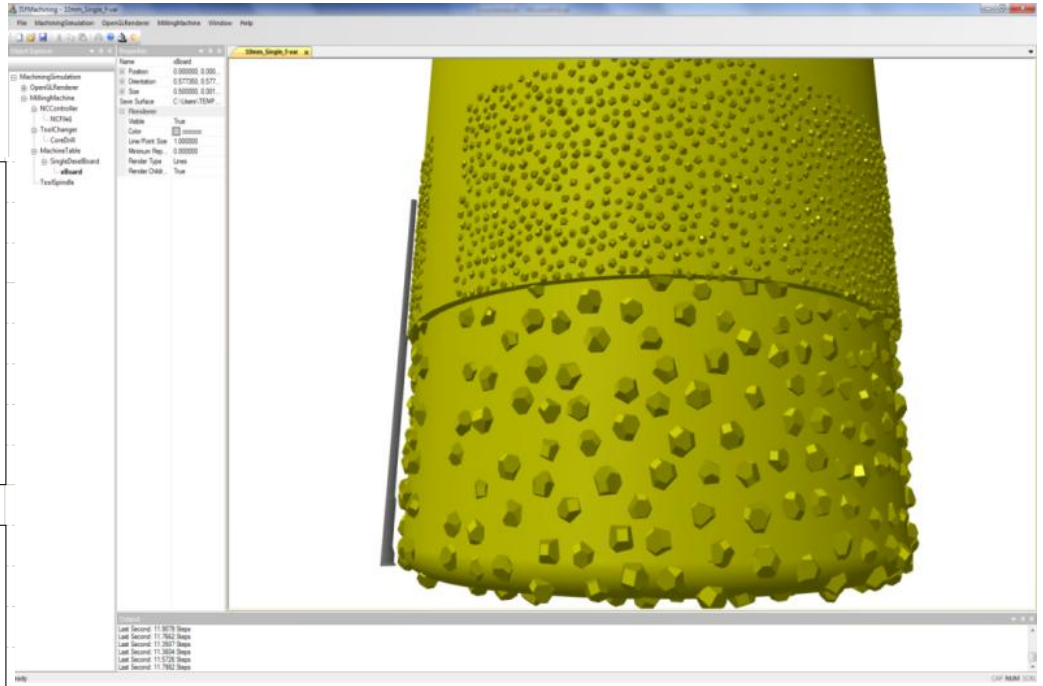

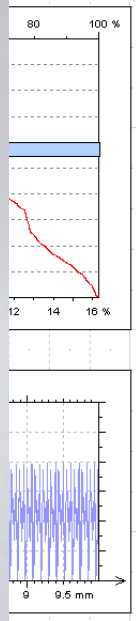

Dynamic characteristics of milling processes

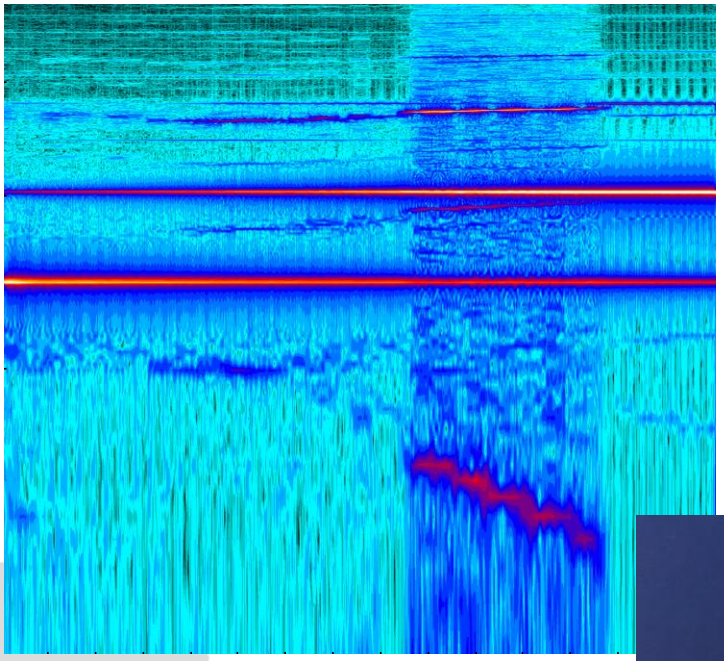

Measurement chain (in the working space of the machine tool)

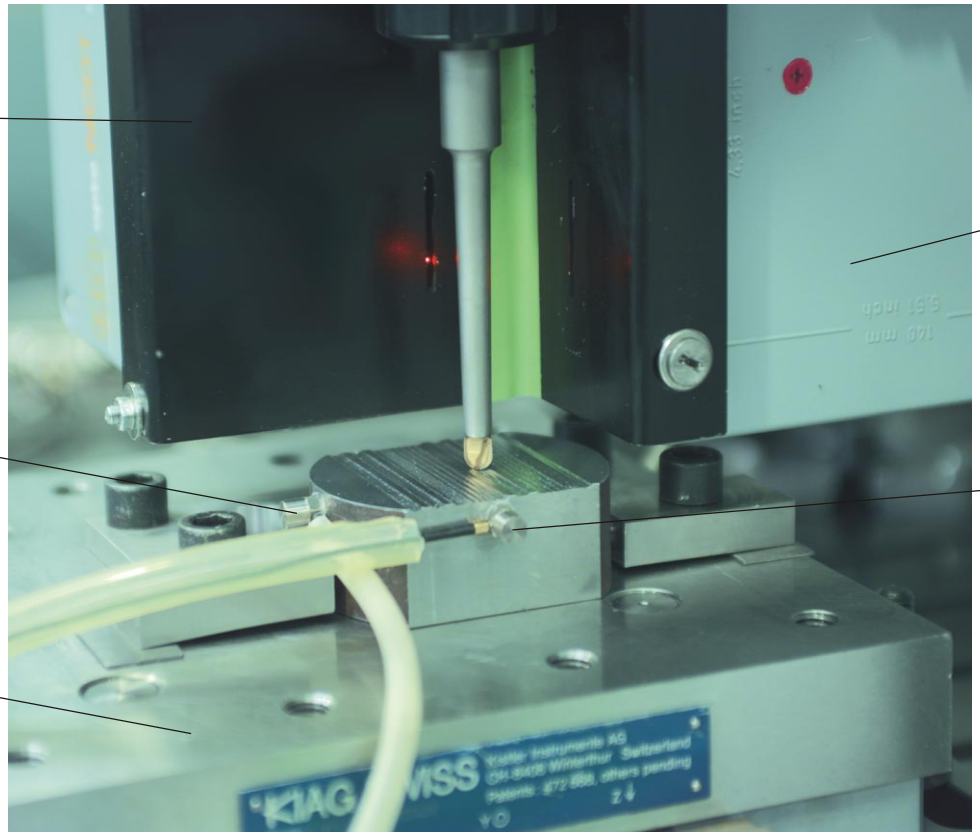

Tip movement with linearly rising depth of cut

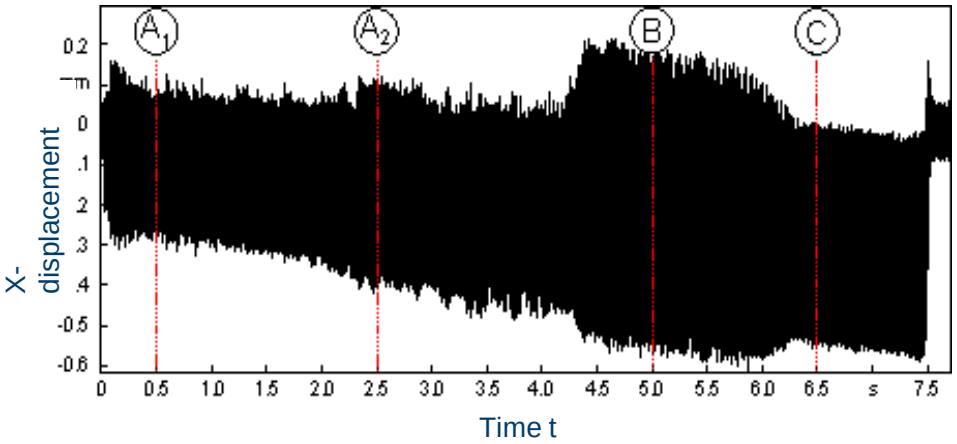

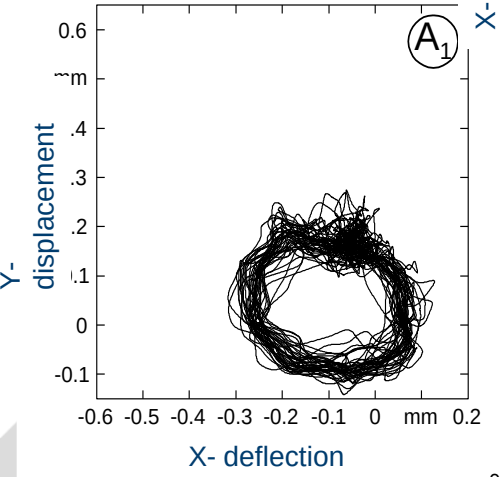

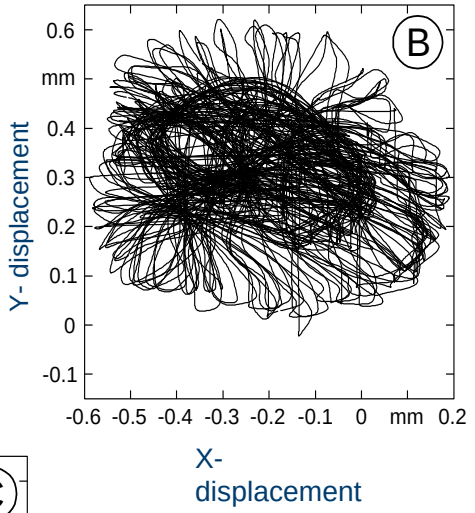

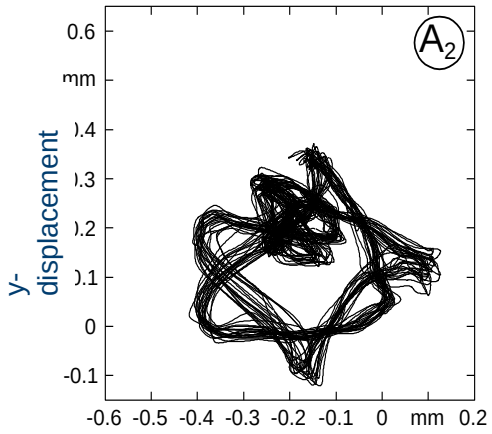

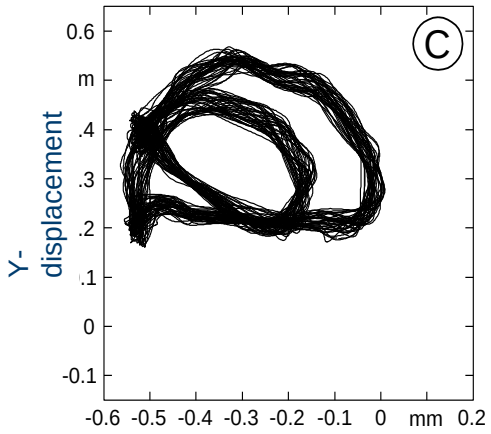

Frequency spectrum of the displacement in x - direction

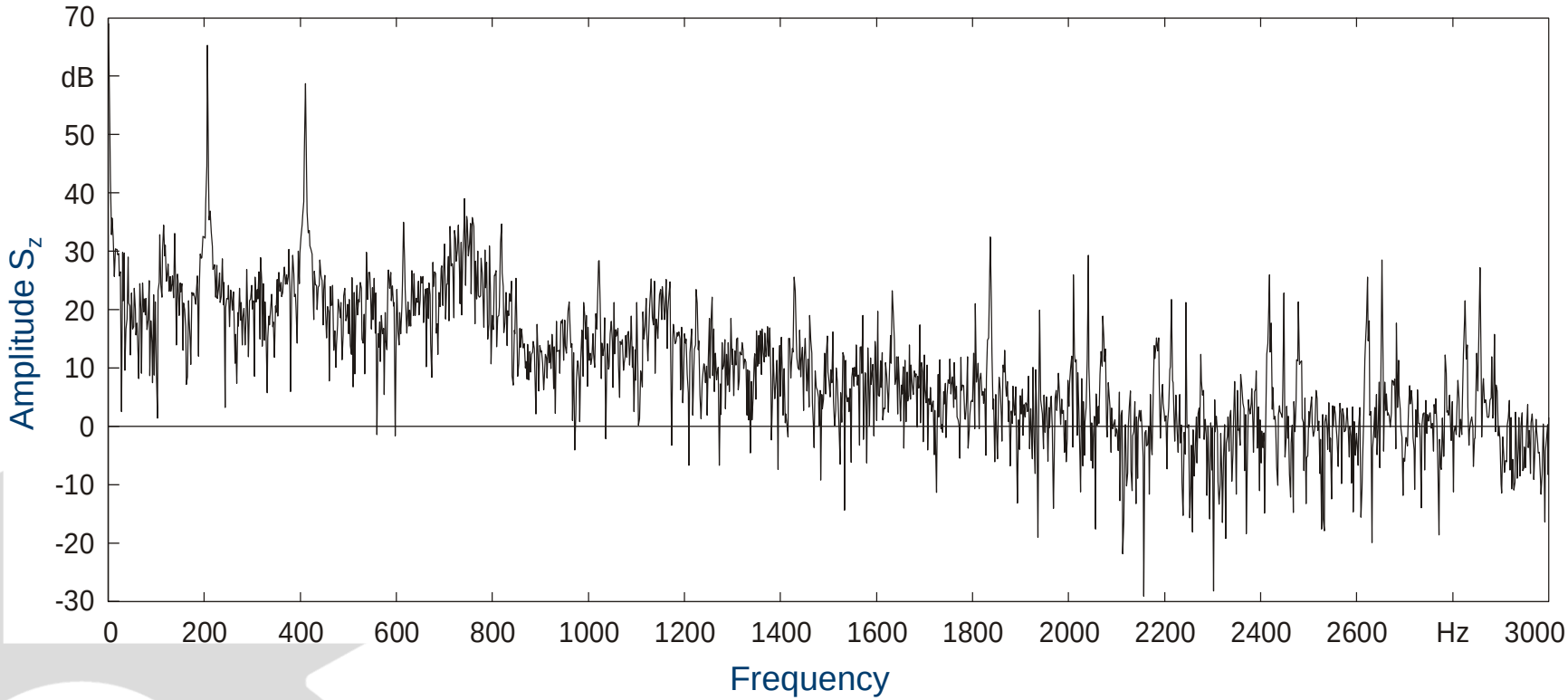

(Phase A_1, t =0.5s) - end milling cutter, v_c = 300m/min, f_z =0.7mm -

Flute machining with linearly rising depth of cut

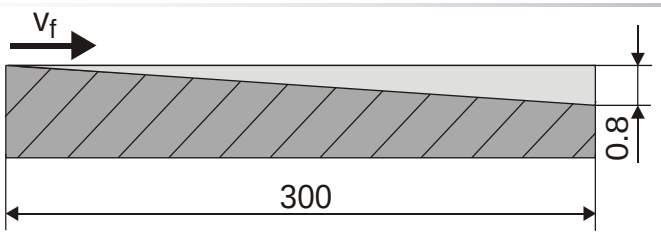

v_c = 300 m/min (n = 12000 min^{-1})

v_f = 2400 mm/min

a_p = 0 ... 0,8 mm

52NiCrMoV7-QT (52HRC)

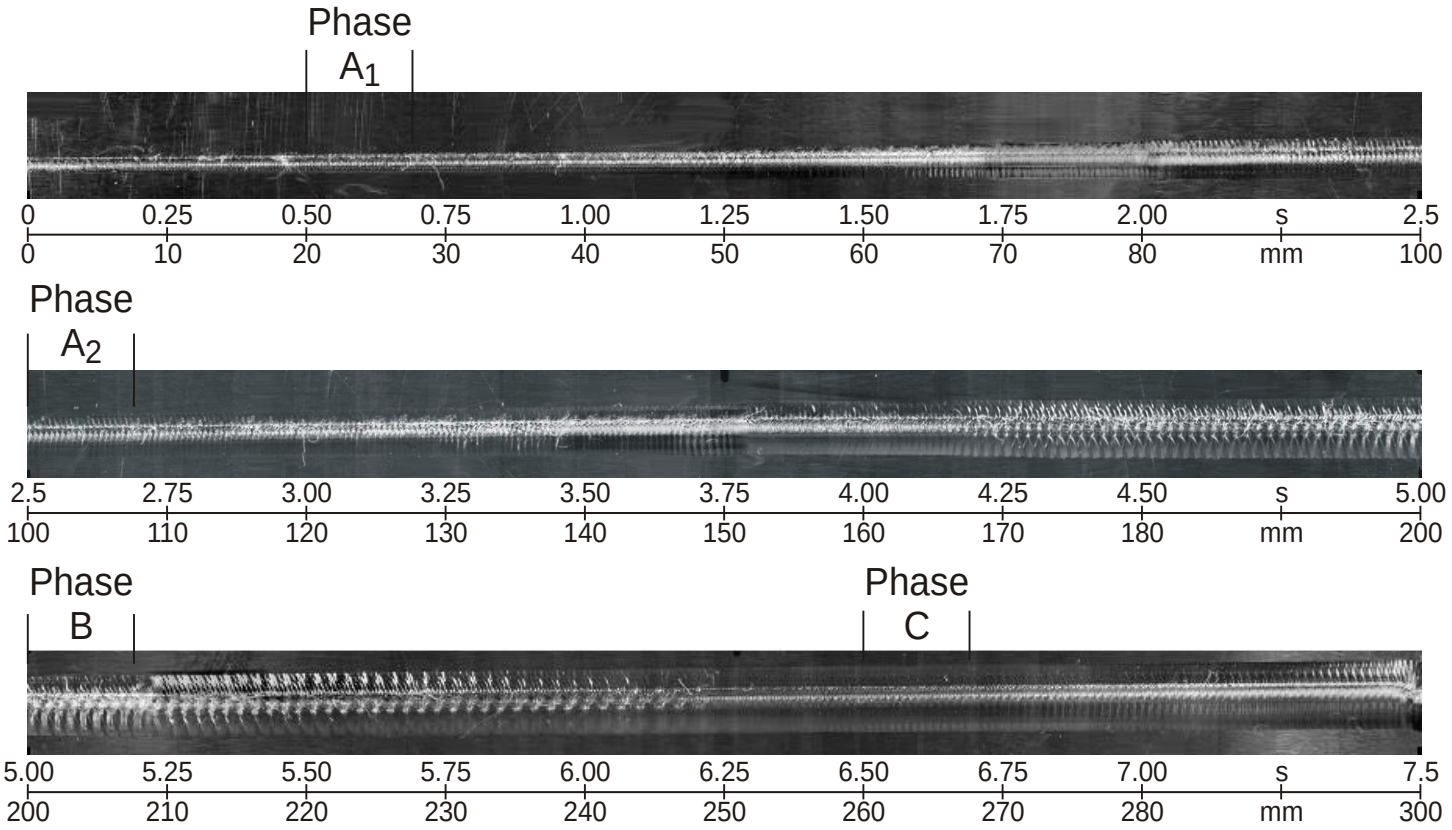

Motivation

Workpiece and close-up view of workpiece surface

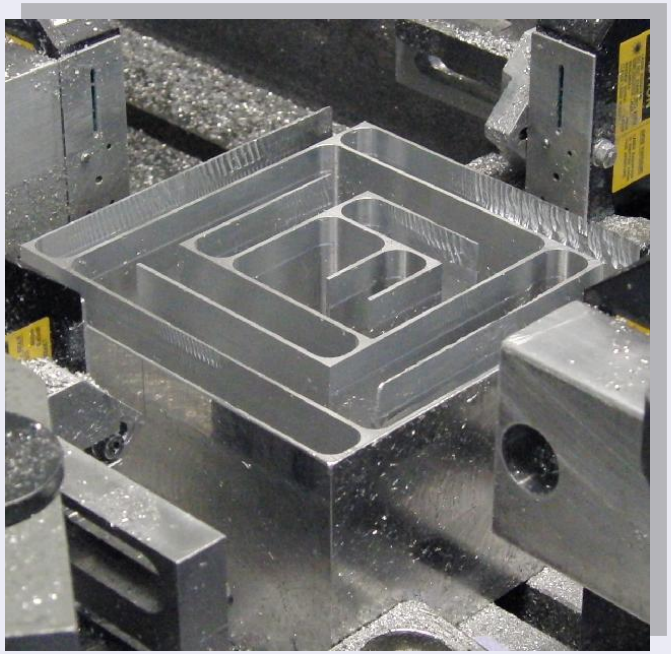

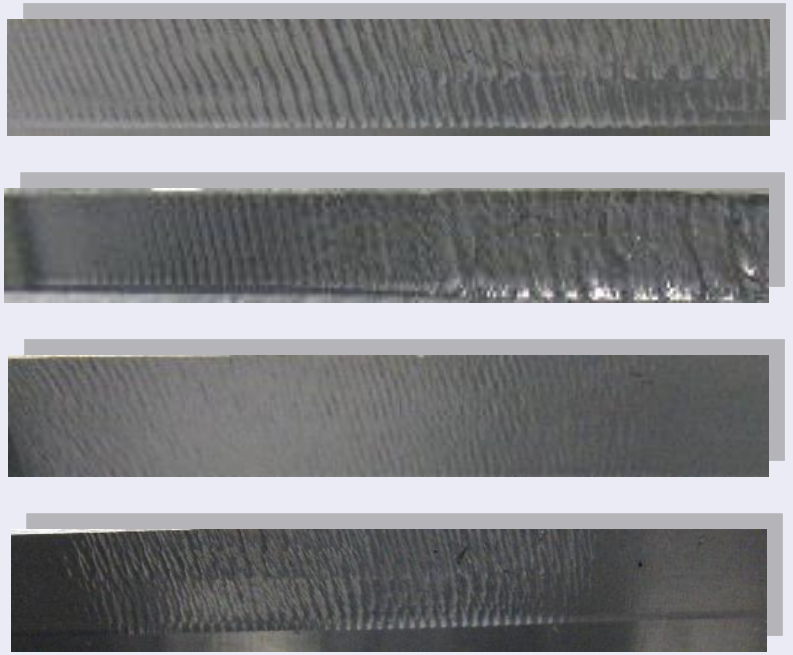

Simulation of NC Milling process

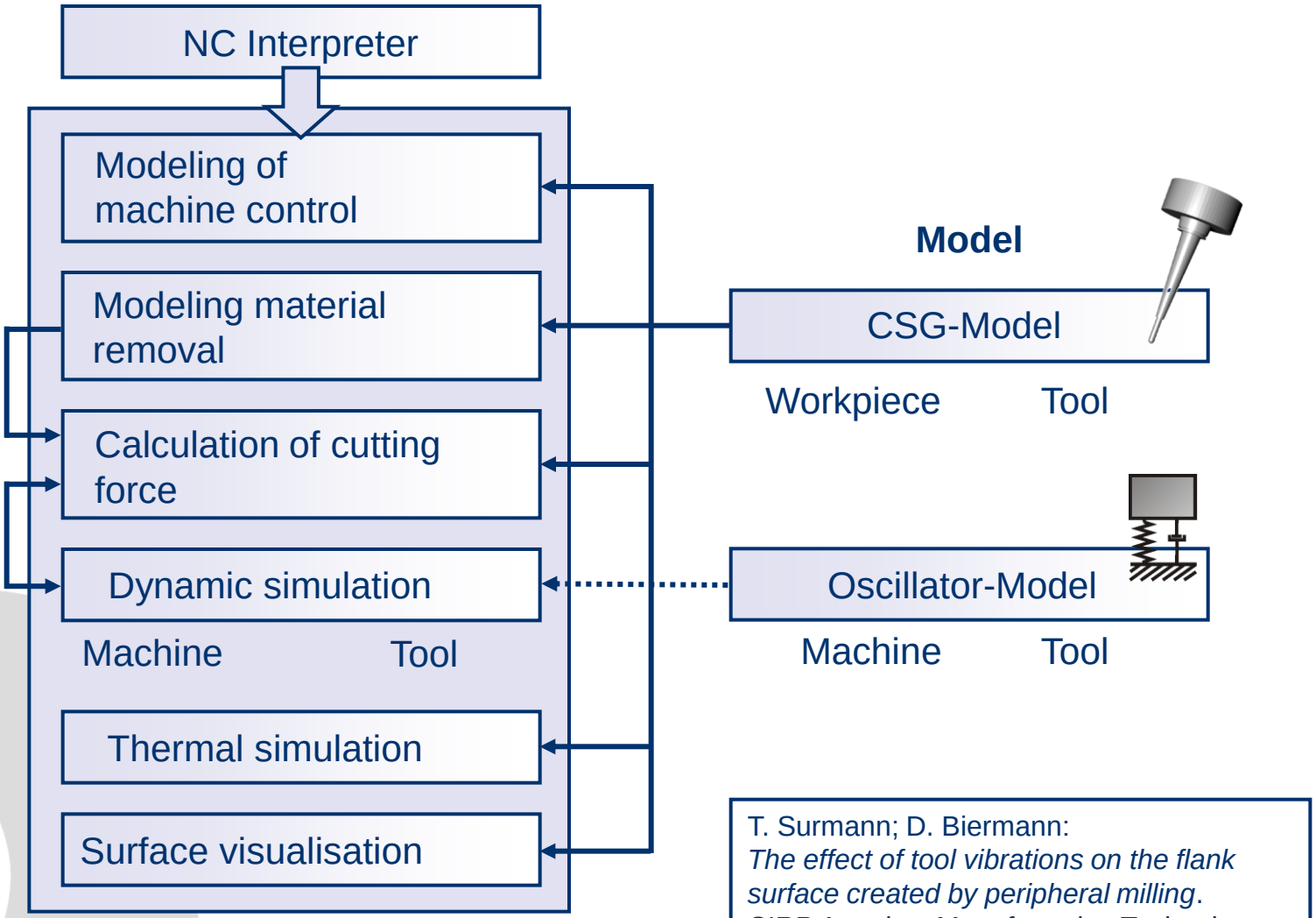

T. Surmann; D. Biermann:
The effect of tool vibrations on the flank surface created by peripheral milling.
CIRP Annals – Manufacturing Technology, 57 (2008) 1

Simulation of NC Milling process

Model

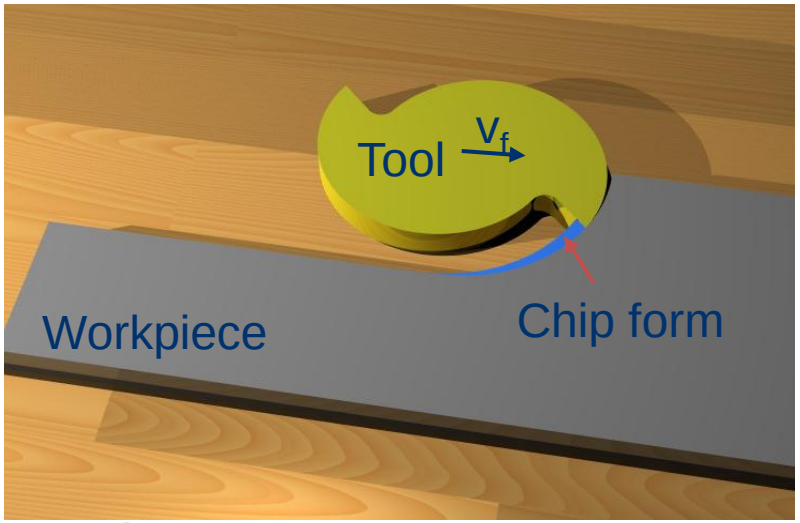

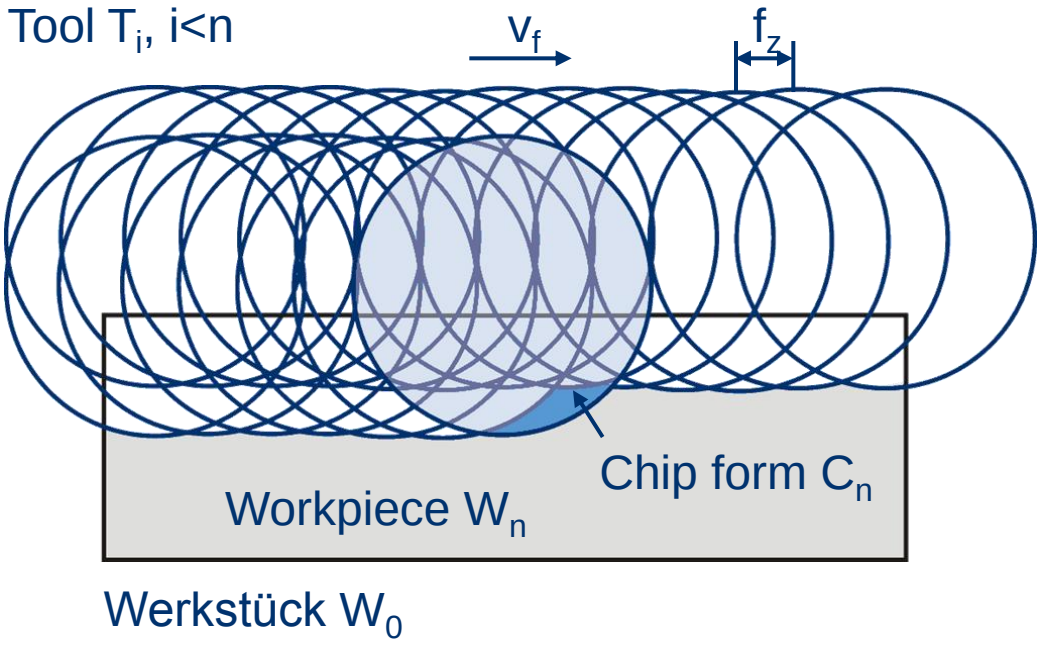

Description of the n-th tooth engangement (n>0)

Workpiece

$$W_n = W_0 \setminus \bigcup_{i=1}^{n} T_i$$

Chip form

$$C_n = \left[\underbrace{\left(W_0 \setminus \bigcup_{i=1}^{n-2} T_i \right)}_{W_{n-2}} \setminus T_{n-1} \right] \cap T_n$$

Simulation of NC Milling process

Hybrid-Simulation-concept takes dynamic workpiece characteristics into account

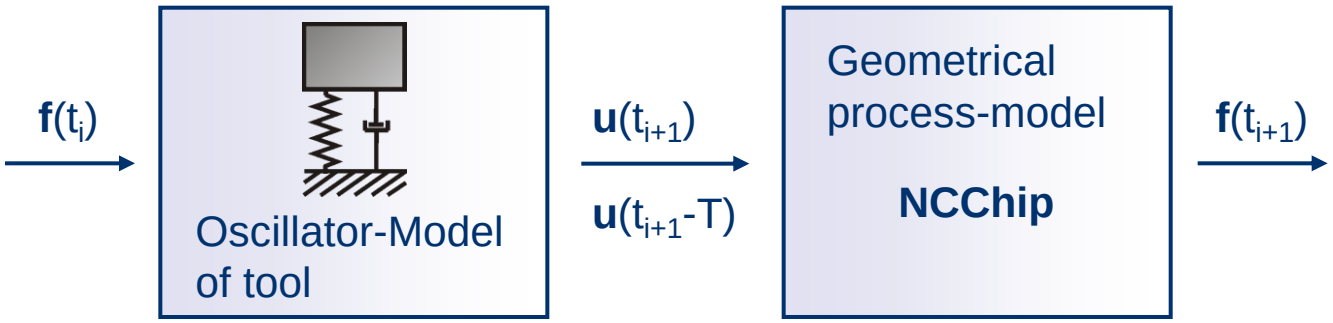

Hybrid-Simulation-concept takes dynamic workpiece characteristics into account

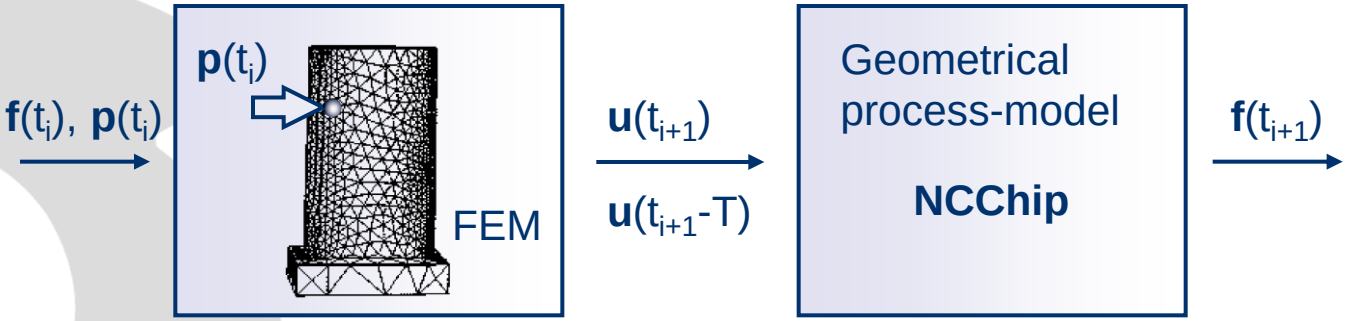

Modeling of workpiece vibrations

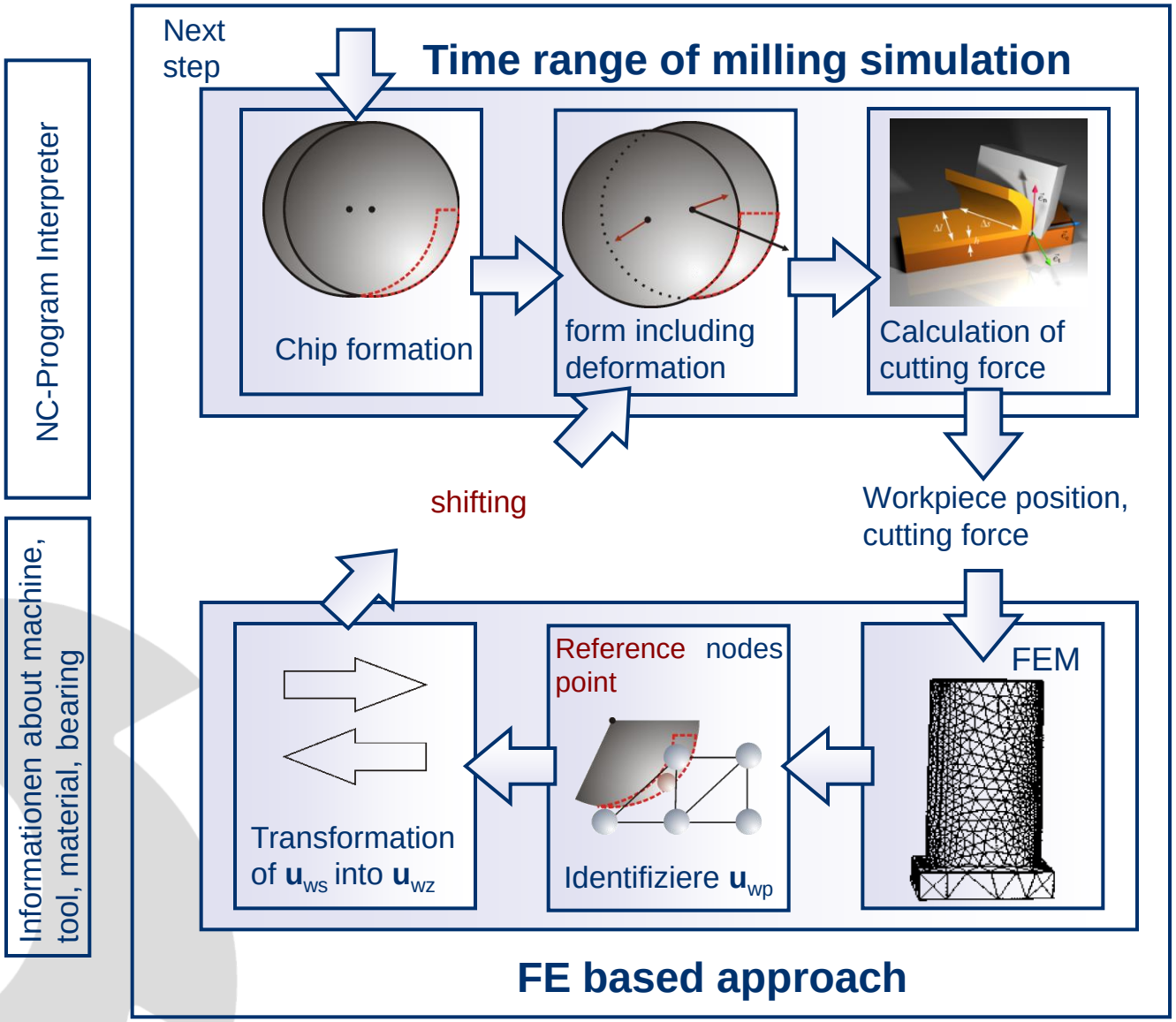

Experimental setup

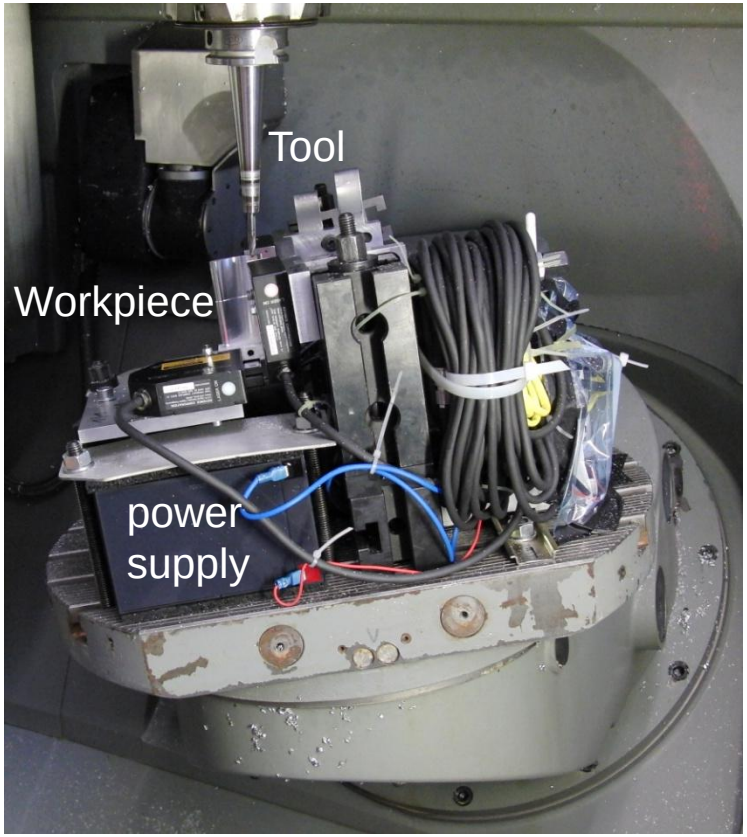

Workpiece	Machine	Tool	Process
Material: AlZnMgCu1.5	5-axis machining centre Deckel Maho 50 eVolution	Rounded edge geometry D = 6mm, double edged	Feed velocity: v_f = 2880 mm/min Rotational speed: n = 18000 min^{-1}

Measurement- und simulation results

Stable part of milling process

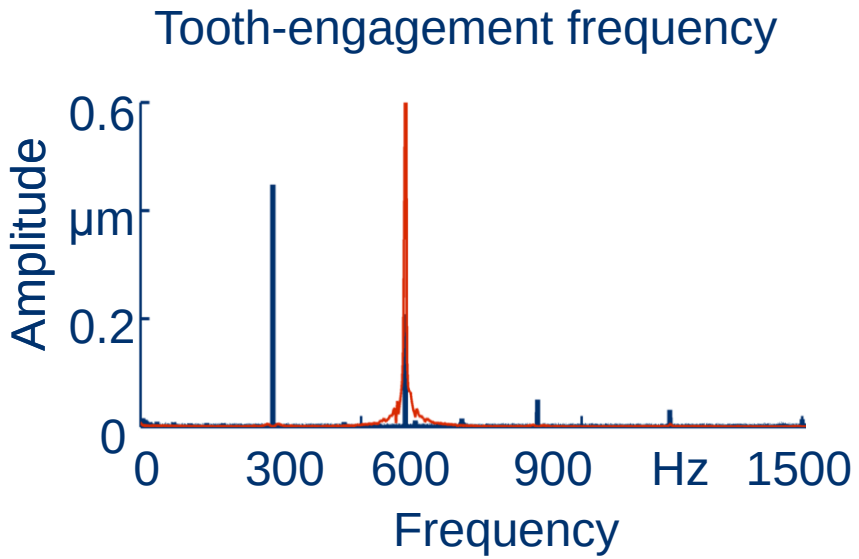

Workpiece surface

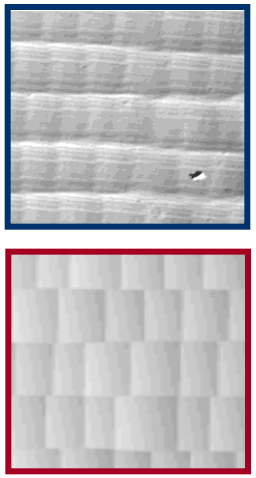

Experiment

Simulation

Workpiece	Machine	Tool	Process
Material: AlZnMgCu1.5	5-axis machining centre Deckel Maho 50 eVolution	Rounded edge geometry D = 6mm, double edged	Feed velocity: v_f = 2880 mm/min Rotational speed: n = 18000 min^{-1}

Measurement- und simulation results

Unstable part of milling process

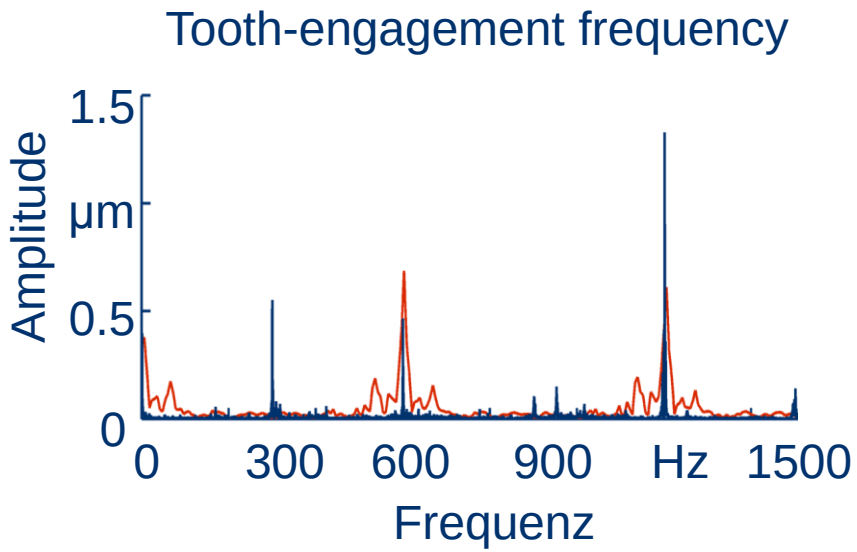

Workpiece	Machine	Tool	Process
Material: AlZnMgCu1.5	5-axis machining centre Deckel Maho 50 eVolution	Rounded edge geometry D = 6mm, double edged	Feed velocity: v_f = 2880 mm/min Rotational speed: n = 18000 min^{-1}

Measurement- und simulation results

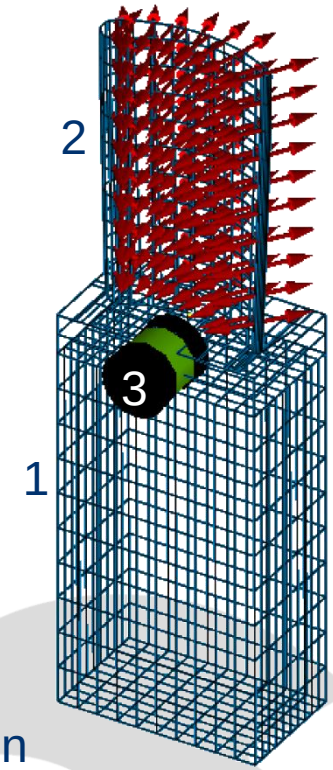

Model in modal-analysis-programm

Numerically controlled modal analysis

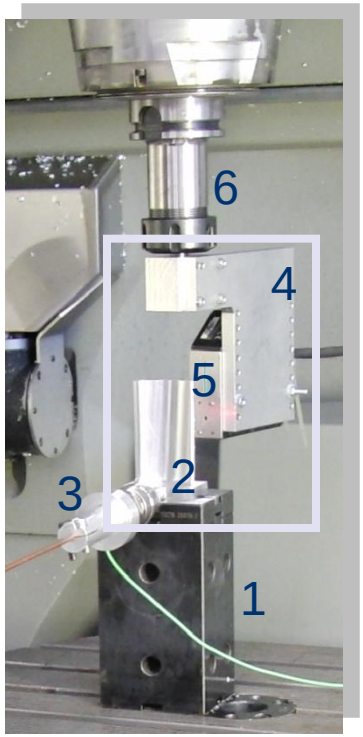

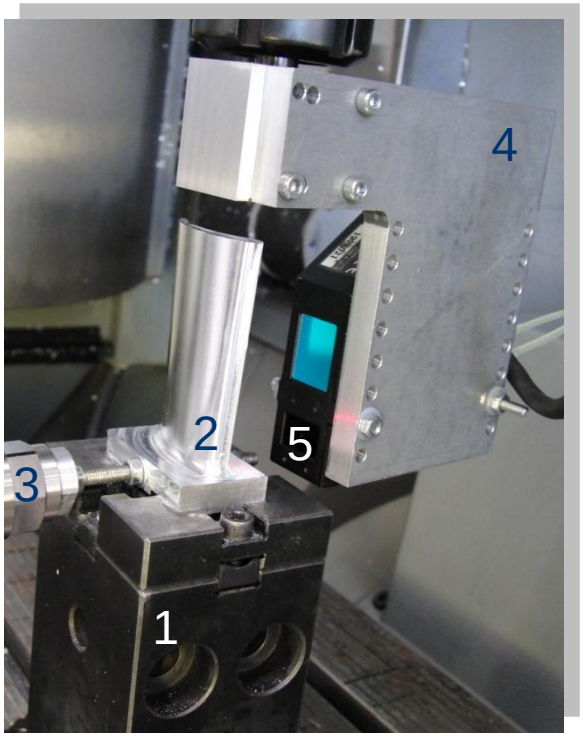

5-axis maching centre Deckel Maho eVolution

1 Work fixture
2 Workpiece
3 Shaker
4 Measurement device
5 Laser system
6 Chuck

→ Measured point

Measurement- und simulation results

Proceeding of measurement

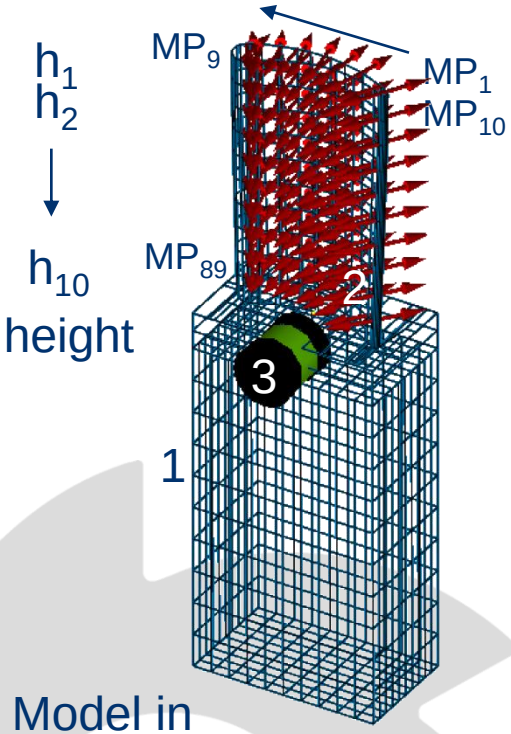

Model in
Modal-analysis-program

Numerical control modal-analysis

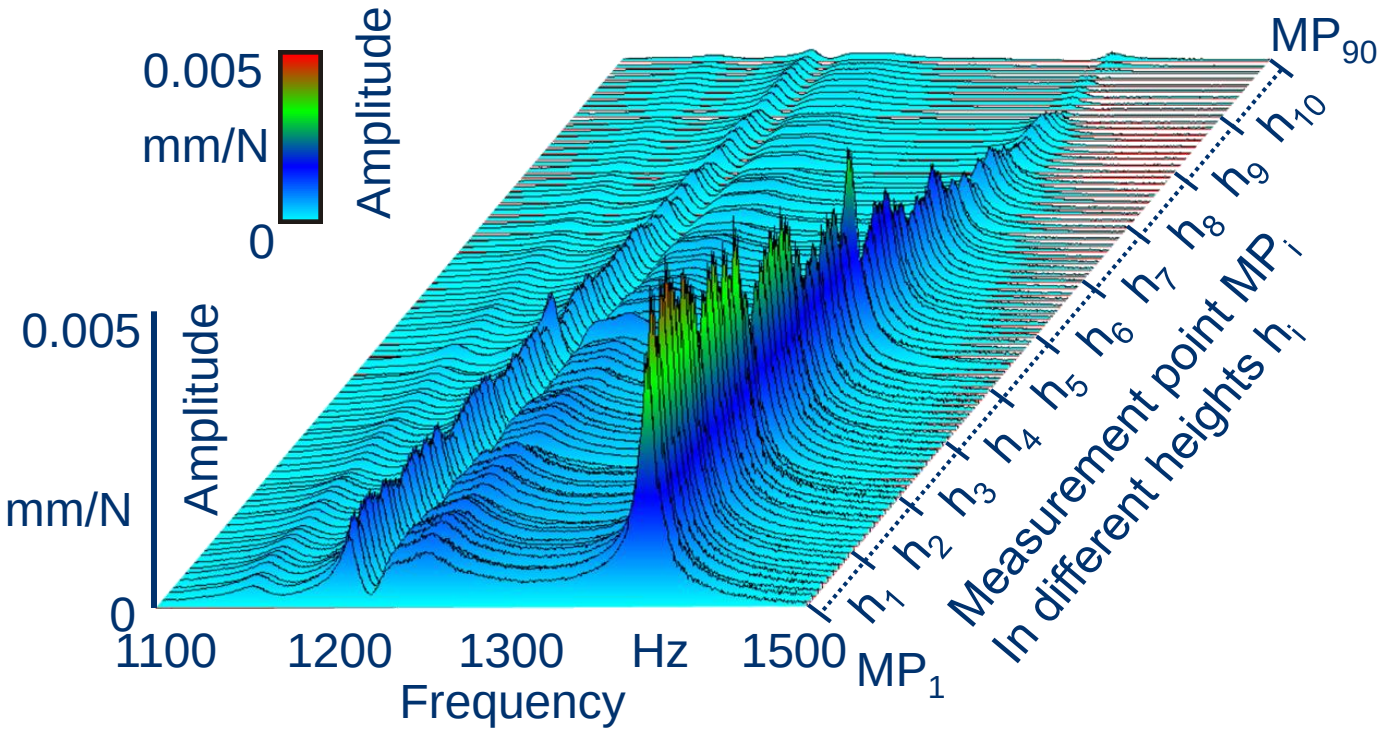

1 Work fixture
2 Workpiece
3 Shaker
4 Measurement device
5 Laser system
6 Chuck

h = height

Measured point

Measurement- und simulation results

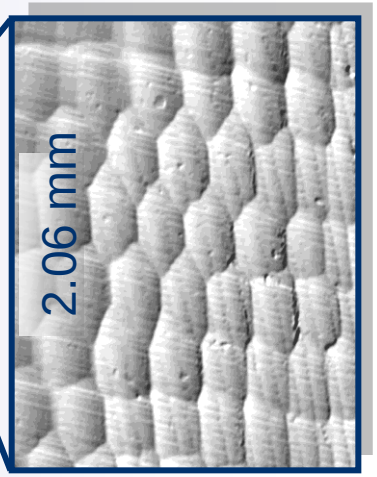

1.5 mm

Microscopic view

— Experiment

1.5 mm

Point based modeling – Close-up view

— Simulation

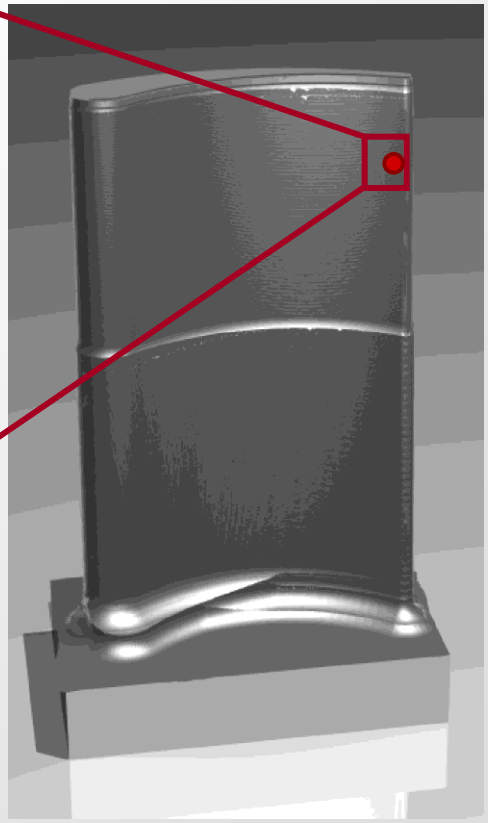

Workpiece	Machine	Tool	Process
Material: AlZnMgCu1.5	5-axis machining centre Deckel Maho 50 eVolution	Rounded edge geometry D = 6mm, double edged	Feed velocity: v_f = 2880 mm/min Rotational speed: n = 18000 min^{-1}

Measurement- und simulation results

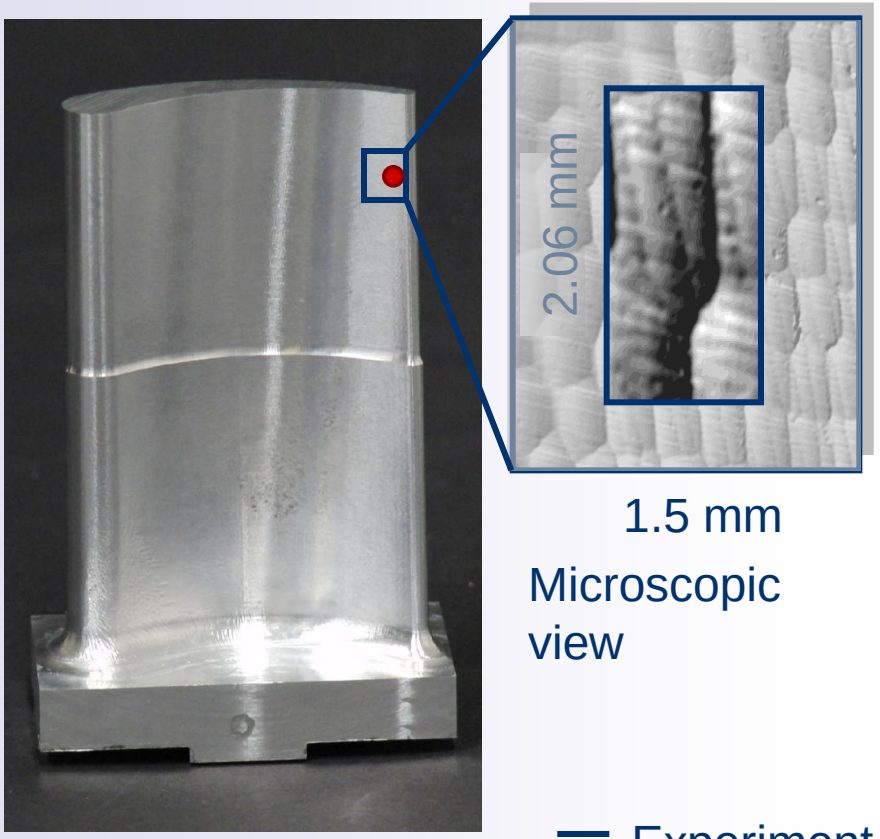

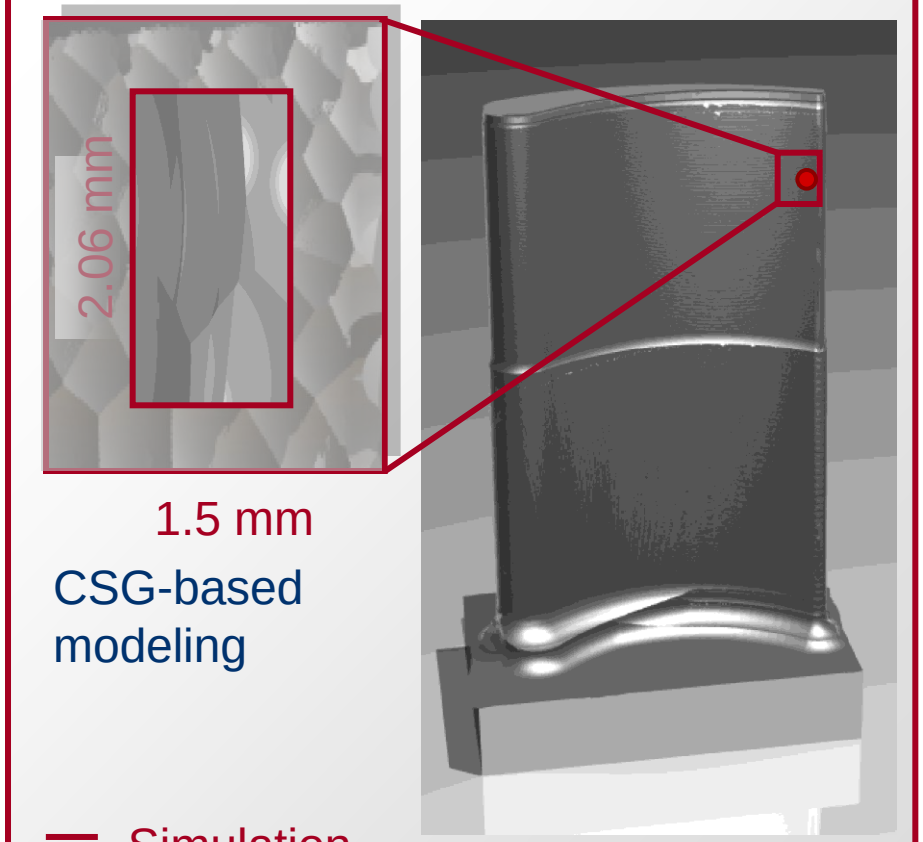

Workpiece	Machine	Tool	Process
Material: AlZnMgCu1.5	5-axis machining centre Deckel Maho 50 eVolution	Rounded edge geometry D = 6mm, double edged	Feed velocity: v_f = 2880 mm/min Rotational speed: n = 18000 min^{-1}

Conclusion and outlook

Summary

- Hybrid-simulation-system for modeling of regenerative workpiece vibrations during NC-milling process
- Result of the workpiece dynamics in the chip form
- Analysis of the measurement and simulation results show advantages for the machining of turbine blades

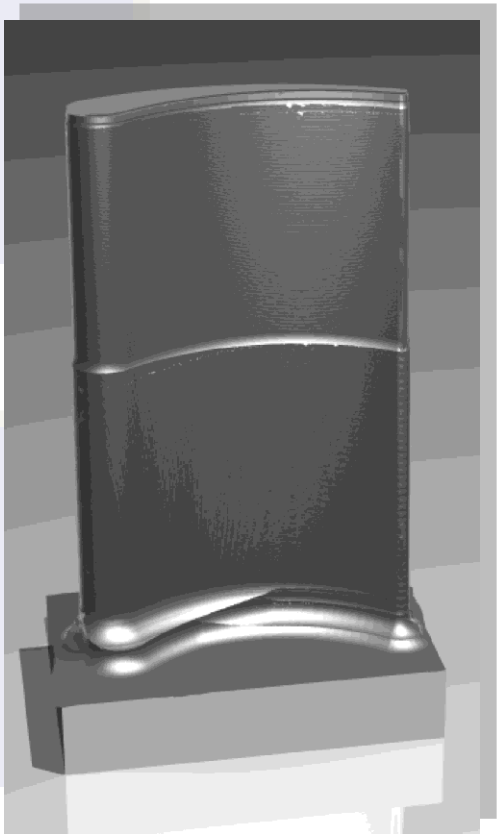

Outlook

- Reduction of computing time and memory requirements
- More efficient models for the calculation of workpiece vibrations and the determination of stability-diagrams

Acknowledgment

This lecture is based on several research projects funded by the German Research Foundation

DFG Deutsche Forschungsgemeinschaft

Thank you for your attention